DISSERTATIONES
MEDICINAE
UNIVERSITATIS
TARTUENSIS
311

PRAKASH LINGASAMY

Development of multitargeted tumor penetrating peptides

DISSERTATIONES MEDICINAE UNIVERSITATIS TARTUENSIS
311

DISSERTATIONES MEDICINAE UNIVERSITATIS TARTUENSIS
311

PRAKASH LINGASAMY

Development of multitargeted tumor penetrating peptides

UNIVERSITY OF TARTU
Press

Laboratory of Cancer Biology, Institute of Biomedicine and Translational Medicine, University of Tartu, Estonia.

The dissertation is accepted for the commencement of the degree of Doctor of Philosophy in Medicine on the 18th of November 2020 by the council of the Faculty of Medicine, University of Tartu, Estonia.

Supervisor:	Professor Tambet Teesalu, Ph.D., Cancer Biology Group, Institute of Biomedicine and Translational Medicine, Faculty of Medicine, University of Tartu, Estonia
Reviewers:	Associate Professor Karin Kogerman, Institute of Pharmacy, Faculty of Medicine, University of Tartu, Estonia
	Dr. Olesja Bodarenko, Senior Researcher, National Institute of Chemical Physics and Biophysics, Estonia
Opponent:	Professor Angelo Corti, Ph.D., Full Professor of Biochemistry, San Raffaele Vita-Salute University of Milan, Director of the Division of Experimental Oncology and Head of the Tumor Biology and Vascular Targeting Unit, San Raffaele Scientific Institute, Milan, Italy
Commencement:	29th of January 2021

Publication of this dissertation is granted by the University of Tartu.

This work was supported by the European Union through the European Regional Development Fund (Project No. 2014–2020.4.01.15-0012), by EMBO Installation grant #2344, European Research Council starting grant GLIOMADDS and GLIOGUIDE (780915) from European Regional Development Fund, Wellcome Trust International Fellowship WT095077MA, Norwegian-Estonian collaboration grant EMP181, and Estonian Research Council (PRG230 and EAG79).

ISSN 1024-395X
ISBN 978-9949-03-526-7 (print)
ISBN 978-9949-03-527-4 (pdf)

University of Tartu Press
www.tyk.ee

TABLE OF CONTENTS

LIST OF ORIGINAL PUBLICATIONS

I. **Lingasamy, P**., Tobi, A., Haugas, M., Hunt, H., Paiste, P., Asser, T., Rätsep, T., Kotamraju, V. R., Bjerkvig, R., Teesalu, T., Bi-specific tenascin-C and fibronectin targeted peptide for solid tumor delivery, *Biomaterials*, 2019 Oct;219:119373.

II. **Lingasamy, P**., Tobi, A, Kurm, K., Sudakov, A., Salumäe, M., Rätsep, T., Asser, T., Bjerkvig, R., Teesalu, T., Tumor-penetrating peptide for systemic targeting of Tenascin-C, *Scientific Reports*, 2020 Apr 2; 10(1):5809.

III. **Lingasamy, P.**, Laarmann, A., Teesalu, T., Tumor penetrating peptide-functionalized Tenascin C targeting antibody for glioblastoma targeting, *Current Cancer Drug Targets*, 2020 Oct 1; 20:11–1

IV. Säälik, P.*, **Lingasamy, P**.*, Toome, K., Mastandrea, I., Rousso-Noori, L., Tobi, A., Simón-Gracia, L., Hunt, H., Paiste, P., Kotamraju, V. R., Bergers, G., Asser, T., Rätsep, T., Ruoslahti, E., Bjerkvig, R., Friedmann-Morvinski, D., Teesalu, T., Peptide-guided nanoparticles for glioblastoma targeting, *Journal of Controlled Release*, 2019 Aug 28; 308:109–118.

V. Ikemoto, H., **Lingasamy, P**., Willmore, A. M. A., Hunt, H., Kurm, K., Tammik, O., Scodeller, P., Simón-Gracia, L., Kotamraju, V. R., Lowy, A. M., Sugahara, K. N., Teesalu,T., Hyaluronan-binding peptide for targeting peritoneal carcinomatosis, *Tumor Biology*, 2017 May; 39(5): 1010428317701628.

* Shared first authorship.

Intellectual Property

VI. Title of Invention: "BI-SPECIFIC EXTRACELLULAR MATRIX BINDING PEPTIDES AND METHODS OF USE THEREOF" By Tambet Teesalu and **Prakash Lingasamy**
Our Ref.: TARTU 100 (095468/00002) and Registered US Provisional Patent
International Publication Number: WO/2020/161602
International PCT No: PCT/IB2020/050847 (Application Number: 62800879).

Contribution to each publication (I–VI) is as follows:

Paper I and II: Designed the experiments with T. Teesalu, developed the methodology, performed all the experiments, analyzed, interpreted the data, and wrote the manuscript.

Paper III: Designed the experiments with T. Teesalu, developed the methodology, performed all the experiments with A. Laarmann, analyzed the data with A. Laarmann, and wrote the manuscript.

Paper IV: Participated in the design of the study and development of methodology with T. Teesalu and P. Säälik. Established a glioblastoma model, performed experimental treatment study, analyzed and interpreted data, performed immunofluorescent staining and confocal microscopy imaging, took part in the interpretation of data, and participated in the writing of the manuscript, and performed the review of the manuscript.

Paper V: Established and performed cell-free binding assay, participated in the analysis and interpretation of data, participated in the writing of the manuscript, and performed the review of the manuscript.

ABBREVIATIONS

2D	Two-Dimensional
Abs	Antibodies
ABX	Abraxane
ADC	Antibody-Drug Conjugate
Ag107	Silver Isotope 107
Ag109	Silver Isotope 109
AgNP	Silver Nanoparticle
ANOVA	One-Way Analysis of Variance
APP	Amyloid Precursor Protein
ATCC	American Type Culture Collection
ATP	Adenosine Triphosphate
AUC	Area Under the Curve
Aβ	B-Amyloid Peptide
B/biot	Biotin
B-AgNP	Silver Nanoparticle Blocked with Biotin
BBB	Blood Brain Barrier
bFGF	Basic Fibroblast Growth Factor
Br	Brain
BSA	Bovine Serum Albumin
CendR	C-End Rule
CF555	Succinimidyl Ester, Fluorescent Dye
CSF	Cerebrospinal Fluid
CTGF	Connective Tissue Growth Factor
CTLA-4	Cytotoxic T-Lymphocyte-Associated Protein 4
DAPI	4`6-Diamidino-2-Phenylindole Fluorescent Dye
DDS	Drug Delivery System
DLS	Dynamic Light Scattering
DMEM	Dulbecco's Modified Eagle Medium
DNA	Deoxyribonucleic Acid
DOX	Doxorubicin
EC	Endothelial Cell

ECM	Extracellular Matrix
EGF	Epidermal Growth Factor
EPR	Enhanced Permeability and Retention
FAM	5(6)-Carboxyfluorescein
FDA	The United States Food and Drug Administration
FGF	Fibroblast Growth Factor
FITC	Fluorescein Isothiocyanate
FN-EDB	Fibronectin Extra Domain B
GBM	Glioblastoma Multiforme
GFAP	Glial Fibrillary Acidic Protein
GL	Granular Layer
GLUT1	Glucose Transporter-1
HA	Hyaluronic Acid
HEPES	4-(2-Hydroxyethyl)-1-Piperazineethanesulfonic Acid
HIPEC	Hyperthermic Intraperitoneal Chemotherapy
ICP-MS	Inductively-Coupled Plasma Mass Spectroscopy
IFP	Elevated Interstitial Fluid Pressure
IMAC	Immobilized Metal Affinity Chromatography
IONP	Iron Oxide Nanoparticle
IONW	Iron Oxide Nanoworm
IP	Intraperitoneal
IP3	Hyaluronan Targeting Peptide, Sequence [CKRDLSRRC]
iRGD	Internalizing RGD, Prototypic Tumor Penetrating Peptide, Sequence [CRGDKGPDC]
IV	Intravenous
K-AgNP	Silver Nanoparticle Functionalized With SGKRK
LA-ICP-MS	Laser Ablation Inductively-Coupled Plasma Mass Spectroscopy
LB	Lysogeny Broth
LinTT1	Lineartt1, P32-Directed Tumor Penetrating Peptide, Sequence [AKRGARSTA]
LRP	Low-Density Lipoprotein Receptor-Related Protein
Lyp-1	P32-Directed Tumor Homing Peptide, Sequence [CGNKRTRGC]

mAbs	Monoclonal Antibodies
MEM	Minimum Essential Medium
MeOH	Methanol
ML	Molecular Layer
MPS	Mononuclear Phagocytic System,
MR	Magnetic Resonance
MRI	Magnetic Resonance Imaging
NA	Neutravidin
NGS	Next-Generation Sequencing
NHS	N-Hydroxysuccinimide
NP	Nanoparticle
NP40	Nonyl Phenoxypolyethoxylethanol
NRP-1	Neuropilin-1
NTA	Nitrilotriacetic Acid
NW	Nanoworm
OBOC	One-Bead-One-Compound
OCT	Optimal Cutting Temperature Compound
p32	Protein 32 (Gc1qr /HABP1/P33/C1qbp)
PAGE	Polyacrylamide Gel Electrophoresis
PBS	Phosphate-Buffered Saline
PC	Peritoneal Carcinomatosis
PD	Parkinson's Disease
PDGC	Patient-Derived Glioma Cell
PD-L1	Programmed Death Ligand 1
PDX	Patient-Derived Xenograft
PEG	Polyethylene Glycol
PET	Positron Emission Tomography
PFU	Plaque-Forming Unit
PL1	Fibronectin Extra Domain B (FN-EDB) And Tenascin-C Extra Domain C (TNC-C) -Targeting Tumor Homing Peptide, Sequence [PPRRGLIKLKTS]
PL3	Tenascin-C Extra Domain C (TNC-C) And NRP1 -Targeting Tumor Homing Peptide, Sequence [CGNKRTRGC]

PV	Pulmonary Vessel
RAGE	Receptor for Advanced Glycation End Products
R-AgNP	Silver Nanoparticle Functionalized with RPARPAR Peptide
Rho	Rhodamine
RNA	Ribonucleic Acid
RPAR/R	Prototypic CendR Peptide, Sequence [RPARPAR]
RT	Room Temperature
SC	Subcutaneous
SD	Standard Deviation
SDS	Sodium Dodecyl Sulfate
SM	Smooth Muscle
TAA	Tumor-Associated Antigens
TEM	Transmission Electron Microscopy
TFA	Trifluoroacetic Acid
TGF	Transforming Growth Factor
THP	Tumor Homing Peptides
TME	Tumor Microenvironment
TNC-C	Tenascin C Extra Domain C
TNF	Tumor Necrosis Factor
TPP	Tumor Penetrating Peptide
TTP	Tumor Targeting Peptide
Tu/T	Tumor
UV-vis	Ultraviolet-Visible
VEGF	Vascular Endothelial Growth Factor
Wt	Wild-Type
Ahx/X	Aminohexanoic Acid

1. INTRODUCTION

Cancer is the secondmost leading cause of mortality worldwide (Bray et al., 2018). The advancement in therapeutic interventions in solid tumors, including surgery, radiotherapy, chemotherapy, and immunotherapy, has resulted in only the incremental improvement of patients' overall survival with advanced disease (Araste et al., 2018). Extensive investigations are being undertaken to identify novel precision anti-cancer treatment strategies such as immunotherapies, personalized molecular therapies, nanomedicine, and affinity cancer targeting. The chemotherapy remains the first line of treatment for metastasized cancer. The majority of existing anti-cancer drugs show poor cancer selectivity and have dose-limiting side effects (Kuncic, 2015; Vrettos et al., 2018; Simón-Gracia et al., 2018a). Tumor-specific markers can be targeted with affinity ligands to selectively deliver chemotherapeutics to the cancer site while limiting the damage to healthy tissues, thereby increasing the therapeutic efficacy (Gerber, 2008; Le Joncour & Laakkonen, 2018; Teesalu et al., 2013; Ruoslahti, 2017). The cancer-targeted precision delivery holds a remarkable potential to selectively transporting the chemotherapeutics to the tumor site, thereby improving the efficacy and reducing off-target cytotoxicity.

An effective strategy for selecting tumor-targeting ligands is to utilize heterogeneity of unique receptors overexpressed in the malignant cells, neovessels, tumor-associated cells, immune cells, and tumor extracellular matrix (ECM) (Valkenburg et al., 2018). Precision-guided delivery of anti-cancer drugs with affinity ligands such as peptides and antibodies showed a great promise in accumulating increased concentration of the drug at the tumor site and reduced systemic exposure in the non-targeted organs (Kennedy et al., 2017; Ruoslahti, 2017; Yoo et al., 2019). The peptides are widely used targeting ligands due to their specificity, small size, relative non-immunogenicity, simple, scalable and cost-effective synthesis, and superior tissue and cell penetration ability (Ruoslahti, 2017; Teesalu et al., 2013). The development of multitargeted peptide may further improve manifold specific targetability, delivery, accumulation and decreases toxicity. Currently development of multitargeted drug delivery ligands such as bi and tri specifics are very challenging, labor intensive, and cumbersome process. Phage display technology is an unbiased tool used for identifying targeting peptide and mapping molecular heterogeneity of the systemically accessible compartment in tumors and other diseases (Pasqualini & Ruoslahti, 1996; Teesalu et al., 2012). Further, the tumor-targeting peptide can be readily armed with cytotoxic drugs, cytokines, toxins, radionuclides, nanoparticles (NPs) loaded with drugs and imaging agents for enhanced avidity, drug stability, improved half-life, and controlled release at the intended target tissue (Jeong et al., 2018; Hua et al., 2018).

The thesis deals with the identification of novel multitargeted tumor homing peptides and their preclinical development for targeted delivery and imaging of solid tumors. Our starting hypothesis was that tumor antigen expression is

heterogeneous within the tumor, and multitargeting may result in a more homogeneous biodistribution of payloads. The multitargeting may also alleviate issues related to a limited number of available receptors for affinity ligands – a widely recognized bottleneck in affinity targeting (Hussain et al., 2014). We used a peptide phage display library to discover dual targeting peptides against selected tumor-specific receptors. To test newly identified peptides as an active targeting ligand, we used different model carrier NP platforms such as iron oxide nanoworms (NWs) and metallic silver NPs (AgNPs). Next, we systemically assessed peptides conjugated NPs *in vivo* for their targeting ability and biodistribution in different xenograft tumor models in mice and rats. The peptide NPs were used for preclinical proof-of-concept studies to investigate the applications of a peptide targeted precision drug delivery and imaging application in different solid tumors.

2. LITERATURE REVIEW

2.1. Cancer drug delivery

2.1.1. Anti-cancer drugs in cancer therapy

Cancer is a complex and heterogeneous pathological condition that originates from virtually any part of the human body due to aberrant and uncontrolled cell proliferation (Hanahan & Weinberg, 2011). Cancer is the secondmost common cause of death globally, and new incidence and mortality rates are rapidly growing worldwide (Bray et al., 2018). Therefore, the development of novel improved therapeutic approaches urgently needed to cure the cancer epidemic. The most widely used anti-cancer therapeutic approaches are surgery, radiotherapy, chemotherapy, and immunotherapy. There are currently >250 the United States Food and Drug Administration (FDA) approved anti-cancer drugs; most of them chemotherapeutics (Vrettos et al., 2018). Chemotherapy, first applied in 1946 using nitrogen mustard in the treatment of non-Hodgkin's lymphoma (DeVita & Chu, 2008), is currently the only treatment option for patients with metastatic cancers.

Typical chemotherapeutic drugs are low molecular weight agents that directly or indirectly kill cancer cells by disrupting the DNA/RNA synthesis of the cells and/or interfering with cell cycle machinery. Chemotherapeutic drugs are classified into several categories based on their mechanism of action. (1) Alkylating agents that directly damage and modify DNA, such as chlorambucil, temozolomide, dacarbazine, carboplatin, mechlorethamine, and melphalan (Fu et al., 2012). (2) Anti-metabolites imitate the natural building blocks of biomolecules: RNA, DNA, and, less frequently, proteins. The most commonly used drugs of this class are methotrexate, 6-mercaptopurine, fluorouracil, gemcitabine, nelarabine, and trifluridine/tipiracil (Tsesmetzis et al., 2018). (3) Topoisomerase inhibitors that prevent the replication of DNA and transcription by inhibiting topoisomerase I or II, such as camptothecin, irinotecan, etoposide, and topotecan (Rothenberg, 1997). (4) Mitotic inhibitors that arrest cell division by inhibiting microtubules, such as paclitaxel, docetaxel, vinblastine, vincristine, and cabazitaxel (Dumontet & Jordan, 2010). (5) Anti-tumor cytotoxic antibiotics interfere with DNA and RNA syntheses, such as bleomycin, daunorubicin, doxorubicin (DOX), and mitomycin-C (Bailly et al., 2020). (6) Steroid hormones that modulate cellular metabolism are typically used to relieve the side effects of other medications; examples are prednisone, methylprednisolone, and dexamethasone (Pufall, 2015; Huang et al., 2017a; Link, 2015). The chemotherapeutic drug uses are limited due to their poor aqueous solubility, metabolic instability, and poor penetration in solid tumors that result in low drug availability and limited therapeutic efficacy (Chabner & Roberts, 2005; Kuncic, 2015; Vrettos et al., 2018).

The second-generation therapies use a disease-specific target to mediate their therapeutic effects. They are categorized into small molecules, antibodies, and vaccines. The small molecules (< 900 Da) that target intracellular effectors and

cell surface receptors are able to diffuse rapidly across tissue barriers and the cell membrane. Examples of the small molecule drugs in clinical use are bortezomib (Velcade®), erlotinib (Tarceva®), imatinib (Gleevec®), and sorafenib (Nexavar®) (Crisci et al., 2019; Link, 2015). On the other hand, antibody-based therapies target specific cell surface receptors to precision-deliver bioactive cargoes, such as radioisotopes, toxins, and immune effectors. Antibody-based therapies can also modulate signaling cascades and immune response. Currently, there are >30 clinically approved antibody drugs, including the anti-CD30 antibody (Bevacizumab), anti-HER2 antibody (Trastuzumab), and anti-CTLA-4 antibody (Ipilimumab) (Alibakhshi et al., 2017; Beck et al., 2017). Vaccines usually target tumor-associated antigens (TAAs) aberrantly expressed self-antigens on cancer cells triggering an anti-tumor immune response. Numerous types of vaccines are developed from either cell, protein, peptide, viral, bacterial, gene-based system, RNA, and DNA. The most widely used immune-based drugs in clinical use include Sipuleucel T and immune checkpoint inhibitors such as anti-CTLA-4, anti-PD-1, and anti-PD-L1 antibodies (Lopes et al., 2019; Hollingsworth & Jansen, 2019). Although immunotherapeutics can lead to a cure, they are ineffective in a majority of patients. The current approved anti-cancer therapies offer only limited cures, a modest extension of life, and novel strategies are needed to deal with their toxicity, intrinsic or acquired resistance, clinical relapse, and limited efficacy.

2.1.2. Drug delivery: Passive and active targeting

The precision tumor delivery of chemotherapeutics and cytotoxic drugs could enhance their therapeutic index – the difference between efficacious and toxic doses. The ideal drug delivery system should result in increased drug accumulation at the tumor site and reduced exposure of healthy tissues, improved solubility and stability, higher internalization and tissue penetration capacity, biocompatibility, and biodegradability. The passive targeting relies on the enhanced permeability and retention (EPR) effect first described by Maeda (Matsumura & Maeda, 1986). The basis of the EPR phenomenon is that solid tumors have angiogenic blood neovessels that are morphologically and functionally different from resting normal vessels; they are tortuous, leaky, and with irregular blood flow. In addition, tumors have poor lymphatic drainage and secrete vascular permeability factors to allow nutrient and oxygen supply to the growing tumor tissue (Zanotelli & Reinhart-King, 2018). The enhanced vascular permeability allows (> 40 kDa) molecules leak out from tumor vessels and accumulate in the tumor tissue. The passive tumor-targeting chemotherapy utilizes this specific property of the EPR effect for delivery. All clinically approved NPs drugs rely on passive targeting for their tumor delivery (Rosenblum et al., 2018). The passively targeted nanocarriers demonstrated reduced toxicity with similar efficacy of conventional chemotherapeutics drugs. However, it is increasingly recognized that the EPR, in particular in clinical tumors, is highly variable and limited, and is influenced by heterogeneity between tumor types and within the individual

tumor (Blanco et al., 2015; Navya et al., 2019; Lingasamy et al., 2019; Säälik et al., 2019).

The tumor drug delivery using nanotechnology gained immense attention over the past two decades due to the multifunctionality and potential theranostic applications. However, current passively targeted monotherapies result in only a small percentage of dosed particles accumulating at the tumor site (Wilhelm et al., 2016). This low efficiency of tumor delivery is likely an outcome of a combination of factors, such as the presence of physical and physiological tissue barriers, clearance of NPs by the mononuclear phagocytic system (MPS), and elevated interstitial fluid pressure (IFP) in tumor extravascular space (Heldin et al., 2004; Ng et al., 2020; Hoshyar et al., 2016; Scodeller & Asciutto, 2020). The combination of inter and intratumoral heterogeneity in hypoxia, the ability of endosomal escape, and penetration of tumor blood vessels and -parenchyma are significant challenges in actively targeted drug delivery. From the translational perspective, nanodrug delivery is further complicated by issues related to the reproducible scale-up of manufacturing and complex regulatory landscape (Rosenblum et al., 2018).

In contrast to EPR-based passive targeting, active targeting, also referred to as affinity (or synaphic or pathotropic) targeting, relies on affinity ligands such as peptides, aptamers, and antibodies (Abs) (Ruoslahti et al., 2010). The targeting ligands bind to specific systemically accessible molecular markers expressed in a target tissue. Affinity targeting allows quantitatively more drugs to be delivered to the tumor site for better efficacy and lower off-target toxicity (Bertrand et al., 2014). The identification of disease-specific markers and developing suitable targeting ligands for clinical application is very challenging. The realization of improved drug delivery with affinity ligands allowed many targeting ligands are undergoing clinical trials with some successes. Three precision antibody-drug conjugates (ADCs) CD30 targeting brentuximab vedotin, HER2 targeting trastuzumab emtansine (T-DM1), and CD22 targeting inotuzumab ozogamicin (CMC-544) are currently approved for cancer therapy (Abdollahpour-Alitappeh et al., 2019). Besides, many active targeting nano-encapsulated chemotherapeutics are undergoing preclinical and clinical testing. Examples of targets of affinity ligands are anti-angiogenic alpha-v integrins, p32, tumor-associated ECM isoforms, aminopeptidase N (CD13), transferrin receptor (TfR), B-lymphocyte antigen (CD19), human epidermal growth factor receptor 2 (HER2), and PSMA (prostate-specific membrane antigen), EGFR (epidermal growth factor receptor), nucleolin, stromal cell-derived factor 1/ C-X-C motif chemokine 12 (CXCL12/ SDF-1)(Shi et al., 2017; Rosenblum et al., 2018; Kaur et al., 2018; Wang et al., 2019; Scodeller & Asciutto, 2020; Simón-Gracia et al., 2018b; Hunt et al., 2017; Venning et al., 2015; Lingasamy et al., 2020b; Lu et al., 2017). The peptides offer advantages such as small size, low immunogenicity, cost-effective and scalable synthesis, and ease of multivalent presentation on NPs. Peptide-targeted NPs have been used for tumor-targeted delivery in numerous preclinical models (Le Joncour & Laakkonen, 2018; Pemmari et al., 2020b; Mishra & Panda, 2019; Zhao et al., 2020; Lingasamy & Teesalu, 2020).

2.2. Tumor homing peptides: discovery and applications for precision tumor delivery of drugs and imaging agents

2.2.1. Vascular heterogeneity of tumors

Recognition that tumor growth requires a supply of oxygen and nutrients inspired Judah Folkman in 1971 to postulate the requirement for inducing the growth of tumor neovessels for solid tumors to grow beyond 1–2 mm^3 (Sherwood et al., 1971). This new vessel formation, angiogenesis, is a hallmark of tumor growth and progression (Ruoslahti, 2002; Hanahan & Folkman, 1996). Unfortunately, the pharmacological modulation of angiogenesis cascades and vascular status to "starve tumors to death" has not proven as successful as initially hoped for (Kremer et al., 2017; Jain et al., 2006; Kim et al., 1993; Maj et al., 2016). Angiogenic blood vessels are morphologically and functionally different from resting mature blood vessels: they are branched, shaped irregularly, exhibit variable intravascular distances, and are hyperpermeable to plasma components (Tonini et al., 2003; Carmeliet & Jain, 2000). The tumor blood vessels have interconnected endothelial cells (ECs) with no regular mural cell association and prominent vesiculo-vacuolar organelles that contribute to increased leakiness and hyper-permeability phenotype (Jain, 2005; Goel et al., 2011). In addition to the generic, angiogenesis-associated, molecular signature tumor neovessels display molecular markers that depend on tumor type, location, and stage (Joyce et al., 2003; Hoffman et al., 2003). Similarly, the lymphatic vessels express markers that are not present in the healthy lymphatic tissue and tumor blood vessels (Laakkonen et al., 2002; Tammela & Alitalo, 2010). This heterogeneity in tumor vasculature can be targeted with specific affinity ligands for the delivery of drugs, imaging agents, and NPs with reduced off-target side effects (Ruoslahti, 2012).

Tumor vascular signature is due to a combination of generic malignancy-associated and type-specific mechanisms. The tumor ECs are derived from pre-existing local vasculature and circulating marrow-derived endothelial progenitor cells (Rafii et al., 2002). Compared to normal ECs, the tumor ECs are highly dependent on glucose metabolism to support significantly higher proliferation and have cytogenetic abnormalities (Cantelmo et al., 2016; Hida et al., 2004). Vascular supporting cells, pericytes, are less abundant and loosely connected in tumor vessels than in healthy blood vessels (Dudley, 2012), and express lower levels of surface markers such as platelet-derived growth factor receptors (PDGF-R) and NG2 proteoglycan (Song et al., 2005; Stallcup & Huang, 2008). Hypoxia in rapidly growing tumor tissue induces the expression of proangiogenic factors such as vascular endothelial growth factor (VEGF), downregulates the activity of oxygen sensors such as prolyl hydroxylase domain proteins (PHD1–3). Furthermore, hypoxia increases the deposition and remodeling of some types of ECM molecules (Goel et al., 2011; Mazzone et al., 2009; Gilkes et al., 2014). Hypoxia in tumors also induces tumor aggressiveness by promoting malignant progression, angiogenesis, metastasis, and resistance to therapies.

The tumor vessels express a signature of angiogenesis-associated markers such as members of VEGF family, basic fibroblast growth factor (bFGF), angiogenin (Ang), transforming growth factors (TGF) α and β, tumor necrosis factor α (TNF-α), platelet-derived endothelial growth factor (PDGF), granulocyte colony-stimulating factor (G-CSF), placental growth factor (PGF), interleukin-8 (IL-8), hepatocyte growth factor (HGF), delta-like ligand 4 (DII4), matrix metalloproteinases (MMP), integrins ($\alpha v\beta_3$ and $\alpha v\beta_5$), semaphorins (Semas), epidermal growth factor (EGF), and ECM components including splice variants of fibronectin EDB (Fn-EDB), tenascin C FnIII C (TNC-C) and hyaluronan (HA) (Rajabi & Mousa, 2017; Chung et al., 2010; Tonini et al., 2003). Also, the expression of proteins that are expressed in resting cells in intracellular space, such as nucleolin, annexin1, plectin-1, and P32 are induced on the cell surface of malignant and tumor-associated cells (Christian et al., 2003; Fogal et al., 2008; Kelly et al., 2008; Oh et al., 2004). Many pathological conditions that involve angiogenesis, including cancer, inflammation, atherosclerosis, thrombosis, sepsis, vascular leak syndromes, and tissue regeneration, share vascular signatures. Importantly for translational relevance, the tumor neovessels are genetically stable compared to malignant cells that are prone to undergo mutations (Quail & Joyce, 2013; Rak et al., 2002).

2.2.2. Exploration of vascular heterogeneity by *in vivo* peptide phage display

The phage display is a powerful high-throughput method that has been widely used as an unbiased tool to map the molecular landscape of the target and to develop systemic homing peptides for diseases or organ of interest (Pasqualini & Ruoslahti, 1996; Bábíčková et al., 2013). Bacteriophages or phages are bacterial viruses composed of deoxyribonucleic acid (DNA) or ribonucleic acid (RNA) genome encapsulated by nucleocapsid proteins that infect and replicate within bacteria. Phage display is a generally used method for peptide and Abs discovery based on different bacteriophage vectors, including M13, T7, T4, and f1. Peptide phage libraries were first developed by George Smith in 1985, followed by Greg Winter, developing the first antibody phage libraries in 1991(Smith, 1985; Clackson et al., 1991).

The commonly used filamentous M13 phage is a lysogenic phage that contains a single-stranded DNA. In contrast, the T7 lytic phage display consists of the double-stranded DNA exhibits increased stability, increased diversity, and is less prone to mutations during replication. The T7 phage DNA is ~40 kb packed into ~55–60 nm diameter icosahedral head formed by capsid proteins (Fig. 1). For display of exogenous peptides at 1–415 peptides/phage particle, the major coat protein 10A or 10B gene is fused at the C-terminal region with foreign DNA encoding a displayed peptide (Teesalu et al., 2012; Deng et al., 2018; Ruoslahti, 2017). Insertion of randomized DNA fragments allows to have ~10^8 of short peptide sequences displayed on phage particles for biopanning for the discovery

of peptidic affinity ligands (Smith & Petrenko, 1997). The peptide density and particle size of T7 virions are similar to typical clinical NPs, allowing the use of discovered peptides on NPs in preclinical settings.

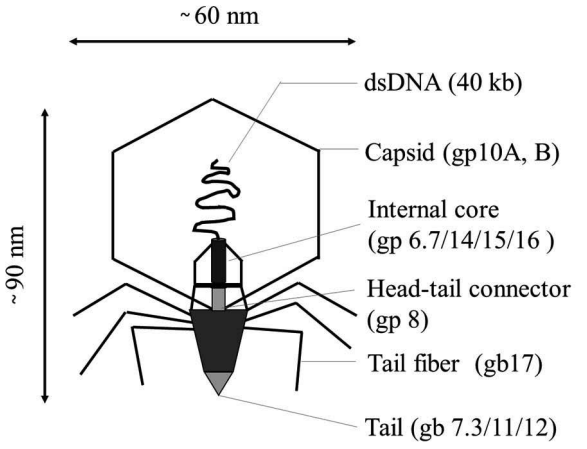

Figure 1. The structure of T7 phage. The genetic material of T7 phage is linear double-stranded DNA protected by capsid head (outer shell) assembled from gp10A and gp10B proteins. The internal core proteins gp14, gp15, gp16 are involved in binding and transformation of phage genomic DNA into *E. coli*.

The tumor-targeting peptides are discovered by phage biopanning using different strategies such as *in vitro, ex vivo,* and *in vivo* selections (Liu et al., 2017). The tumor vascular heterogeneity can be explored by agnostic *in vivo* phage display to identify peptides that target systemically accessible receptors, whereas *in vitro* phage display is used to identify peptides targeting known tumor vascular receptors. The *in vivo* phage display considers the heterogeneity and complexity of living animals and allows unbiased identification of targeting peptides (Pasqualini & Ruoslahti, 1996). For *in vivo* biopanning for tumor homing peptides, the peptide phage libraries (10^8–10^{10} pfu) are injected systemically in tumor-bearing mice; after 10–60 min circulation, the unspecific and unbound phage particles are removed by perfusion (Fig. 2). Finally, the target and control organs are collected for phage quantification and rescue by amplifying phages in *E. coli* for the next biopanning round. The biopanning steps are repeated until enrichment at the target site, and the collapse of diversity of the library are observed.

The candidate peptides can be identified by next-generation sequencing (NGS) to comprehensively assess the representation of individual peptide-phages in different organs and tumors through the screen. The candidate peptides are then synthesized and evaluated for homing as fluorescent peptides and, after successful validation, used as a targeting ligands on the surface of NPs, drugs, and imaging agents for targeted delivery (Matochko & Derda, 2015; Teesalu et al., 2012). Besides the search for malignant disease-targeting peptides, *in vivo* peptide phage display has been applied for the identification of systemic homing

peptides for other diseases and healthy organs (Yang et al., 2011; Mann et al., 2016, 2017; King et al., 2016; Bábíčková et al., 2013; Cureton et al., 2017; Pemmari et al., 2020a; Acharya et al., 2020).

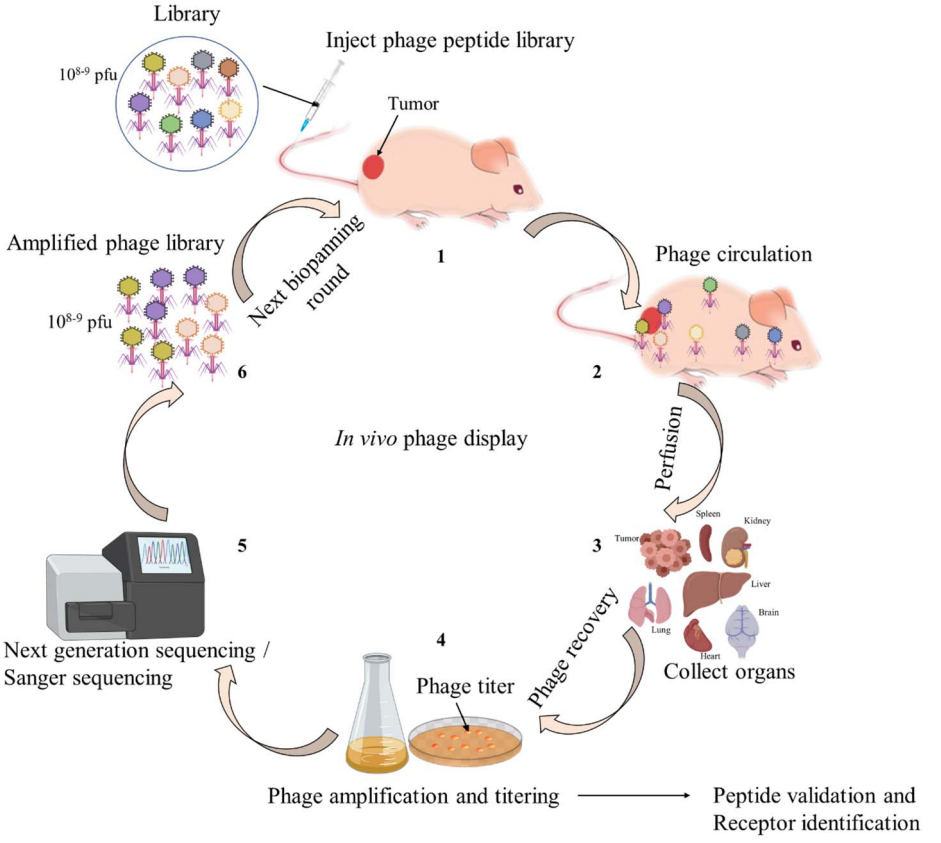

Figure 2. *In vivo* phage peptide biopanning. (1) Peptide phage library is injected through the tail vein of tumor-bearing mice. (2–3) After 10 to 60 min circulation, unspecific peptide phages are removed from circulation by perfusion through the heart, and organs are collected for analysis. (4, 6) The bound peptide phage from the tumors is titered, amplified in *E. coli*, and used as input for the next biopanning round. (5) After biopanning, the peptide-encoding phage genome is subjected to next-generation sequencing, and enriched candidate peptides are individually validated for target specificity. The newly identified synthetic peptides are used for affinity targeting and delivery.

2.2.3. Classes of tumor homing peptides

Over the past years, numerous tumor homing peptides have been discovered that target tumor cell surface receptors, angiogenic tumor vessels, blood vessels, tumor ECMs, tumor-associated macrophages and pericytes, tumor-associated cell such as fibroblast, murine and endothelial cells to achieve tumor-specific payload

delivery in preclinical and clinical settings (Fig. 3)(Saw & Song, 2019; Simón-Gracia et al., 2018a; Zhao et al., 2020; Andrieu et al., 2019; Le Joncour & Laakkonen, 2018).

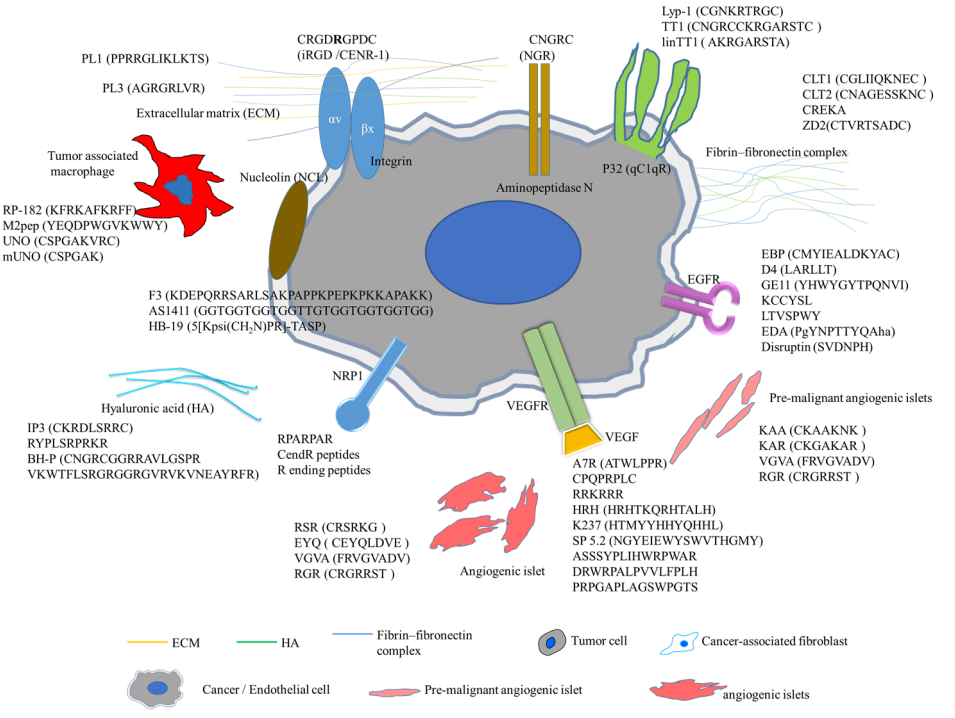

Figure 3. **Overview of tumor homing peptides and their receptors.** Tumor targeting peptides and their receptors are shown within and around the tumor and associated cells. The image was adopted from book chapter (Lingasamy & Teesalu, 2020).

Tumor homing peptides can be classified into two subcategories. First, docking-based tumor homing peptides that use systemically accessible molecular markers in the tumor tissue that are specifically expressed at the surface of the endothelial cells or target extravascular structures at the sites of vascular leakiness. Second, tumor penetrating peptides (TPPs) that trigger a multistep mechanism to allow extravasation and penetration deep into the tumor parenchyma (Teesalu et al., 2013; Ruoslahti, 2017). The TPPs work by the multistep process, described below for prototypic TPP, iRGD (CRGDKGPDC). First, the vascular homing RGD motif binds to tumor-associated systemically accessible receptor molecules (alpha-v integrins); second, the tumor recruited iRGD peptide is proteolytically processed to activate its cryptic C-end Rule (CendR) motif (CRGDK/R). The cleaved peptide loses its affinity for integrins and acquires the ability to bind to neuropilin (NRP-1 and 2)- transmembrane receptors with critical roles in regulating vascular permeability and cellular uptake (Roth et al., 2012). This secondary NRP-1/2 binding activates the CendR pathway for enhanced extravascular transport of drugs into

tumors. Detailed understanding of the iRGD pathway has enabled the development of other TPPs with different primary receptors and activating protease susceptibilities (Braun et al., 2016; Alberici et al., 2013; Paasonen et al., 2016).

2.3. Tumor extracellular matrix as a target for affinity ligands

2.3.1. Extra Domain B of Fibronectin

Fibronectin (FN) is an abundant, multifunctional, and multidomain ECM glycoprotein that has been demonstrated to play roles in survival, proliferation, and invasion of malignant cells (Wierzbicka-Patynowski & Schwarzbauer, 2003). FN is a disulfide-bridged dimer of ~250–280 kD subunits (Ruoslahti, 1988; McDonald, 1988). FN is a modular protein: it consists of three repeated motifs, referred to as type I, II, and III repeats. These contain binding sites for other ECM proteins and cell surface receptors (Kaspar et al., 2006) (Fig. 4). The fibronectin pre-mRNA undergoes alternative splicing during embryogenesis and tumorigenesis to give rise to 20 different variants. "Oncofetal fibronectins" – fibronectin type III extra-domain A (EDA) and extra-domain B (EDB) are overexpressed in most solid tumors and during wound healing but undetectable in normal adult tissues (Tamkun et al., 1984; Schwarzbauer et al., 1983; Pagani et al., 1991; Colombi et al., 1986; Castellani et al., 1994). The FN-EDB and EDA domains have been considered one of the most specific markers of angiogenic blood vessels (van Obberghen-Schilling et al., 2011). Single FN-EDB or EDA null mice show healthy development, but mice lacking both domains of FN show vascular defects that result in embryonic death (Fukuda et al., 2002).

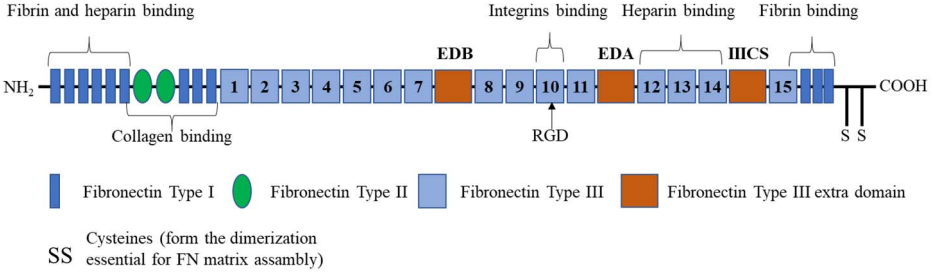

Figure 4. The modular structure of fibronectin. Fibronectin is a large modular protein composed of type I, II and III domains. The three extra-domain type III repeats shown in orange can be either inserted or omitted in the molecule by the mechanism of alternative RNA splicing: EDB, EDA, and IIICS.

The EDB domain was discovered during the experiment of proteolytic cleavage of FN molecules obtained from different tumor sources (Borsi et al., 1985). FN-EDB consists of 91 amino acids encoded by a single exon that is identical in mouse, rat, rabbit, dog, monkey, and human (Neri & Bicknell, 2005). The EDB domain-containing fibronectin is abundantly expressed in many aggressive solid tumors such as breast (D'Ovidio et al., 1998), hepatic (Rybak et al., 2007), pulmonary (Oyama et al., 1990), colorectal (Pujuguet et al., 1996), head and neck carcinoma (Birchler et al., 2003), lymphoma (Schliemann et al., 2009b), glioma (Ohnishi et al., 1998; Teesalu & Lingasamy, 2020; Lingasamy et al., 2019) and melanoma (Frey et al., 2011), but is undetectable in healthy adult tissues (Kumra & Reinhardt, 2016).

The FN-EDB is expressed prominently in the perivascular space, and expression is activated during angiogenesis in the tumors and during wound healing and embryogenesis (Castellani et al., 1994; Kaspar et al., 2006; Schliemann et al., 2009a; Rybak et al., 2007; Villa et al., 2008). The transforming growth factor-beta (TGF-β), glucose levels, and reduced intracellular pH were shown to regulate the alternative splicing to yield the deposition of EDB (Borsi et al., 1990; Khan et al., 2005). Fn-EDB has gained significant interest in the development of ligand-based targeted imaging and for therapeutic applications. During the last decades, various EDB ligands have been identified, including Abs BC-1 and ScFV L19 (Carnemolla et al., 1989; Pini et al., 1998), peptides ZD2 and aptides (APT_{EDB}) (Han et al., 2015; Kim et al., 2012b). These ligands are investigated for their potential applications as targeting vehicles of therapeutic payloads in preclinical and clinical settings. Notably, Neri and his colleagues in Philogen S.p.A. showed Fn-EDB targeting antibody fragment (L19)-mediated delivery of immune cytokines (interleukin 2 (IL 2), IL12, TNF) have anti-tumor activity in various advanced solid tumors with mild reversible toxicities. A combination therapy with drugs or radiotherapy in the clinical trial showed a positive outcome in solid tumor patients (Kumra & Reinhardt, 2016; List & Neri, 2013; Johannsen et al., 2010; Weide et al., 2019).

2.3.2. Tenascin C extra domain C

Tenascin-C (TNC) is a large hexameric multidomain ECM glycoprotein enriched in the stroma of gliomas and mammary tumors (Chiquet-Ehrismann et al., 1986; Bourdon et al., 1983). Whereas TNC is expressed during embryogenesis, most healthy adult tissues are negative for its expression. TNC is expressed abundantly in the stroma of most solid tumors and inflammation (Brösicke & Faissner, 2015). TNC comprises different domains: EGF-like repeats, fibronectin type III domains (FNIII), and fibrinogen globular domain (FBG) domain (Fig. 5). The nine different FNIII domains (A1-A4, B, AD2, AD1, C, D) are differentially included or excluded by RNA alternative splicing between the fifth and sixth constant FN3 domains. The TNC monomer has a molecular weight between 190 and 330 kDa due to differential glycosylation and alternative splicing (Tucker & Chiquet-

Ehrismann, 2015; Midwood & Orend, 2009; Giblin & Midwood, 2015). The large isoforms of TNC are expressed during tissue remodeling, angiogenesis, wound healing, and tumorigenesis of various cancers (Jones & Jones, 2000; Ishiwata et al., 2005). The TNC knockout mice are born alive but exhibit abnormal behavior like impaired mobilization, hyperactivity, and structural aberrations such as compromised lung branching and downregulation of fibronectin (Fukamauchi et al., 1996; Mackie & Tucker, 1999; Roth-Kleiner et al., 2004; Orend & Chiquet-Ehrismann, 2006).

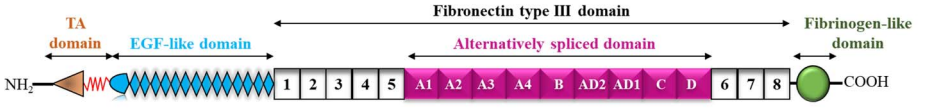

Figure 5. The domain structure of human tenascin-C. The organization of tenascin-C domains illustrated with amino terminus starting with TA domain, 14.5 epidermal growth factor-like domains (EGF)-like repeats, the universal eight constant FNIII domains (FNIII repeats 1–5 and FNIII repeats 6–8), where nine additional domains included in a depending on alternative RNA splicing, and single fibrinogen-like domain at carboxyl end.

The FNIII C domain of TNC-C, a 91 amino acid domain inserted by alternative splicing, is 95% conserved between mice and humans (Joester & Faissner, 1999; Lingasamy et al., 2020b, 2019; Teesalu & Lingasamy, 2020; Lingasamy et al., 2020a). The oncofetal TNC-C domain is highly expressed during embryogenesis, in the stroma of most solid tumors, and in angiogenic vasculature. In contrast, the expression of TNC-C is undetectable in healthy adult tissues by immunohistochemistry and northern-blot analysis (Carnemolla et al., 1999; Tucker et al., 1994; Dörries & Schachner, 1994). The TNC-C strongly expressed in aggressive brain tumors and various carcinomas such as high-grade astrocytoma (grade III), glioblastoma, most of the lung cancers, renal cell carcinoma, malignant melanoma, and urothelial carcinoma. TNC-C domain shows the restricted pattern of expression around angiogenic vasculature, proliferating cells, and tumor stroma with a predominantly perivascular staining pattern (Carnemolla et al., 1999; Silacci et al., 2006; Schliemann & Neri, 2007; Tanaka et al., 2006; Talmadge, 2011).

The upregulation of TNC-C correlates with tumor grade and is associated with poor prognosis in most solid tumors (Talmadge, 2011). The presence of the TNC-C domain is a marker of vascular proliferation in cerebral cavernomas (Viale et al., 2002). Radiolabeled monoclonal antibody targeting the A1-D domain of tenascin C has been used for imaging and radiotherapy in patients with cancer for years (Paganelli et al., 1999; Riva et al., 1999). Various TNC affinity targeting ligands, including single-chain antibody (ScFV) G11, aptamers, and FH peptide, have been identified for targeted tumor payload delivery (cytokines, radionuclides, drugs) (Spenlé et al., 2015; Lingasamy et al., 2020b, 2019).

2.3.3. Hyaluronan

Hyaluronic acid (HA) is a ubiquitously expressed non-sulfated glycosaminoglycan (GAG) discovered in 1934 that consists of an alternatively repeating disaccharide of D-glucuronic acid and N-acetyl-D-glucosamine units (Meyer & Palmer, 1934; Schanté et al., 2011). HA is a ~106 kDa molecule that is synthesized by an integral plasma membrane glycosyltransferase, hyaluronan synthase, and degraded by hyaluronidases (Necas et al., 2008). HA plays an essential role in maintaining the mechanical integrity of the ECM network and in modulating cell growth. HA is critically involved in a wide range physiological, biological functions ranging from control of hydration of tissues and water transport, ECM organization, cell adhesion, migration, mitosis, angiogenesis, morphogenesis, and in disease and tissue repair (wound healing, inflammation, tumorigenesis, and dissemination of tumors) (Simón-Gracia et al., 2018a; Zhang et al., 2018; Necas et al., 2008). HA is a hydrophilic, biocompatible, and non-immunogenic molecule with clinical applications in tissue engineering, arthritis treatment, ocular surgery, drug delivery, and molecular imaging. Importantly, HA and its derivatives have been used to develop drug carriers for the specific and sustained delivery of different classes of therapeutic payloads (Lee et al., 2020; Ikemoto et al., 2017). The overexpression of HA at metastatic sites in ovarian cancer contributes to the peritoneal dissemination, and the HA level correlates with high tumor grade and poor disease outcome (Ween et al., 2011; Zhong et al., 2020). HA is found in the tumor-associated ECM in many types of tumors, and affinity targeting of HA may allow the delivery of drugs and imaging payloads to tumors.

2.4. Peptide targeting of cell surface receptors

2.4.1. Neuropilin-1

Neuropilins (NRPs) are conserved cell surface proteins, first described in neurons, expressed in all vertebrates (Takagi et al., 1987). NRP family consists of two homologous transmembrane glycoproteins, NRP1 (120 kDa) and NRP2 (112 kDa). NRP1 acts primarily as a co-receptor for various secreted ligands such as Semaphorins (SEMAs) (Nakamura & Goshima, 2002), VEGF family, heparin (Mamluk et al., 2002), transforming growth factor-β, hepatocyte growth factor (HGF) (Vivekanandhan & Mukhopadhyay, 2019) and integrins (Goel et al., 2013). The NRP1 knockout results in embryonic lethality due to defects in vascular patterning and development (Takashima et al., 2002; Kawasaki et al., 1999). NRP1 plays an essential role in physiological and pathological processes, including angiogenesis, cardiovascular development, neuronal guidance, immunity, inflammation, and cancer (Staton et al., 2007; Chaudhary et al., 2014). NRP1 is widely expressed in endothelial cells and other cells, and its expression is robustly upregulated in a most of cancers, including prostate cancer (Tse et al., 2017; Teesalu et al., 2009), oral squamous cell carcinoma (Stasikowska-Kanicka et al., 2018), glioblastoma

(Nasarre et al., 2010), breast cancer (Stephenson et al., 2002), gastric cancer (Ding et al., 2018), leukemia (Karjalainen et al., 2011), and melanoma (Huang et al., 2017b). NRP1 plays a functional role in tumor progression by promoting lymphatic metastasis by increased tumor lymphangiogenesis and modulating invasiveness, and thus correlates with tumor stage, progression, and a poor prognosis (Ellis, 2006; Chaudhary et al., 2014; Prud'homme & Glinka, 2012; Niland & Eble, 2019).

A tumor-penetrating peptide motif, containing R/KXXR/K consensus C-end Rule (CendR) motif, binds to the b1b2 domain of NRP-1 and potentiates vascular permeability and trans-tissue transportation (Teesalu et al., 2009; Sugahara et al., 2009). The CendR motif is present in several growth factors, including VEGF-A165, HGF/SF, and semaphorins that bind to the b1 domain of NRP-1 (Acevedo et al., 2008; Becker et al., 2005; Lambert et al., 2009). Targeting NRP1 through the CendR pathway allows enhanced transporting payloads from small molecules, drugs, imaging agents, and NPs deep into a target tissue.

2.4.2. P32 protein

The p32 (also called gC1qR /HABP1/P33/C1qBP) is a trimeric 32 kDa acidic mitochondrial chaperone (Saha & Datta, 2018; Van Leeuwen & O'Hare, 2001; Ghebrehiwet & Peerschke, 1998). In mitochondria, p32 shifts metabolism from oxidative phosphorylation (OXPHOS) to glycolysis (Fogal et al., 2010) and regulates kinase activity (Storz et al., 2000). Interestingly and relevant for affinity targeting, P32 is a multicompartmental protein: it is expressed in mitochondria in quiescent cells and upregulated at the surface of malignancies in endothelial cells (blood and lymphatic), malignant cells, and tumor-associated macrophages (Saha & Datta, 2018). High cell surface P32 expression has been observed in many cancers, including ovarian (Yu et al., 2013) and breast (Chen et al., 2009) carcinoma, and cultured cells of breast cancer (MCF7, 4T1, MDA-MB-231, MCF10-CA1a) (Fogal et al., 2008), endometrial cancer (Zhao et al., 2015), melanoma (MDA-MB-435), prostate cancer (PC3) (Amamoto et al., 2011), and glioblastoma (Agemy et al., 2013; Säälik et al., 2019) origin. In patients, overexpression of p32 in cancer correlated with stage and prognosis in patients (Saha & Datta, 2018). The distinct expression pattern of P32 in cancer and its role in metabolism makes p32 a promising target for therapy and diagnostic application.

Several peptide ligands have been developed to target P32 protein. Lyp-1 (CGNKRTRGC) peptide was the first P32 targeting peptide identified using the *in vivo* phage display (Laakkonen et al., 2002). Another peptide, CGKRK, has shown to use cell surface p32 protein as its receptor (Agemy et al., 2013). Recently, improved P32-targeting TT1 peptide (active both as a disulfide-bridged cyclic CKRGARSTC and as linear linTT1 peptide, AKRGARSTA) was developed by cell-free biopanning on recombinant p32 (Sharma et al., 2017; Paasonen et al., 2016). TT1 peptide belongs to the class of TPPs and thus has additional properties for tumor penetration apart from P32 binding. TT1 peptide first binds in P32 on the cell surface, followed by processing by tumor-associated protease urokinase-

type plasminogen activator (uPA) to expose the CendR motif (AKRGAR to enable NRP-1 binding to trigger vascular exit, parenchymal spreading, and cellular internalization of the peptide (Sharma et al., 2017; Paasonen et al., 2016). The TT1 peptide has been evaluated in preclinical studies for targeting breast, gastric cancers (Hunt et al., 2017; Simón-Gracia et al., 2018b) and glioblastoma (Säälik et al., 2019). Interestingly, linTT1 peptide has also been used for the development of precision nanosystems for targeting macrophages during myocardial infarction (Torrieri et al., 2020).

2.4.3. Integrins

Integrins are a family of structurally related heterodimeric transmembrane proteins built in humans from 18 α and 8 β subunits (Hynes, 2002). Integrins are best-understood cell adhesion receptors with critical roles in embryonic development, innate and antigen-specific immunity, leukocyte trafficking, regulation of cell growth and differentiation, wound healing, hemostasis, signaling, and pathogenesis of many disease states (Shimaoka & Springer, 2003). Integrins interact with many components of the ECM, such as laminin (LAM), paxillin, POSTN, vitronectin, fibronectin, fibrinogen, and collagen, as well as growth factors (e.g., TGF-β) and cell surface receptors (e.g., uPAR). Integrins are expressed in a cell-type-specific manner (Desgrosellier & Cheresh, 2010; Takada et al., 2007). The expression of αvβ3, αvβ5, a5β1, a6β4, a4β1, and αvβ6 integrins regulates migration, proliferation, and survival in many solid tumors, and expression is correlated with disease progression in various tumor types such as colon, non-small-cell lung carcinoma, glioblastoma, pancreatic, prostate, breast, melanoma (Hamidi & Ivaska, 2018).

In the early 80s, Arg-Gly-Asp (RGD) sequence in fibronectin was identified integrin (α5β1, αVβ1, αVβ3, αVβ5, αVβ6, αVβ8, and αIIbβ3) binding motif (Pytela et al., 1985; Pierschbacher & Ruoslahti, 1984). Since then, many different RGD-based peptides and peptidomimetics have been developed to target integrins for tumor-targeted delivery of therapeutics, imaging agents, and NPs.

Among the integrin-binding peptides, the cyclic 9–amino acid iRGD tumor penetrating peptide (clinically developed as CEND-1) is a landmark discovery in precision cancer delivery (Sugahara et al., 2009). Different from monospecific integrin-targeting peptides, iRGD (CRGDRGPDC or CRGEKGPDC) is a modular peptide with both tumor homing and CendR-dependent tumor penetrating properties. The iRGD peptide binding and internalization is a multistep process (involving vascular homing, protease processing, and engagement of tissue penetration receptor NRP-1). The unique feature of iRGD-triggered CendR pathway (endocytic transcytosis and trans-tissue transport pathway) is that it potentiates tumor accumulation and penetration of both chemically conjugated payloads and payloads that have been co-injected with the peptide (Ruoslahti, 2017; Teesalu et al., 2013; Sugahara et al., 2010; Teesalu et al., 2009).

2.5. Nanoparticles in therapeutic and diagnostic use

2.5.1. Clinically approved nanoparticles

NPs possess unique physicochemical properties that can be used to achieve multimodal theranostics applications in cancer. NPs are widely investigated for different applications, such as biosensors, microfluidics, drug delivery, and disease diagnosis, detection, and imaging (Patra et al., 2018). There are over 15 FDA and EMA (European Medicines Agency)-approved NP-based therapeutics and imaging agents for the treatment of malignant diseases (Rosenblum et al., 2018). Inorganic iron oxide-based NP systems such as Nanotherm® (MagForce), Feridex®/ Endorem® (AMAG pharmaceuticals) were approved for superparamagnetic MR imaging of glioblastoma. In 2009, their use was discontinued for cancer treatment but continued to be used for iron deficiency in chronic kidney disease (Anselmo & Mitragotri, 2015; Bashir et al., 2015). NBTXR3/Hensify (NBTXR3) crystalline hafnium oxide (HfO2) metal NPs are used to enhance external radiotherapy of locally advanced soft tissue sarcoma, prostate and lung cancer (Maggiorella et al., 2012; Bonvalot et al., 2019).

Liposomal approved NPs include DaunoXome® (Galen) used for the treatment of Kaposi's sarcoma, Onivyde® (Merrimack) for pancreatic cancer, Doxil®/ Caelyx™ (Janssen) for Kaposi's sarcoma, ovarian cancer, and multiple myeloma (Shi et al., 2017). Vyxeos is a new liposomal system encapsulated with cytarabine and daunorubicin, used to treat adults with newly diagnosed acute myeloid leukemia (Chen et al., 2018). Eligard® (Tolmar) is a leuprolide acetate and polymer-based system for controlled delivery of payload for prostate cancer (Bobo et al., 2016). Abraxane /ABI-007 (Celgene) is an albumin-bound paclitaxel nanoformulation used for breast, NSCLC, and pancreatic cancer (Anselmo & Mitragotri, 2019, 2016; Patra et al., 2018).

2.5.2. Current trends in nanoparticle development

The first generation of approved nanomedicines were simple monofunctional systems, essentially formulation aids, with the key advantage of improving tolerability and reducing the toxicity of the parental chemotherapeutic drugs. All currently approved nanoformulations are nontargeted – for tumor delivery, they rely on the enhanced permeability and retention (EPR) effect. The heterogeneity in the tumor EPR and its extent limits the uses of these nontargeted nanoformulations effects contributing to reduced efficacy (Rosenblum et al., 2018). Coadministration with iRGD peptide and other TPPs described above may overcome this problem and improve the tissue distribution profile of nontargeted NPs for more tumor selectivity. iRGD peptide is undergoing clinical trials as an adjuvant to potentiate paclitaxel and gemcitabine in combination therapy of pancreatic cancer (ClinicalTrials.gov Identifier: NCT03517176, "CEND-1 in combination with Nab-paclitaxel and Gemcitabine in Metastatic Pancreatic Cancer"). Actively

targeted NPs decorated with affinity ligands for tumor-specific target molecules may offer increased efficacy and reduced toxicity, as has been clinically demonstrated with DOX-loaded anti-HER2 immunoliposomes (Park et al., 2002; Kirpotin et al., 2006). Compared to other classes of drug candidates, more NP compounds have entered clinical trials in recent years (Rosenblum et al., 2018; Ventola, 2017).

2.6. Summary of the literature

Clinical utility of most approved anti-cancer drugs and nanocarriers is limited by their low efficacy, off-target dose-limiting toxicities, intrinsic or acquired drug resistance, and tumor relapse. A solid tumor is a complex ecosystem composed of malignant cells, endothelial cells, immune cells, fibroblasts, and noncellular factors. The tumor stroma and ECM are critical components of the tumor microenvironment (TME) that interact with circulatory and lymphatic systems to influence tumor progression, metastatic dissemination, and response to anti-cancer therapies. *In vivo* peptide phage display has been instrumental for the development of tumor-specific affinity ligands and for deciphering the molecular signature on malignant and tumor-associated cells and tumor EC (composed of molecules such as TNC-C, FN-EDB, HA, NRP1, P32, and integrins). The recent availability of tumor homing peptides with tissue penetration properties allows targeting extravascular tumor-associated markers and high capacity cargo delivery to tumor parenchyma otherwise limited to the receptors.

3. AIM OF THE STUDY

Precision targeting of cancer suffers from spatiotemporal heterogeneity, low capacity, and reduced availability of receptors of affinity ligands. We hypothesized that multitargeted peptide ligands could improve affinity tumor targeting for more efficacious cancer therapy. The aim of this thesis was focused on the development of novel multitargeted tumor penetrating peptides against a stable and abundant component in solid tumors, ECM. We have used a panel of strategies and advanced techniques to identify ECM-specific peptidic ligands and to study tumor homing, biodistribution, and therapeutic efficacy of peptide guided NPs on purified recombinant proteins, cultured cells, and *in vivo* animal models.

Specific aims:

1) To identify bispecific peptides that recognize both FN-EDB and TNC-C and carry out preclinical proof-of-concept preclinical studies using newly identified peptides for the development of peptide-targeted anti-cancer nanodrugs and imaging agents (I).
2) To identify bispecific peptides that recognize both TNC-C and NRP-1 and carry out preclinical proof-of-concept preclinical studies using newly identified peptides for the development of peptide-targeted anti-cancer nanodrugs and imaging agents (II).
3) To study the effect of genetic fusion of iRGD TPP to C-terminus of TNC targeting single-chain antibody on its systemic glioblastoma homing and penetration (III).
4) To develop of TT1 peptide-functionalized NPs for glioblastoma targeting (IV).
5) To develop peritoneal carcinomatosis targeting peptides for locoregional IP delivery (V).

4. MATERIALS AND METHODS

The detailed description of the materials and methods presented in this thesis are found in the original publications. This section provides a summary of the methods used in the studies.

The Estonian Ministry of Agriculture, Committee of Animal Experimentation, approved all the experimental procedures that required animal usage under project #42 and #48. The animal experiments performed at the Tel Aviv University were approved by the Institutional Animal Care and Use Committee of the Tel Aviv University.

The Ethics Committee of the University of Tartu approved protocols for obtaining and using fresh surgical human tumor samples from Tartu University Clinics, Tartu, Estonia (permit #243/T27).

4.1. Recombinant proteins and antibody preparation

4.1.1. Recombinant protein preparation

The TNC-C and Fn-EDB domain coding DNA sequences were PCR amplified from human TNC (pF1K, Promega, # FXC00319) and pASK75-Fn7B8/pASK75-Fn789 plasmids. PCR fragments were cloned in pET28a+ plasmid for expression as an N-terminal His-tagged protein and expressed in *E. coli* BL21 Rosetta™ 2 (DE3) pLysS (Novagen, #70956). HiTrap IMAC HP columns (GE Healthcare # 17-0920-05) on the ÄKTA purification system (GE healthcare) or a manual pump were used for protein purification. His-tagged NRP-1 b1b2 domain and P32 proteins were expressed and purified as described previously.

4.1.2. Single-chain antibody preparation

The cDNA sequences encoding FN-EDB-L19-ScFv and TNC-C-G11- scFV were retrieved from US patent applications (US8455625 B2 and EP2157102 A1) and cloned into pET28a+ plasmid for expression in *E. coli* (BL21(DE3) Rosetta pLysS strain). The ScFV proteins were purified by A GraviTrap Sepharose (GE Healthcare # 28-9852-54) column, followed by affinity purification on immobilized proteins. The purified ScFV was analyzed by SDS-PAGE, pull-down assays, and ELISA.

4.1.3. Polyclonal and monoclonal antibody preparation

Rabbits were immunized with recombinant TNC-C, FN-EDB, NRP1 b1b2, and P32 proteins at LabAs LLC (Tartu, Estonia). Rabbit polyclonal antibodies (RPAbs) were purified on protein G columns, followed by affinity purification on respective

immobilized proteins. ELISA and Western blot were used to confirm the specificity of RPAbs. The mice were immunized with recombinant TNC-C, FN-EDB, NRP1 b1b2, and P32 for monoclonal antibody (mAb) production, and hybridoma clones were selected based on ELISA. The purified mAbs were validated using ELISA with respective proteins.

4.2. T7 peptide phage library biopanning

To identify bispecific peptides that interact with TNC-C, FN-EDB, and NRP1, we performed T7 phage binding studies. We used NNK-encoded cyclic CX7C and linear X7 peptide libraries with diversity ~5×10^8 displayed on the T7 415-1b phage scaffold (Novagen, EMD Biosciences, MA, USA). We performed biopanning cross-screens on TNC-C and FN-EDB. The first and fourth rounds of biopanning were performed on 20 µg/ml TNC-C, and Fn-EDB immobilized on the costar 96-Well ELISA plate (#3590, Corning Life Sciences, Tewksbury, MA, USA). To block unspecific binding, 1% BSA in PBS was added to the wells at 4 °C overnight. The peptide phage library (5×10^8 pfu in 100 µl of PBS-BSA) was incubated overnight, followed by 6 washes with PBS containing 1% BSA and 0.1% Tween-20 (washing buffer) to remove background phages. The bound phages were rescued and amplified in the BLT5403 strain of *E. coli* (Novagen, EMD Biosciences, MA, USA).

The subsequent selection rounds were performed on Ni-NTA magnetic agarose beads (QIAGEN, Hilden, Germany) coated with 400 µl His-6X tagged TNC-C or Fn-EDB (30 µg/10 µl beads) in PBS at room temperature for 1 h. The beads were washed and blocked with washing buffer and incubated with 5×10^8 pfu T7 phages in 100 µl in washing buffer at RT for 1 h. The background phages were removed by rinsing 6 times with washing buffer, and bound phages were eluted with 1 ml PBS containing 500 mM imidazole. The eluted phages were titered and amplified for the next round of selection. The random set of clones were selected for Sanger sequencing of peptide-encoding phage DNA. The cell-free binding studies with individual phage clones were performed using Ni-NTA magnetic agarose beads coated with His-6X tagged proteins TNC-C, FN-EDB, and NRP1. The G7 heptaglycine peptide (GGGGGGG) phage (or insert-less phage) were used as negative controls.

To address the specificity of the peptide phage binding to the FN-EDB and TNC-C, we pre-incubated protein-coated NiNTA beads with 20 µg/ml rabbit polyclonal antibodies against FN-EDB and/or TNC-C. For structure-function studies, we performed an alanine scanning mutagenesis by genetically substituting the amino acids in the peptide one-by-one with an alanine residue and tested the effect of the mutations on the binding of peptide-phages to the target proteins.

4.3. Cell lines and cell culture experiments

In this research work, we have used 11 different cell lines that originate from human or mouse tumors (Table 1). The U87-MG (human glioblastoma, HTB-14) cells and PC3 (prostate carcinoma, CRL1435) cells were obtained from ATCC. NCH421K cells from CLS Cell Lines Service GmbH (Eppelheim, Germany). P3, P13 stem cell-like cells were a gift from Rolf Bjerkvig (Bergen, Norway). 005 cells were established from murine GBM, as previously described (Marumoto et al., 2009). M21 cells were a gift from David Cheresh at the University of California San Diego (UCSD). PPC-1 cells were obtained from the Ruoslahti laboratory at Sanford-Burnham-Prebys Medical Discovery Institute (SBPMDI). Human MKN-45P gastric cancer cells were isolated from parental MKN-45 (Koga et al., 2011). Cells were cultured as described in the publications (Lingasamy et al., 2020b; Säälik et al., 2019; Lingasamy et al., 2019; Ikemoto et al., 2017; Bougnaud et al., 2016; Talasila et al., 2013; Keunen et al., 2011).

Table 1. Cell-lines used in the *in vitro* and *in vivo* studies

Cell line name		Application	Publication in thesis
U87-MG	Human glioblastoma	*In vitro* /*In vivo*	I, II, III, IV
NCH421k	Human glioblastoma	*In vitro* /*In vivo*	I, II, IV
P3	Human glioblastoma	*In vivo*	II
P13	Human glioblastoma	*In vivo*	II
WT-GBM	Mouse glioblastoma	*In vitro* /*In vivo*	I, II, IV
VEGF-KO-GBM	Mouse glioblastoma	*In vitro* /*In vivo*	IV
005	Mouse glioblastoma	*In vitro* /*In vivo*	IV
PC3	Human prostate carcinoma	*In vivo*	I, II
M21	Human melanoma	*In vitro*	I, II, IV
PPC-1	Human primary prostate carcinoma-1	*In vitro*	I, II, IV
MKN-45P	Human gastric carcinoma	*In vitro* /*In vivo*	V

4.4. Peptides

Peptides used in this research work (Table 2) were ordered from TAG Copenhagen (Frederiksberg, Denmark) or synthesized using Fmoc/t-Bu chemistry on a microwave-assisted automated peptide synthesizer (Liberty, CEM Corporation, NC, USA). The peptides were purified to 90%–95% purity by high-performance liquid chromatography (HPLC) using 0.1% trifluoroacetic acid (TFA) in acetonitrile-water. The quadrupole time-of-flight (Q-TOF) mass spectral analysis was used

for quality control of the peptides. All peptides were synthesized with free carboxyl termini; 5(6)-carboxyfluorescein (FAM) or biotin was attached via the 6-aminohexanoic acid spacer to the N-terminus of the peptide.

Table 2. Peptides used in *in vitro* and *in vivo* studies in this thesis

Peptide name	Amino acid sequence	Receptor	Publication in thesis	References
PL1	PPRRGLIKLKTS	Fn-EDB, TNC-C	I,	(Lingasamy et al., 2019)
PL5	PPRRGLIKLKTSS NTKENSVVASLRP	Fn-EDB, TNC-C		
PL3	AGRGRLVR	TNC-C, NRP-1	II	(Lingasamy et al., 2020b)
LinTT1	AKRGARSTA	p32	IV	(Paasonen et al., 2016)
IP3	CKRDLSRRC	HA	V	(Ikemoto et al., 2017)
iRGD	CRGDKGPDC	αvβ3 and αvβ5 integrins, NRP-1	III	(Sugahara et al., 2010, 2009)
RPAR	GRPARPAR	NRP-1, NRP-2	I, II	(Teesalu et al., 2009)
ᴅ[KLAKLAK]$_2$	**ᴅ[**KLAKLAKKLAK LAK]	Mitochondrial membrane	I, II, IV	(Ellerby et al., 1999)

4.5. Targeted nanoparticles

Two classes of synthetic NPs (NWs and AgNPs) were used in the studies described in the thesis (Fig. 6). All the nanoplatforms were previously reported to facilitate delivery and imaging applications in tumors (Braun et al., 2014; Willmore et al., 2016; Toome et al., 2017; Hunt et al., 2017; Sharma et al., 2017). We have used IONW for tumor homing, targeted payload delivery, and MRI T2 contrast imaging in publications I, II, and IV. The AgNPs system was used for homing, cellular internalization, quantification, and imaging in laser ablation-ICP-MS in publications I, II, IV, and V.

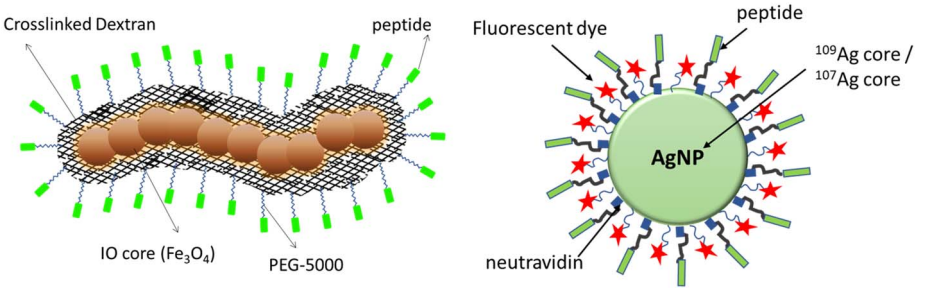

Figure 6. Nanoparticle platforms used in this thesis.

4.5.1. Iron oxide nanoworms

The iron oxide nanoworms (NWs) were prepared as previously described (Park et al., 2008; Hunt et al., 2017) with minor modifications. Briefly, the aminated NWs were PEGylated using maleimide-5K-PEG-NHS (JenKem Technology, TX, USA). Peptides with the thiol group of extra cysteine residue were coupled to the NWs through a maleimide PEG (5000)-NHS linkers (Jenkem, TX, USA). The concentration of the NWs was determined at 400 nm with a NanoDrop 2000c spectrophotometer (Thermo Scientific, Washington, USA) and confirmed by ICP-MS. The size, zeta potential, and polydispersity of NWs were measured using Dynamic Light Scattering (DLS; Zetasizer Nano ZS, Malvern Instruments, UK). The NWs were imaged using Transmission electron microscopy (TEM; Tecnai 10, Philips, Netherlands).

4.5.2. Silver nanoparticles

Silver nanoparticles (AgNPs), including isotopic (Ag^{107} and Ag^{109}) AgNPs, were synthesized and functionalized as previously described (Willmore et al., 2016; Toome et al., 2017; Braun et al., 2014). The CF555-N-hydroxysuccinimide-dye (NHS-dye) or CF647-N-hydroxysuccinimide-dye (NHS-dye) was conjugated to the terminal amine group of PEG. The biotinylated peptides were coated on the NeutrAvidin (NA) on the surface of the AgNPs. The control AgNPs were prepared by blocking a biotin-binding pocket with free D-biotin. The concentration of AgNPs was measured at the 405-nm Ag plasmon peak with a NanoDrop 2000c spectrophotometer. The AgNP image was acquired with transmission electron microscopy (TEM, Tecnai 10, Philips, Netherlands). The zeta potential, polydispersity, and size of AgNPs measured using DLS (Zetasizer Nano ZS, Malvern Instruments, UK).

4.6. *In vitro* experiments

4.6.1. Cell-free peptide-binding assay

The binding of FAM-labeled peptides to target proteins was performed in an enzyme-linked immunosorbent assay (ELISA). The FAM-labeled peptides were immobilized on ELISA plates (Nunc Maxisorp, Thermo Fisher Scientific Inc., MA, USA), blocked with blocking buffer (1% BSA in PBS buffer, 0.1% Tween®-20), and incubated with recombinant proteins at 2 µg/ well in PBS for 6 h. The bound proteins were detected using a primary anti-His-tag antibody and horseradish peroxidase-conjugated secondary antibody. The peroxidase chromogenic reaction was done by adding 100 µL/well of freshly prepared solution from TMB Peroxidase EIA Substrate Kit (Bio-Rad, Hercules, CA, USA). The absorbance was measured at 450 nm with a microplate reader (Tecan Austria GmbH, Grödig, Austria).

FAM IP3 peptide binding to HA was evaluated using ELISA assay. 200 µg/mL HA (cat. no. 53747; Sigma-Aldrich) in 100 µL PBS was coated on 96 well plates (Corning Life Sciences, Tewksbury, MA, USA) at 4 °C overnight, blocked with 300 µL of blocking solution for 1 h at 37 °C, and washed 3X with PBS. To evaluate the specificity of IP3, the immobilized HA was treated with 20 µg untreated hyaluronidase (HAase) or heat-inactivated HAase (100 °C for 10 min) at 37 °C for 2 h. The wells were incubated with 10 µg peptide/well at RT for 4–6 h, washed, and incubated with a blocking buffer. Rabbit anti-FAM primary antibody and rabbit-HRP secondary were added sequentially at 37 °C for 1 h to detect the peptide binding. The peroxidase reaction was performed with the substrate, and absorbance was measured at 450 nm with a microplate reader.

4.6.2. Cellular binding and internalization of nanoparticles

The peptide binding and cell internalization of AgNPs was studied in 3 different cell lines: U87-MG, PPC1, and M21. The cells were cultured on glass coverslips until 80% confluency. The cells were incubated with peptide conjugated CF555-labeled AgNPs (PL1-AgNPs, PL3-AgNPs, and Biotin-AgNPs) at 37 °C for 1 h. The background AgNPs were removed by washing with culture medium. To remove surface-bound AgNPs, an etching solution containing 10 mM of $Na_2S_2O_3$ and $K_3Fe(CN)_6$, freshly diluted in PBS, was applied to cells for 3 min.

Confocal microscopy imaging was performed to visualize the AgNPs. The cells on the coverslips were fixed using –20 °C methanol for 1 min. The cells were stained with Alexa Fluor 488-labeled wheat germ agglutinin (WGA) at 1:1000 at RT for 1 h to visualize the cell membrane, and target receptors were stained with respective primary and secondary antibodies.

Cell nuclei were counterstained with 4′,6-diamidino-2-phenylindole (DAPI, Molecular Probes) at 1 µg/mL. Fluoromount-G (Electron Microscopy Sciences,

PA, USA) medium was used to mount the coverslips on microscope slides for confocal imaging (Zeiss LSM 510; Olympus FV1200MPE, Germany).

Flow cytometry was performed to assess the binding and uptake of AgNPs. Briefly, the U87-MG, PPC1, and M21 cells in suspension were incubated with targeted and control AgNPs in the culture medium for 1 h at 37 °C. The cells were washed, and etching was performed with controls. The cells were analyzed using the BD Accuri flow cytometer by monitoring the 555 on channel FL2.

4.6.3. Fluorescence anisotropy assay

To study PL3 peptide-binding saturation and dissociation constant (Kd) for its receptor, we used solution-based fluorescence anisotropy (FA) assay. The FA saturation binding experiments were carried out as described previously (Veiksina et al., 2015, 2014). 100 µl of PBS and 0.1% Pluronic F-127 were added to 96-well flat-bottom polystyrene NBS multi-well plates (Corning, Cat# 3686). The different concentrations of NRP1 b1b2 (0–112 µM) and TNC-C (0–275 µM) proteins were combined with 0.66 µM FMA-PL3 peptide. The total binding and non-specific was measured with or without 500 µM Biotin-PL3 after 24 h incubation at 25 °C in the dark; during incubation, wells were sealed with the moisture barrier (4Titude, Cat#4ti-0516/96). The FAM-PL3 and protein concentration measured by absorbance at 25 °C on a Synergy NEO (BioTek) microplate reader. The plate reader optical module was set 485 nm (slit 20 nm) excitation filter, 528 nm (slit 20 nm) emission filter, and polarizing beam splitting for dual-channel detection. The polarized light and emission intensities from the sample were collected from channels that were parallel ($I_{\parallel}$) and perpendicular ($I_{\perp}$) to the plan of excitation light. Due to the sensitivity of measurements, the grating factor (G-factor) was calibrated with gain adjustment of the photomultiplier tubes using 1 µM fluorescein standard. The total and non-specific binding ligand depletion data were measured for both binding studies. The FA values were analyzed with the widely used equation $FA = (I_{\parallel} - G \cdot I_{\perp})/(I_{\parallel} + 2 \cdot I_{\perp})$ and estimated the binding affinity by the global fitting (Veiksina et al., 2014).

4.7. Animal experiments

Athymic nude mice (Hsd/Athymic Fox1 nu Harlan) were purchased from Envigo (Netherlands) and maintained under pathogen-free standard housing conditions of the Animal Facility of the Institute of Biomedicine and Translational Medicine, University of Tartu (Tartu, Estonia).

4.7.1. Experimental tumor mice

We used orthotopic or subcutaneous human and mouse xenograft tumor models. For orthotropic GBM tumor models induction, the cell lines have grown and maintained as adherent or non-adherent spheroids. The dissociated individual cells (700,000 for U87-MG, WT-GBM, VEGF-KO-GBM, 300,000 for NCH421K, P3 stem cell-like, P13, and 005) in 3 μL PBS were intracranially implanted into mice right striatum (coordinates: 2 mm right and 1 mm anterior to the bregma at 2.5 mm depth). The intracranial tumors were allowed to develop for 10–15 days (U87-MG), 6–7 days (WT-GBM), 12–14 days (VEGF-KO-GBM), 30–45 days (NCH421K), 30–45 days (P3), 35 days (P13), and 10 days (005) before conducting experiments.

For the subcutaneous GBM and prostate carcinoma model, cells were grown in 2D until 80% confluence. 2–9 × 10^6 (U87-MG, PC3) cells in 100 μl PBS were subcutaneously injected into the right flank of 11 to 15-week old male and female nude mice. The subcutaneous U87-MG GBM and PC3 prostate carcinoma tumors were allowed to grow until 100mm^3 before starting the experiment.

4.7.2. *In vivo* playoff phage auditioning

The *in vivo* playoff auditioning of phage was performed for competitive systemic peptide phage homing study with internally controlled in mice bearing tumor xenografts models. The selected candidate phage displaying TNC-C binding peptide and control peptides were individually amplified and purified with PEG-8000 (Sigma-Aldrich, St. Louis, MO, USA) precipitation, followed by $CsCl_2$ gradient ultracentrifugation and dialysis. The peptide phage was pooled at equimolar representation as a cocktail mix and intravenously (IV) injected at 1 × 10^{10} pfu (in 200 μl PBS) in tumor-bearing mice. The cocktail mix was circulated for 2 h, followed by anesthesia and cardiac perfusion with 20 ml DMEM. The tumor and control organs were collected in lysogeny broth (LB) medium containing 1% NP40, and tissues were homogenized using a hand-held homogenizer. The bound peptide phage in the tissue lysates was amplified in *E. coli* and purified with PEG-8000 precipitation. The phage genomic DNA was extracted using a DNA extraction kit (High Pure PCR Template Preparation Kit; Roche, Basel, Switzerland). The phage genomic DNA was subjected to high throughput sequencing (HTS) using next-generation sequencing (NGS) with the Ion Torrent system (Thermo Fisher Scientific, Waltham, MA, USA). The NGS was used to evaluate the representation of different peptides in the input mixture, tumors, and control organs using a custom python script. The script identifies the length of the read, barcodes, and constant flanking residues of the peptide for identification and analysis.

4.7.3. Tumor-targeted delivery and biodistribution studies

We used different mouse models to investigate the tumor homing specificity and targeted delivery of peptide-NWs. FAM-peptide (PL1, PL3, and LinTT1) conjugated NWs or control FAM-NWs (7.5 mg /kg Fe) in PBS were injected IV into the tail vein of mice bearing orthotropic WT-GBM, VEGF-KO-GBM, NCH421K, 005 tumors, or subcutaneous U87-MG and PC3 tumors. After 5 h circulation, intraventricular perfusion was performed with 20 ml PBS/DMEM under deep anesthesia, and the tumors and control organs were collected for further analysis. The Illuminatool Bright Light System LT-9900 (Lightools Research, Encinitas, CA, USA) with a 520 nm band-pass filter was used for *ex vivo* imaging of tissues. The organs were snap-frozen in liquid nitrogen and stored at −80 °C for further analysis.

To study the receptor-dependent homing and specificity *in vivo*, we performed *in vivo* receptor blocking experiment. The tumor mice were preinjected with rabbit polyclonal blocking antibody against FN-EDB and/or TNC-C (30 μg/mouse) 15 min before injection of the peptide targeted NWs. The mice were perfused after 5 h circulation through the heart with PBS/DMEM, and organs were collected and snap-frozen for further analysis.

4.7.4. Immunofluorescence and confocal microscopy

We performed immunofluorescence and confocal fluorescence microscopic imaging to visualize the targeted homing, delivery, analysis biodistribution, and validating targeting receptors. The snap-frozen tumor and control organs were cryosectioned at 8–10 μm and mounted on a Superfrost+ slides. The sections were equilibrated at RT, fixed in 4% paraformaldehyde for 20 min, or in cold methanol (−20 °C) for 1 min, wash in PBST (PBS+ 0.05% Tween 20), blocked with PBST, 5% BSA, 5% fetal bovine serum (FBS), and 5% goat serum for 1 h at RT.

The immunostaining was performed with primary antibodies rabbit anti-fluorescein IgG fragment (cat. no. A889, Thermo Fisher Scientific, MA, USA), rat anti-mouse CD31 (BD Biosciences, CA, USA), mouse anti-human nestin (#MA1-110, Thermo Fisher Scientific Inc.), rat anti-mouse CD31, rat anti-mouse CD11b (cat. no. 553370; 557395, BD Biosciences, CA, USA), rat anti-mouse LYVE-1 (cat. no. 14044382, eBioscience, CA, USA), rat anti-mouse CD68 (#MCA1957A488, Bio-Rad, CA, USA), rabbit polyclonal anti-Ki67 (cat. no. NB500-170, Novusbio, UK), rabbit anti-cleaved caspase-3 (cat. no. 966, Cell Signaling Technology, MA, USA), in-house prepared CF647 (or CF546)-labeled single-chain antibodies ScFV L19 (against FN-EDB) and ScFV G11 (against TNC-C), rabbit anti-p32, rabbit anti-NRP1 b1b2, rabbit anti-TNC-C, rabbit anti-Fn-EDB. The following secondary antibodies were used, Alexa 488 goat anti-rabbit IgG, Alexa 488-goat anti-rat IgG, Alexa 546 goat anti-mouse IgG, Alexa 546-goat anti-rabbit IgG, Alexa 647-goat anti-rat IgG, and Alexa 647-goat anti-

rabbit IgG (all from Invitrogen, CA, USA). Cell nuclei were counterstained with DAPI at 1 μg/ml, mounted on glass slides using anti-fade mounting media Fluoromount-G (Electron Microscopy Sciences, PA, USA). The stained sections were imaged using confocal microscopy (Olympus FV1200MPE, Hamburg, Germany) and analyzed using the FV10 –ASW4.2 viewer, Imaris, and Fiji ImageJ software tools.

4.7.5. Intravital fluorescence imaging

The peptide homing in mice bearing U87-MG xenografts was assessed by *in vivo* fluorescence imaging using the IVIS Spectrum imaging system (PerkinElmer, Waltham, MA). The CF647 AgNPs were intravenously injected via the tail vein to s.c U87-MG tumor mice. The mice were placed in a dark IVIS system imaging chamber under isoflurane anesthesia (2–3% isoflurane and oxygen flow rate of 2 L/min) for imaging. The images were acquired at pre-injection (0 h) and 5 h post-injection with the following parameters: specific excitation filter, 650 nm; emission filter, 665 nm; auto exposure time; binning, medium; the field of view, 12; f/stop, 2). The regions of interest (ROIs) of the whole tumor after tissue background correction were quantitated, expressed as total radiant efficiency [p/s] / [μW/cm²], and an automated spectral unmixing algorithm was used for background tissue autofluorescence correction. The images from 3 animals/ experimental groups were analyzed using Living Image 4.4 software (Caliper Life Sciences, Hopkinton, MA). For *in vivo* the receptor blocking studies, systemic pre-injection of blocking TNC-C and/or NRP1 antibodies (30 μg/mouse) 15 min before injection of the AgNPs was performed. After imaging, the mice were perfused through the heart with PBS/DMEM, and organs were collected for cryosectioning and confocal microscopy.

4.7.6. Magnetic resonance imaging (MRI)

To investigate the potential use of PL1 targeted NWs as tumor detection and as a contrast agent for MRI imaging, the nude mice bearing orthotopic NCH421k GBM were IV injected with NWs (PL1-NWs or control NWs) at 5 mg/kg Fe per injection. The mice were subjected to MRI imaging before NWs injection for pre-scan. Five h after NW injection, the mice were anesthetized with isoflurane and subjected to MRI using a 9.4 Tesla BioSpec 94/21 (Bruker BioSpin MRI GmbH, Ettlingen, Germany) equipped with ParaVision Acquisition 6.0.1 software (Bruker, Ettlingen, Germany). Mice received isoflurane in an oxygen mix (1.5%, flow rate of 200 ml/min) for anesthesia; the body temperature and breathing rate were monitored throughout the experiments. T2* map MGE (Multiple Gradient Echo) sequences were acquired in sagittal and coronal orientations. The following parameters were used during the data acquisition: slice thickness, 0.375 mm (3 slices averaged offline for improved signal/noise ratio); inter-slice gap:

0.375 mm; repetition time: 800; Echo time: 3.5–38.5 ms; flip angle: 50°; the number of axial slices: 128; pixel bandwidth: 292.9; imaging frequency: 400.3; matrix: 256 × 256; magnetic field strength: 9.4. The regions of interest (ROIs) were drawn manually on the images by using image sequence analysis (ISA) tool package (Paravision 5, Bruker), T2 relaxation times calculated using T2vtr fit function y= A+C*exp (–t/T2) (A: absolute bias; C: signal intensity; T2: spin-spin relaxation time) for T2 evaluation. To calculate mean signal intensity in the tumor to a reference region, ROIs were drawn manually on the images at a given echo time (TE). Following intravital MRI, the animals were perfused with PBS to remove blood and background circulating NWs and subjected to postmortem MRI. After imaging, tumors and control tissues were harvested and sectioned for immunofluorescence staining and confocal microscopy.

4.7.7. Multiphoton intravital imaging

To investigate the ability of PL1-NWs to target angiogenic vessels *in vivo*, we induced angiogenesis by intradermal injection of adenoviral vector driving expression of mouse VEGF164 (Ad-VEGF164). Briefly, 2.5×10^{8} PFU were intradermally injected into the left ear of 7–8-week-old female nude mice, and the right ear served as an internal control. The PL1-NW or NW (7.5mg/kg Fe) were IV injected 4 days after induction of angiogenesis and intravital imaging performed after circulated for 24 h. To visualize blood vessels, Texas Red/Evans Blue was IV injected at 30mg/kg. The ear was fixed on the coverslip using a veterinary-grade glue tape, and agarose mold was prepared around the ear for imaging. The body temperature of mice was maintained during the experiment with a heat mat. Intravital imaging was performed with a multi-photon laser scanning fluorescence microscope (Olympus FV1200MPE-BX61WI) equipped with MaiTai DeepSee IR laser (Spectra-Physics) and with XLPLN25x/1.05 NA water-immersion objective (Olympus). The images and videos were acquired at an excitation wavelength of 920 nm, optical sections were taken under identical conditions, and experiments were repeated in triplicates. For immunofluorescence staining and confocal microscopy, the angiogenic ear and control ear was collected, fixed with 4% PFA overnight, followed by overnight incubation with 30% sucrose before freezing with OCT. The 8–10 μm sections were immunostaining with antibodies against ScFvG11 anti-TNC-C or ScFvL19 anti-FN-EDB, endothelial cells (CD31, red), and the nuclei were stained with DAPI (blue).

4.7.8. Laser ablation ICP-MS-based bioimaging and biodistribution studies

To analyze and quantify *in vivo* biodistribution of systemic peptide-AgNPs in tumor mice, we used laser ablation inductively coupled plasma mass spectrometry (LA-ICP-MS) to measure Ag. The isotopically pure Ag^{107}NPs and

Ag^{109}NPs were functionalized with biotinylated peptide (peptide-Ag^{109}NPs) or biotin (biotin-Ag^{107}NPs). The peptide-Ag^{109}NPs and biotin-Ag^{107}NPs were mixed at a 1:1 ratio. The mice bearing orthotopic U87-MG GBM tumor were IV injected and allowed to circulate for 5 h, perfused via the left ventricle of the heart with 20 mL PBS, and Organs were snap-frozen for cryosectioning and ICP-MS analysis. The snap-frozen organs were cryosectioned at 30 μm thickness on Superfrost+ slides and stored at –20ºC.

The sections were thawed and air-dried in a desiccator before ICP-MS. The tissue sections isotopes (^{109}Ag and ^{107}Ag) were mapped with 2-D mapping, and line scans using a Cetac LSX-213 G2+ laser ablation (LA) system equipped with HelEx 2-volume ablation cell, coupled to Agilent 8800 QQQ ICP-MS. The LA-ICP-MS settings were optimized using NIST 612 glass. The ^{13}C, ^{107}Ag, and ^{109}Ag isotopes were monitored with dwell times (9.5 and 14 ms) or (47.5 ms, 95 ms, and 95 ms) corresponding to a duty cycle of 0.05 s. ^{13}C was used as an internal standard to account for differences in the volume (carbon content) of ablated tissue. Multiple parallel line raster scans were performed to generate distribution maps. The raster lines were directly adjacent to each other (with 65 μm offset), and the whole mapping area was ablated. The sample area was around 14 × 8 mm, and the run time for a single sample was ~ 4 h. For ratiometric biodistribution studies, frozen tissue samples were thawed, digested, and analyzed using Agilent 8800 ICP-MS. The Chromium 2.2 and Iolite v3.62 software were used for data reduction, and elemental and isotope ratio maps.

4.8. Experimental tumor therapy

To test the *in vivo* efficacy of peptide (PL1, PL3, and LinTT1) targeted NWs in tumor mice, U87MG 4×10^6 cells in 100 μl PBS were implanted subcutaneously into under the skin of the right dorsal flank of 11–15 week old male nude mice. The tumor volume [calculated with the formula: length × (width x width)/2] and animal weight were recorded every other day until tumor volume reached ~100 mm^3. Animals were randomized into 4 groups (PBS, FAM-$_D$[KLAKLAK]$_2$-NWs, FAM-peptide-NWs, and FAM-peptide-$_D$[KLAKLAK]$_2$-NWs). For the PL1 peptide study, we used 8 animals per group, and for PL3 and LinTT1 studies, 6 mice per group. 100 μl of NWs (at 5 mg/kg body weight of iron) or PBS was IV-injected into mouse tail vein every other day, with 10 injections for PL1 and 8 injections for PL3 and linTT1. Tumor size, body weight, survival, and animal well-being (behavior, appearance, grooming) were recorded during treatment and post-therapy. The digital caliper was used for tumor volume measurement. When the tumor volume reached 1.5 cm^3 (or >10% body weight), the mice were sacrificed, and organs and tumors were excised and snap-frozen for further analysis.

4.9. Overlay assay on clinical tumor samples

We performed the overlay assay to access the binding of the targeted peptide NPs to the human tumor sections. Freshly excised human GBM samples were obtained during surgeries at the Department of Neurosurgery, Tartu University Hospital, Estonia. The tumor tissue samples were snap-frozen in liquid nitrogen and cryosectioned at 8–10 µm. The sections were fixed with methanol, permeabilized with PBST buffer, followed by blocking unspecific sites with blocking buffer (5% BSA, 5% goat serum, 5% FBS in PBST). For the overlay assay, the blocked tissue sections were incubated with 20 µg/slide PL1-NW, PL3-NW, and NW at 4 °C overnight. The tumor sections were washed and blocked with a blocking buffer, followed by immunostaining with rabbit anti-fluorescein, and detection with anti-rabbit Alexa-488. The peptide receptors were stained with mouse anti-TNC-C or ScFV G11 TNC-C-CF555, and ScFV L19 FN-EDB-CF647.

4.10. Statistical analysis

All the statistical analyses performed using GraphPad Prism 6 software (GraphPad Software Inc., CA, USA). The results were shown as mean with error bars indicating either ±SEM or ± SD and otherwise indicated. Student unpaired / paired t-test was used comparing two groups, and the ANOVA test was used for multiple groups comparison. All the statistical analysis $P < 0.05$ was considered significant. The P-values were shown as ns – not significant, * – $P \leq 0.05$, ** – $P \leq 0.01$, *** – $P \leq 0.001$ and **** – $P \leq 0.0001$. The details of the statistical methods used can be found in the experimental section of each publication.

5. RESULTS

5.1. Identification of bispecific TNC-C and FN-EDB binding peptide

(Publication I)

To identify TNC-C and FN-EDB binding bispecific peptides, we employed cross-screening of T7 phage X7 peptide libraries on recombinant human FN-EDB and TNC-C proteins. The first round of selection was performed on TNC-C immobilized on a high protein binding multiwall plate. The subsequent rounds of biopanning were carried out on FN-EDB coated magnetic Ni-NTA beads.

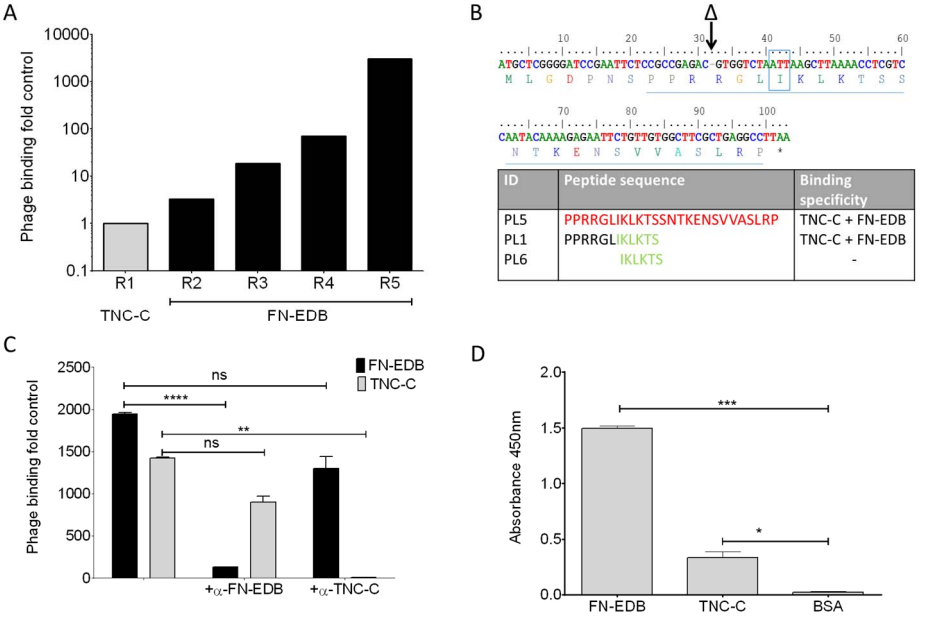

Figure 7. Identification of PL1 bispecific peptide targeting FN-EDB and TNC-C. (A) Biopanning using T7 phage-displayed X7 peptide library on immobilized TNC-C and FN-EDB resulted in ~3000-fold enrichment in binding to FN-EDB in round 5 of selection. (B) Genomic DNA and amino acid sequence of the C-terminal portion of the T7 major coat protein 10 and the adjacent exogenous PL5 peptide (underlined); Arrow indicates single nucleotide deletion in the peptide-encoding DNA. PL5 and its shorter derivative PL1 peptide retain the ability to bind both target proteins. (C) PL1 phage binds to immobilized FN-EDB and TNC-C. The specificity of PL1-phage binding to EDB and TNC-C was evaluated by preincubation of protein-beads with 50µg/ml of anti-FN-EDB or anti-TNC-C blocking antibody. PL1 phage binding is expressed as fold over control phage displaying heptaglycine. (D) Synthetic PL1 peptide interacts with FN-EDB and TNC-C. Immobilized FAM-PL1 was probed with recombinant His-tagged EDB and TNC-C (or control BSA), followed by sequential incubation with rabbit anti–His-tag primary antibody, secondary goat anti-rabbit HRP antibody, and a chromogenic peroxidase reaction. Values represent mean ± SD from 3 independent experiments; P-values were determined by Student unpaired t-test; all statistical tests were two-sided; * $P < 0.05$; ** $p < 0.01$; **** $p < 0.0001$.

At the biopanning round 5, significant enrichment of >1000 fold in phage binding was obtained (Fig. 7A). The randomly selected 48 peptide phage clones from round 5 conferred phage binding to either target alone. Interestingly, a 27-amino acid (aa) peptide PPRRGLIKLKTSSNTKENSVVASLRP (PL5) possessed the desired dual binding ability. The PL5 phage genome harbored a single nucleotide deletion in the peptide-encoding region, resulting in a frameshift and conversion of 7-aa peptide displayed at the C-terminus of the phage major capsid protein to a 27-aa peptide (Fig. 7B). The several shorter derivatives of the PL5 peptide phage were then created, among them a 12-aa peptide that we designated PL1 (PPRRGLIKLKTS). PL1 peptide retained the ability of PL5 to bind to both target proteins when displayed on phage and as a FAM-labeled synthetic peptide (Fig. 7C–D). Function-blocking polyclonal Abs against FN-EDB and TNC-C inhibited the PL1 binding, and PL1 peptide did not interact with other control proteins NRP1 and BSA, demonstrate that PL1 peptide binding is selective for FN-EDB and TNC-C (Fig. 7C).

5.1.1. Systemic PL1-NWs home to solid tumors in mice

We next studied PL1 peptide homing and biodistribution in a panel of GBM and prostate xenograft tumor models. FAM-PL1 or FAM was conjugated to dextran-coated PEGylated paramagnetic NWs and systemically administered into mice bearing orthotopic (NCH421K, WT-GBM) and s.c. (U87MG) GBM, as well as prostate carcinoma (PC3) xenografts. PL1-guided NWs accumulated in the tumor perivascular matrix in all models tested (Fig. 8A–D). After 5 h circulation PL1 targeted NWs showed increased uptake (NCH421K tumors 8.8-fold, U87MG 5-fold, in WT-GBM 3.3-fold, and PC3 4.7-fold over nontargeted particles). In contrast, the control organs (liver, kidney, spleen, and lung) showed similar levels of peptide-guided and non-targeted NW. Uptake of PL1-targeted NWs was specific as coadministration of PL1-NWs with blocking rabbit polyclonal Abs against either FN-EDB or TNC-C, or a combination of both inhibited the uptake (Fig. 8E).

As target ECM components of PL1 peptide are upregulated in angiogenic neovessels, we next studied the contribution of PL1-NW homing on induced nonmalignant angiogenic vessels in mice. To induce angiogenesis, the ears of mice were intradermally injected with an adenoviral vector driving the expression of Ad-VEGF-A[164]. Four days post-injection, both FN-EDB and TNC-C expression was upregulated in angiogenic sites (Fig. 10B). *In vivo* multiphoton imaging showed >3-fold increase in accumulation of PL1-NWs (relative to non-targeted NWs) in the angiogenic vessels, whereas the normal contralateral ear shows no PL1-NW signal. These results show that PL1 acts as an affinity ligand for angiogenic neovessels.

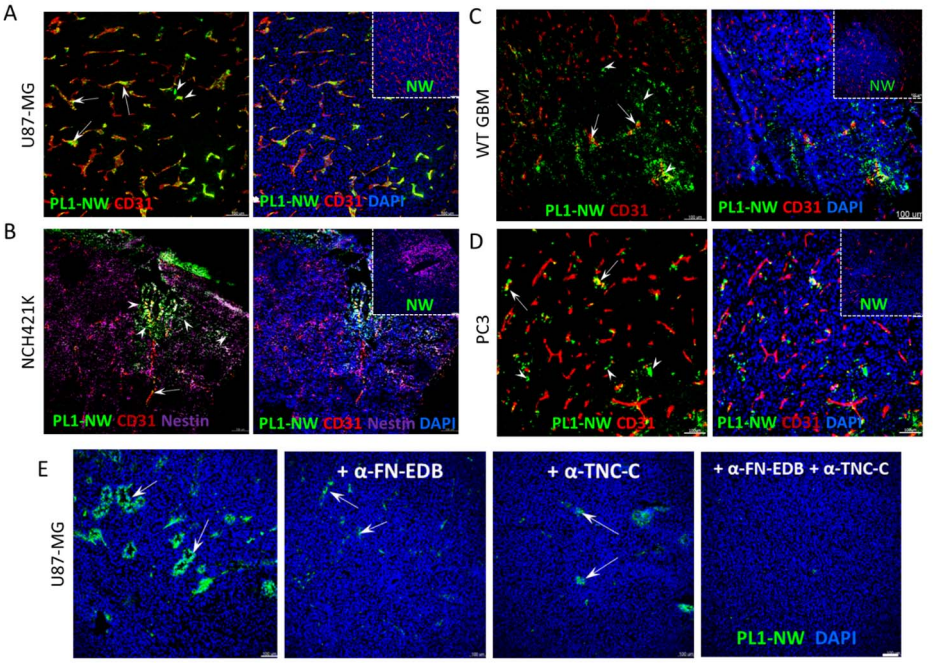

Figure 8. Systemic PL1-NWs home to solid tumor lesions. (A, B, C, D) NWs coated with FAM-labeled PL1 peptide, or FAM only were IV injected at 7.5 mg/kg into mice bearing s.c. U87-MG (A), orthotopic NCH421K (B), orthotopic WT GBM (C) glioblastoma xenografts, and s.c. PC3 human prostate tumors (D). After 5 h circulation, the mice were perfused, and organs were collected. Cryosections were immunostained with antibodies against fluorescein to amplify the NW signal (green), CD31 to visualize the endothelial cells (red), and nestin to label stem cell-like cells (magenta) and examined using confocal microscopy. Images were acquired under the same conditions. Tumor sections from mice injected with control non-targeted FAM-NWs are shown in the boxes. The arrows point to PL1-NWs (green) along the tumor blood vessels, and the arrowheads point to extravasated PL1-NWs. (E) The specificity of *in vivo* homing of PL1 NPs probed with antibody blockade. PL1-NWs (7.5 mg iron/kg body weight) alone or in different combinations with anti-EDB and anti-TNC-C Abs were IV injected into mice bearing U87 xenograft tumors. Five h after the injection, perfused, organs were collected for cryosectioning and examination by confocal microscopy. Arrows point to PL1-NWs (green) in tumor tissue. Nuclei were stained with DAPI (blue). Scale bars, 100 μm.

5.1.2. PL1-NWs as a MR imaging agent

The elongated shape of dextran-coated PEGylated paramagnetic NWs is known to produce a hypointense signal and enhance magnetic relaxivity in T2-weighted MRI (Park et al., 2008). To explore the potential of PL1-NWs as a targeted MRI contrast agent, MRI was carried out on NCH421K GBM mice at the following time points: at pre-injection, at 5 h post-administration, and terminal imaging. In T2-weighted and T2* images of PL1-NW-injected tumor mice, we observed a hypointense signal and a 27–36% increase in T2* relaxation time (from about

23±2 ms at preinjection to 17±1 ms at 5 h, and 14±4 ms at termination) within the tumor lesions. The non-targeted NWs showed no time-dependent changes in signal intensity (relaxation time remained the same (21±5 ms, 22±3 ms, and 20±6, respectively) (Fig. 9A). These results suggest potential applications for PL1-guided contrast agents for tumor detection and imaging.

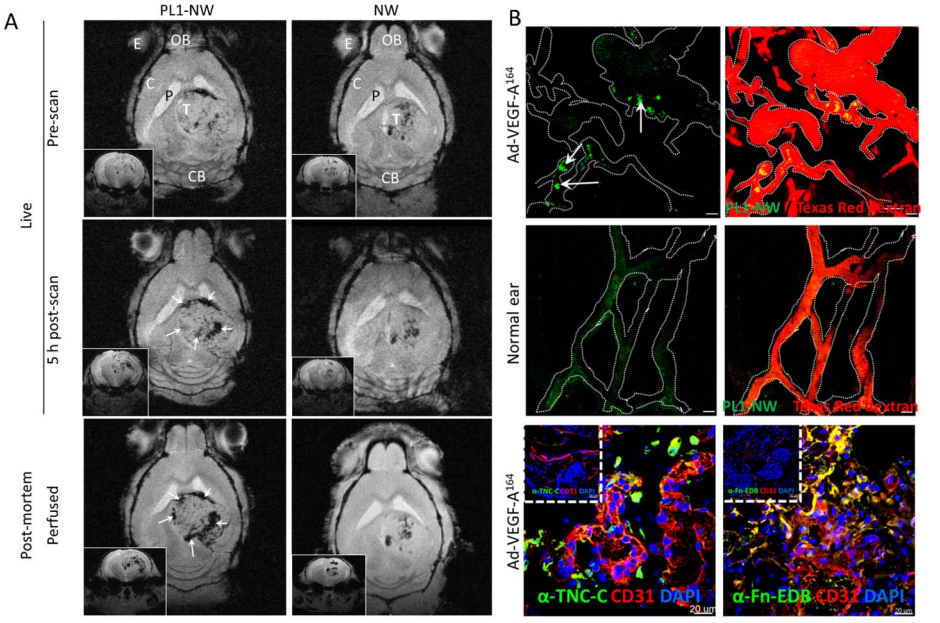

Figure 9. PL1-NWs act as an MRI contrast agent and target angiogenic vessels. (A) PL1-NWs or control NWs (5mg/kg iron) were IV injected into NCH421K glioblastoma mice and subjected to MRI. The top panel images are axial slice views of T2-weighted images before NW injection, the middle images are 5 h after NW circulation (post-scan), and the bottom images are terminal after perfused with PBS (perfused; T, tumor). Arrows indicate increased dark signal in a tumor of a mouse injected with PL1-NWs, but not with control NWs. Insets: coronal T2-weighted views of the same tumor. The images were taken from 3 independent experiments. (B) The left ear of nude athymic mice was intradermally injected with Ad-VEGF-A^{164}; 4 days later, the angiogenic response was apparent, and the animal was injected with PL1-NWs for homing studies and multiphoton imaging after 24 h. PL1-NWs accumulate in the angiogenic blood vessels indicated by arrows, whereas PL1-NWs shows no signal. Green: PL1-NWs or NWs; red: blood vessels stained by Texas Red/Evans Blue, the dashed white lines delineate the vascular tree, and arrows point to PL1-NWs angiogenic vessels. Scale bars: 20 μm. The angiogenic ears were immunostained with antibodies against ScFvG11, recognizing TNC-C (left panel, green), ScFvL19 recognizing FN-EDB (right panels, green), endothelial cells (CD31, red) and the nuclei were stained with DAPI (blue). The control ear shows no expression of TNC-C and FN-EDB (inbox). The representative tissue sections of angiogenic and control ears are shown (N=3), Scale bars: 20 μm.

5.1.3. LA-ICP-MS-based profiling of PL1-AgNPs

To study whether PL1 affinity targeting is independent of the nanocarrier system, we studied the effect of PL1 functionalization on tumor homing of silver nanoparticles (AgNPs) – a model nanoscale platform that we have developed for quantitative biodistribution studies *in vitro* and *in vivo.* To overcome issues related to interanimal differences in the dosing and physiological status of tumors, we injected tumor-bearing orthotopic U87-MG GBM mice with a cocktail of isotopically barcoded PL1-targeted and nontargeted AgNPs. The tissues were subjected to the line- and rasterized laser ablation mapping of the isotopic content by ICP-MS (LA-ICP-MS). The distribution mapping of targeted PL1-Ag^{109}NPs and Ag^{107}NPs showed higher accumulation in the GBM tumor but not in the

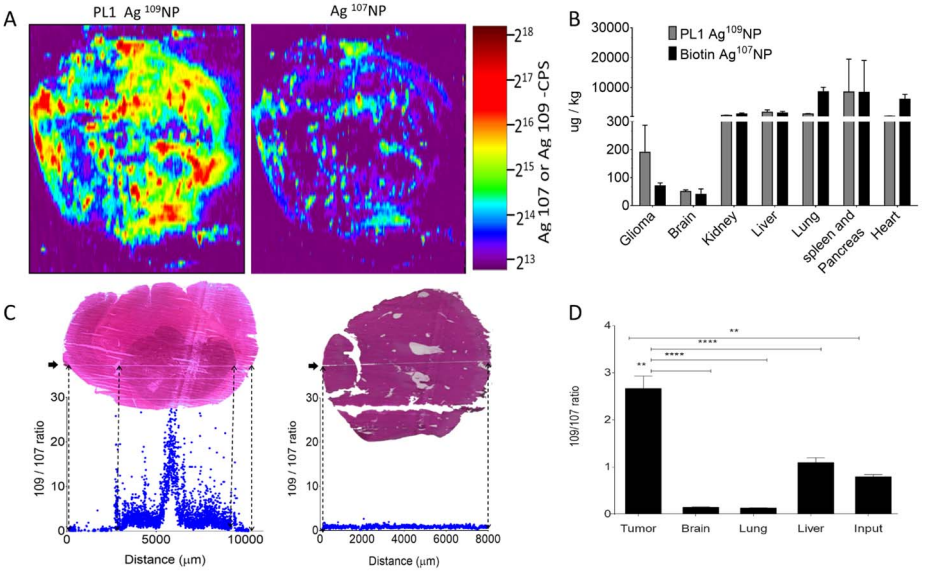

Figure 10. Quantitative distribution analysis of PL1-functionalized and control AgNPs by LA-ICP-MS. An equimolar mixture of targeted PL1-Ag^{109}NPs and control Ag^{107}NPs were IV injected in mice bearing orthotopic U87MG xenografts. After 5 h circulation and perfusion, the organs were collected, snap-frozen, and cryosectioned at 30 µm for LA-ICP-MS. (A) The selected tumor regions were subjected to LA-ICP-MS analysis. The distribution of targeted PL1-Ag^{109}NPs and control Ag^{107}NPs in the tumor, and surrounding brain parenchyma were color scaled according to isotope counts per second. The pixel size was 6.5 × 65 µm. (B) ICP-MS-based quantification of PL1-functionalized and control AgNPs in tissue extracts. The bar chart is showing PL1-Ag^{109} and Ag^{107} in different organs in µg/kg. (C) Laser ablation line scans for Ag^{109}/ Ag^{107} profile using 40 µm spot diameter. The ablation path is indicated by an arrow in H&E-stained glioma brain (left) and control (liver) tissue (right). The blue-dot graphs show the Ag^{109}/ Ag^{107} ratio on the laser ablation path across the tissue. (D) PL1-Ag^{109}NPs tissue distribution based on analysis of Ag^{109}/ Ag^{107} ratio from line scans. PL1-AgNP concentration in glioma is 2.6–30-fold higher than in the control tissues. Data are representative of 3 independent animals. P-value was determined by one-way ANOVA Bonferroni's multiple comparisons test with brain, lung, and liver. Error bars: mean ± SD (n = 3 mice per group, each 5 data points per organ), ** $p < 0.01$; **** $p < 0.0001$. Scale bars: 200 µm.

healthy brain area (Fig. 10A). ICP-MS quantification of tissue extracts demonstrated preferential tumor accumulation of PL1-Ag^{109}NPs (~190 µg/kg of Ag^{109}) over control Ag^{107}NPs (71 µg/kg of Ag^{107}), and similar levels of the two Ag isotopes in the control organs (Fig. 10B). The comparative spatial tissue analysis of Ag^{109}/ Ag^{107} showed intratumoral heterogeneity with some areas showing the Ag^{109}/ Ag^{107} ratio ~30 and above (Fig. 10C). The homing of the PL1-Ag^{109}NPs was tumor-specific, as the Ag^{109}/ Ag^{107} ratio in control organs was close to the input 1:1 ratio (liver), or <1 (in the lung and normal brain) (Fig. 10C). Analysis of the Ag^{109}/ Ag^{107} ratio showed that PL1 functionalization increased AgNP homing to the GBMs on average ~2.7 fold (Fig. 10D).

5.1.4. Proapoptotic PL1-NWs have anti-tumor activity

To evaluate the therapeutic efficacy of PL1 functionalization of anti-cancer NPs, we used as a model nano-drug payload $_D$[KLAKLAK]$_2$ proapoptotic peptide (known to destabilize mitochondrial membranes to trigger apoptosis) in two GBM models (s.c. U87-MG and orthotopic NCH421K). Mice bearing s.c. U87-MG tumor growth was significantly inhibited in the PL1- $_D$[KLAKLAK]$_2$-NW-treated group compared to the negative control group (PBS treated), whereas only a slight reduction in tumor growth was seen in animals treated with PL1-NWs, or $_D$[KLAKLAK]$_2$-NWs (Fig. 11A). In the NCH421k mice treated with PL1-$_D$[KLAKLAK]$_2$-NWs, the median survival was significantly longer than in control mice treated with PBS, FAM-$_D$[KLAKLAK]$_2$-NWs, or PL1-NWs (Fig. 11B).

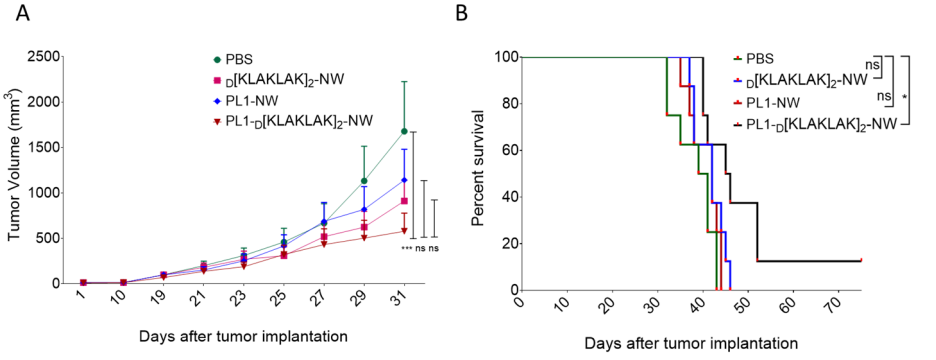

Figure 11. Anti-tumor activity of PL1-targeted NWs in U87-MG and NCH421K GBM models. Mice bearing (A) subcutaneous U87-MG and (B) orthotopic NCH421K xenografts were IV injected with different NWs formulations ($_D$[KLAKLAK] $_2$-NWs, PL1-NWs or PL1-$_D$[KLAKLAK] $_2$-NWs; all at 5mg iron/kg), or PBS. In total, 10 injections were performed every other day (n=8 mice/group). (A) Dynamics of tumor volume in response to treatment with different NWs formulations. Statistical analyses were performed with two-way ANOVA Bonferroni's multiple comparisons test and log-rank test (n = 8 mice/group), error bars: mean ± SEM; ns – $P > 0.05$; *** – $p<0.0001$; (B) Kaplan-Meier survival analysis. Mice bearing intracranial NCH421K tumors showed a statistically significant extension of survival when treated with PL1-$_D$[KLAKLAK] $_2$-NWs compared to other treatment groups.

5.1.5. PL1-NWs bind to clinical GBM lesions

To explore the translational relevance of PL1-NWs, we studied the binding of PL1-NWs to clinical GBM samples. The human GBM tissue sections were overlaid with FAM-PL1-NWs or FAM-labeled control NWs and subjected to confocal imaging. PL1-NWs showed binding to all human GBM samples tested, with binding primarily at perivascular structures as well as deep in the tumor parenchyma (Fig.12). Further, PL1-NWs colocalized with tumor FN-EDB and TNC-C receptors that are highly overexpressed in clinical GBM samples. Control non-targeted NWs exhibited no binding to the tumor sections (Fig.12).

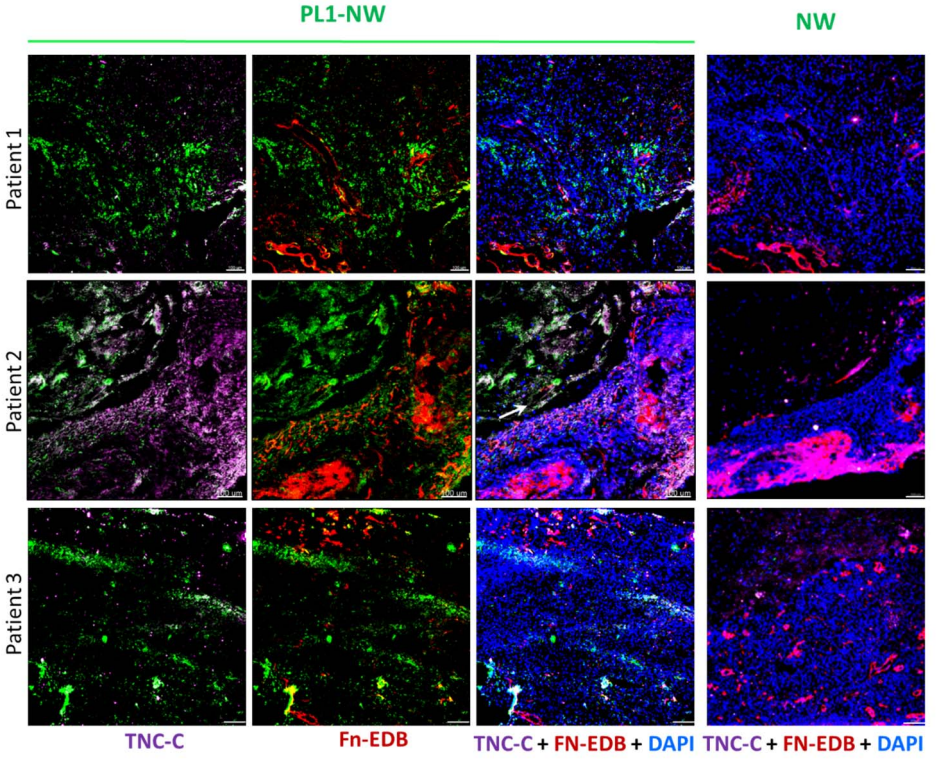

Figure 12. PL1-NWs bind to cryosections of clinical GBM. The cryosections of clinical GBM samples were incubated with PL1-NWs or nontargeted NWs, immunostained, and examined by confocal microscopy. Tissues were stained for FAM (anti-FITC, green), EDB (ScFv L19, red), TNC-C (ScFv G11, magenta), and nuclei (DAPI, blue). Scale bar: 100 μm for all panels.

5.2. Identification of tumor-penetrating peptide targeting TNC-C and NRP1

(Publication II)

The biopanning of CX7C peptide phage libraries against TNC-C resulted in round 5 ~1000-fold enrichment. A random set of 38 peptide phage clones from TNC-C-selected phage pool contained the following predominant motifs: RGRLXR (7 repeats), RGRLR (18 repeats), and RLXR (12 repeats) (Fig. 13A). We created a panel of phages displaying permutations of the RGRLXR motif and audited it using *in vivo* phage playoff in 4 glioma models and 1 prostate cancer model.

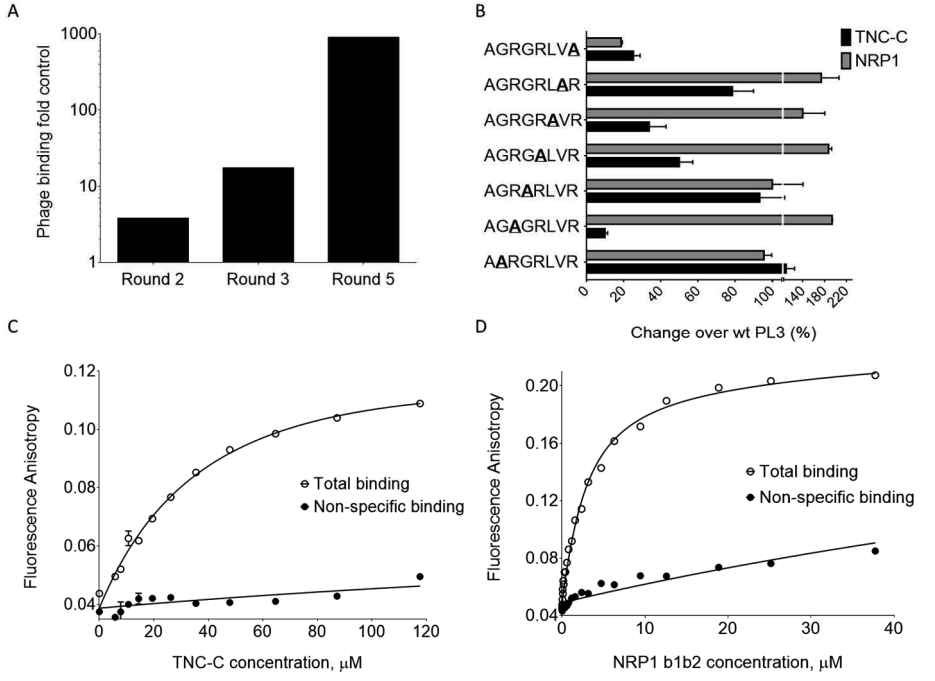

Figure 13. Identification and cell-free binding of PL3 peptide. (A) The CX7C T7 phage library biopanning on TNC-C resulted in ~1000-fold enrichment by the round 5 of selection. Binding is shown fold over control G7 (heptaglycine)-displaying phage. (B) The effect of alanine scanning mutagenesis (alanine substitutions indicated by underlined bold) on interaction of PL3 phage with its receptors TNC-C and NRP-1. The PL3 phage binding to TNC-C and NRP-1 was expressed as a percentage relative to parental PL3 phage. (C–D) The fluorescence anisotropy (FA) saturation curve assay showing FAM-Cys-PL3 binding to TNC-C and NRP1. The 0.66 μM FAM-Cys-PL3 incubated with different protein concentrations in the absence (total binding, open circles) of 0.5 mM Biotin-Ahx-PL3. The FA values were calculated according to FA= (I|| - G·I⊥)/ (I|| + 2·I⊥) and fitted globally after 24 h incubation at 25 °C. The values are shown mean ± SD from 3 independent experiments.

The AGRGRLVR octapeptide (codenamed PL3) was overrepresented in tumors across the models tested. Interestingly, the PL3 peptide contains a C-terminal RXXR motif known to bind to NRP-1. We studied the binding of PL3-displaying phage to NRP-1 and found that the peptide phage binds to NRP-1 >200 fold more than the control phage displaying heptaglycine peptide. Next, we studied the binding of alanine substituted PL3 phage to TNC-C and NRP-1. The alanine substitution of arginine or leucine residues resulted in decreased binding to recombinant TNC-C. The NRP-1 binding was abolished when the C-terminal arginine residue was substituted with alanine (Fig. 13B).

We next used fluorescence anisotropy (FA) assay to determine Kd of PL3 for its receptor proteins. The FAM-Cys-PL3 (1.46 kDa) binding to TNC-C (12.3 kDa) and NRP1 b1b2 domain (37.8 kD) were saturable at different levels due to different rotational mobility of the receptors. The Kd values were calculated by assuming a single binding site with ligand depletion in the global fitting. The Kd of PL3 binding to TNC-C was 51 ± 19 μM (Fig. 13C). Dequenching of the FAM signal after tryptic digestion of the PL3/TNC-C complex suggested the involvement of more than one binding site and lower Kd value. The Kd of PL3-NRP-1 interaction was 1.1 ± 0.2 μM (Fig. 13D), similar to previously published Kd for CendR peptide-NRP-1(Wang et al., 2011)

5.2.1. NRP-1-dependent internalization of PL3-functionalized AgNPs

To explore the binding and internalization of PL3 peptide-functionalized AgNPs, we used 3 cell lines of known PL3 receptor expression status. The U87-MG glioma cells are positive for TNC-C and NRP-1, PPC1 prostate carcinoma cells are positive for NRP-1, and M21 melanoma cells negative for NRP-1. To enable the fluorescence microscopy detection, PL3-AgNPs were labeled with CF555. PL3-AgNPs were strongly bound and endocytosed in U87-MG and PPC1 cells with perinuclear accumulation. The control AgNPs showed only weak background signal in both cell lines (Fig. 14A–B). The M21 cells displayed only a weak background signal that was similar for both PL3-functionalized and control AgNPs (Fig. 14C). The treatment of biocompatible and non-toxic etching solution removes extracellular AgNPs and allows distinguishing extracellular and internalized AgNPs. Removing extracellular AgNPs from U87-MG and PPC1 cells showed only a slight reduction in cell-bound PL3-AgNP signal, suggesting that most of PL3-AgNP were internalized and protected from etching by the cellular membrane. The blocking of the NRP1 receptor by anti-NRP-1 antibody in U87-MG cells abolished PL3-AgNP internalization (Fig. 14D), suggesting that the uptake of PL3-AgNPs in U87-MG cells was NRP-1-dependent.

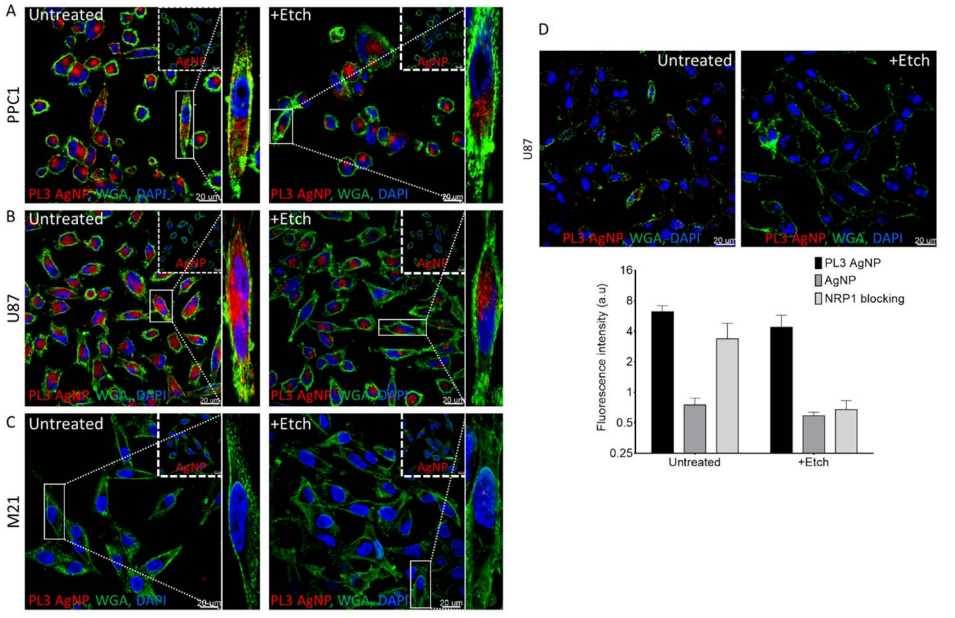

Figure 14. PL3-functionalized AgNPs are taken up in NRP-1-positive PPC1 and U87-MG cells. The U87-MG glioma (A), PPC1 prostate carcinoma(B), and M21 melanoma (C) cells incubated with CF555 labeled PL3-AgNPs, or control AgNP particles for 1h. The cells were washed and treated with an optional hexacyanoferrate/thiosulfate redox-based etching solution to dissolve extracellular particles before confocal imaging. PL3-AgNPs (red) bound to and were internalized in NRP-1-positive PPC1 and U87-MG cells but not in NRP-1-negative M21 cells. The high-magnification images on the right of PL1-AgNP images show binding and internalization. The control particles in the box show negative binding in all cell lines studied. Scale bars: 20 µm in main images, 2 µm in insets. (D) The U87-MG cells were preincubated with NRP1 blocking antibody (30 µg/ml) for 1 h, followed by incubation with PL3 AgNPs (red). The plasma membrane was stained with wheat germ agglutinin (green) and nuclei with DAPI (blue). Scale bars, 20 µm. Quantitation of binding and internalization of CF555-labeled AgNPs using ImageJ. >3 independent experiments were carried out. The error bars show mean ± SD (N=6), and P-values were determined using unpaired Student's t-test (** $P \leq 0.01$).

5.2.2. PL3-nanoparticles accumulate in malignant lesions

The systemic *in vivo* phage playoff experiment showed robust homing of PL3 peptide phages to different solid tumor models. Next, we studied the effect of functionalization with synthetic PL3 peptide on the *in vivo* biodistribution of synthetic NPs. First, we tested the homing of PL3 and control NWs in mice bearing glioma lesions (s.c. U87-MG and orthotopic WT-GBM) and prostate cancer xenografts (PC3 s.c. tumors). Confocal imaging demonstrated that in all the models, PL3-NWs showed tumor tropism, mainly colocalizing or associated with CD31-positive vascular structures (Fig. 15A–C). In some regions, PL3-NWs extravasated

from blood vessels and accumulated in the tumor parenchyma (Fig. 15A–C, arrowheads). Macroscopic imaging showed preferential tumor accumulation of the PL3-NWs in U87-MG tumor mice (Fig. 15D). In the U87-MG tumors, PL3-NWs were found primarily overlapping with immunoreactivities of cognate receptors of PL3 peptide – TNC-C and NRP-1 (Fig. 15E-F, arrowheads).

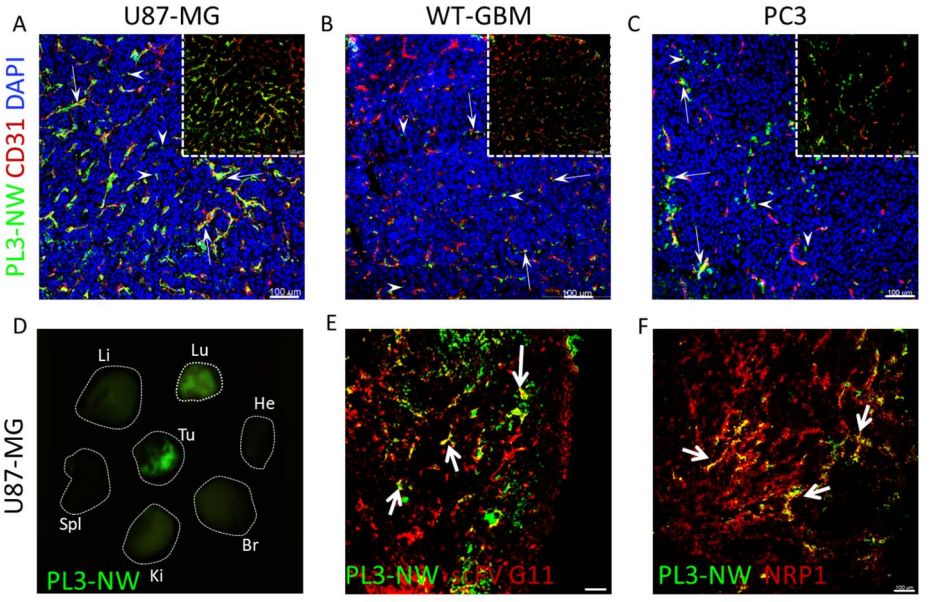

Figure 15. Systemic PL3-NWs accumulate in solid tumors. PL3-NWs or control FAM-NWs were IV injected (7.5 mg/kg) into mice bearing s.c. U87-MG glioblastoma (A), orthotopic WT-GBM glioblastoma (B), and s.c. PC3 prostate carcinoma (C). The animals perfused after 5 h, organs were immunostained with rabbit anti-FAM (green), rat anti-CD31 (red) Abs, and nuclei counterstained with DAPI (blue). In the confocal microscopy image, arrows point to PL3-NWs localization in CD31-positive vessels, and arrowheads showing to extravasated PL3-NWs in the tumor parenchyma. Insets show the image without the DAPI channel. (D) *Ex vivo* macroscopic Illumatool imaging of PL3-NWs IV injected U87-MG tumor and control tissues (green channel, tumor: Tu, brain: Br, Kidney: Ki, spleen: Spl, liver: Li, lung: Lu and heart: He). (E–F) The confocal images of PL3-NWs tumor tissue stained with rabbit anti-FAM (green), anti-TNC-C (red), and rabbit anti-NRP1 (red) Abs. Arrow points to the colocalization of PL3-NW with TNC-C and NRP1 and Scale bar: 100 µm. The representative images shown from 3 independent experiments.

Next, we studied the effect of PL3 peptide functionalization on *in vivo* tumor tropism of near-infrared CF647 dye-labeled AgNPs. The PL3-AgNP or non-targeted AgNPs were systemically injected into s.c. U87-MG mice. Whole-body intravital imaging was performed by the IVIS spectrum at pre-injection and at 5 h post-injection time points. After 5 h circulation, fluorescent surface radiance imaging of PL3-CF647-AgNPs showed ~10-fold accumulation in U87-MG lesions compared to control CF647-AgNPs (Fig. 16A–B). The PL3-AgNP blocking by a

coadministered cocktail of anti-TNC-C and NRP-1 polyclonal function-blocking Abs revealed in near-complete inhibition of the PL3 tumor homing, whereas PL3-AgNP coadministration with single blocking Abs resulted in decreased tumor accumulation (Fig. 16C, D). These results demonstrate the ability of PL3 peptide in precision-targeted delivery and specific tumor homing in different NP systems.

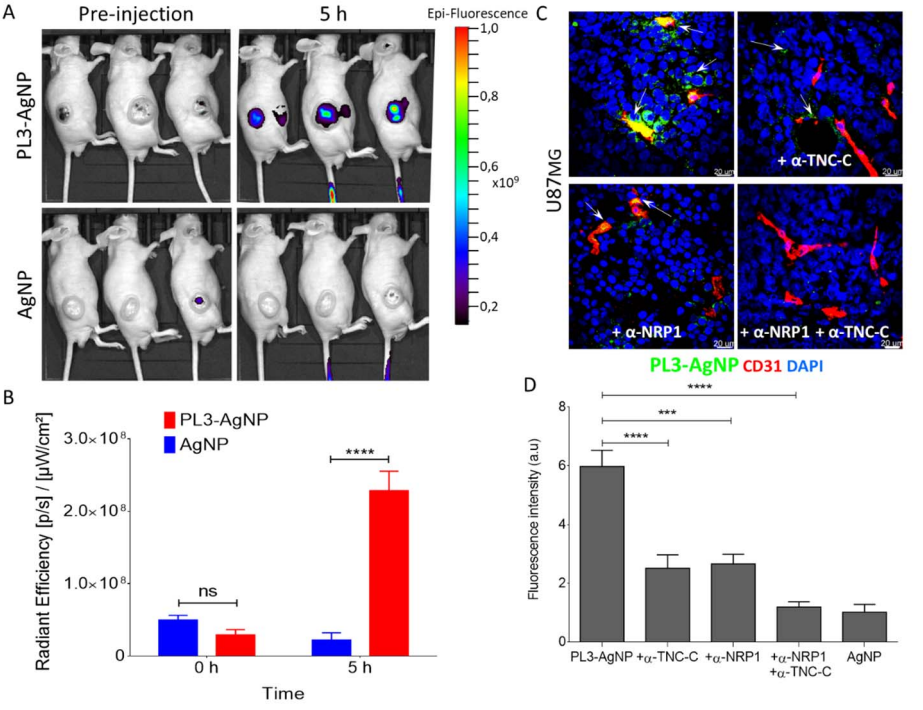

Figure 16. Specific homing of systemic PL3-AgNPs to U87-MG tumors. (A) Alexa-647-labeled PL3-AgNPs and control AgNPs were IV injected into s.c. U87-MG mice (3 mice per group) for *in vivo* imaging. The fluorescence images were taken at pre-injection and 5 h post-injection time points using IVIS Lumina Imaging System. The images are shown after spectral un-mixing. (B) The Alexa-647 signal was quantified from PL3-AgNPs and control AgNPs groups. Y-axis shows Average Radiant Efficiency [p/s]/[µW/cm²], and error bars show mean ± SEM (N=3). P-values were determined using two-way ANOVA, ns, $P > 0.05$; **** $P \leq 0.0001$. (C) The specificity of *in vivo* homing of PL3-AgNPs to s.c. U87-MG tumors were studied by blockade with anti-TNC-C or anti-NRP1 Abs, or both. The confocal imaging of PL3-AgNPs (green), CD31-positive blood vessels (red), and DAPI (blue). (D) The green signal from images was quantified using Fiji ImageJ. The error bars indicate mean ± SEM (N=3 mice per group). The scale bar corresponds to 20 µm and p-values were determined using Student unpaired t-test *** $p \leq 0.001$; **** $p < 0.0001$.

5.2.3. PL3-guided proapoptotic nanoparticles have anti-glioma activity

Having demonstrated specific tumor homing of PL3-displaying biological and synthetic NPs, we next evaluated the therapeutic efficacy of PL3 peptide on proapoptotic $_D$(KLAKLAK)$_2$ peptide-loaded NW in the U87-MG GBM model. The use of s.c. U87-MG allowed monitoring tumor size, rather than survival, as the endpoint (Fig. 17A). The treatment was initiated at 36 days after tumor induction when the tumor volume reached 100 mm^3. During therapy, tumor volume increased rapidly in control (PBS, PL3-NW, and $_D$(KLAKLAK)$_2$–NW) treatment groups. In contrast, tumor growth was significantly delayed in mice treated with PL3-$_D$(KLAKLAK)$_2$-NWs (Fig. 17B). The PL3- $_D$(KLAKLAK)$_2$-NW-treated mice had 50% extension in survival compared to the animals in the other treatment groups (Fig. 17C). These data show that PL3 functionalization improves the therapeutic index of anti-cancer NPs.

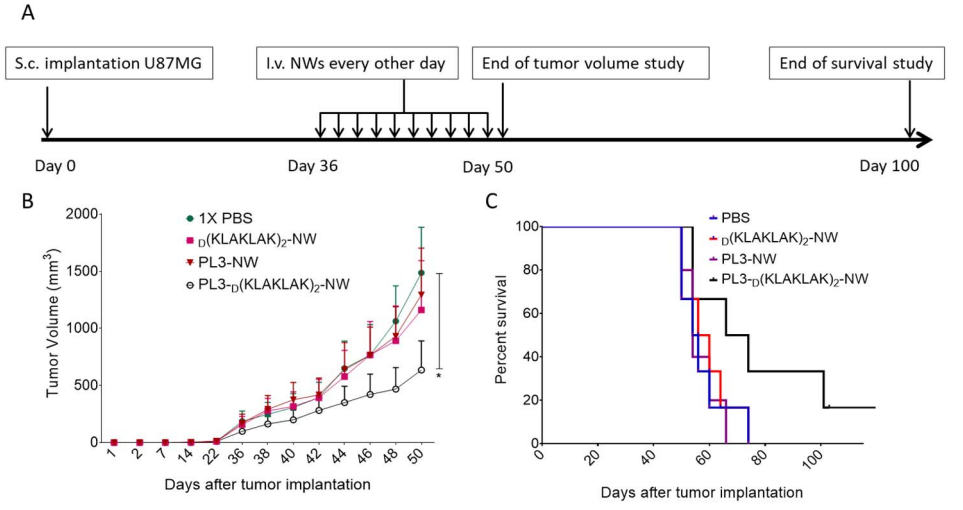

Figure 17. Treatment with PL3-D(KLAKLAK)2-NWs inhibits GBM progression. (A) The flow of tumor treatment study. The treatment of s.c. U87-MG bearing mice with PL3-$_D$(KLAKLAK)$_2$-NW and controls (PL3-NW, $_D$(KLAKLAK)$_2$-NW, and PBS) began when the tumor volume reached 100 mm^3 (on day 36 after tumor induction). The mice were randomized in 6 groups and treated with 10 IV injections (5 mg/kg Fe in 100µl PBS) every other day. (B) The tumor size was recorded daily, and data were analyzed with 2-way ANOVA and log-rank test. Error bars: mean ± SEM; *P< 0.05. (C) Kaplan-Meier survival analysis and body weight were calculated for each group using GraphPad Prism 6 software with p values < 0.05 considered significant.

5.2.4. PL3-NWs bind to surgical explants of human GBM

To address translational relevance of PL3-guided nanosystems, we studied the binding of PL3-NW to clinical GBM lesions. The PL3-NWs or control NWs were overlaid on the GBM cryosections and subjected to confocal imaging. The PL3-NWs bind to TNC-C positive regions in all the tested clinical glioblastoma, diffuse astrocytoma, anaplastic oligodendroglioma, and oligodendroglioma tissue samples (Fig. 18).

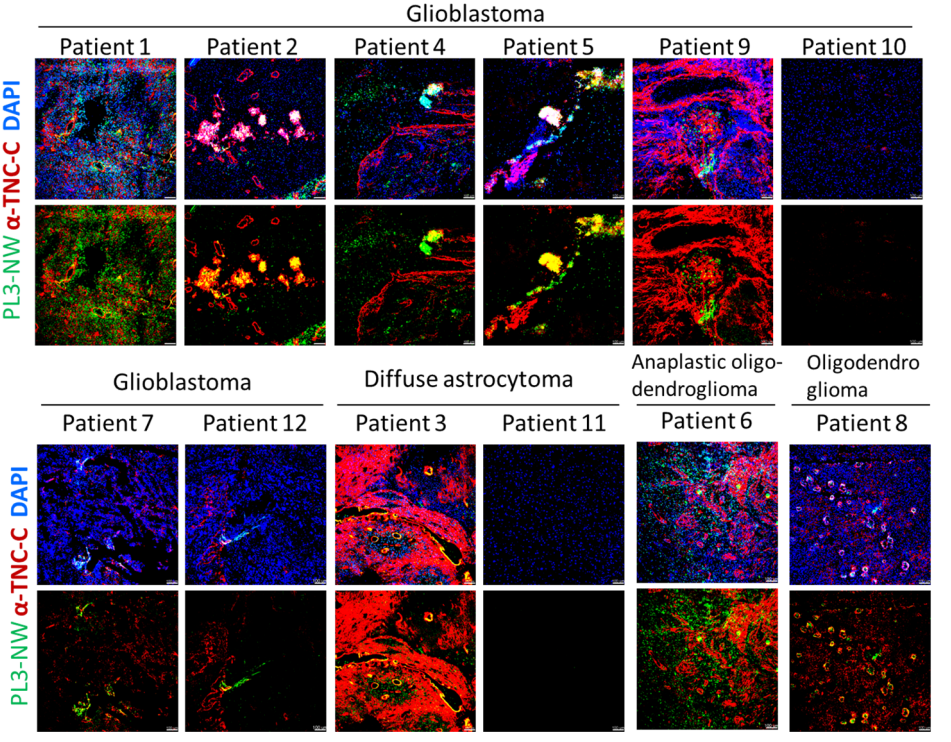

Figure 18. PL3-NWs bind to surgical explants of human glioma tissues. The snap-frozen clinical human glioma tissues were sectioned and incubated with FAM-labeled PL3-NWs or non-targeted NWs, stained with anti-FAM (FITC, green), anti-TNC-C Abs (red) and nucleus (DAPI, blue). Scale bar, 100 μm for all panels.

5.3. iRGD functionalization confers TNC-C-targeting G11 single-chain antibody the ability to bind to angiogenic integrins

(Publication III)

To test if the fusion of TPP to ECM targeting antibody improves its tumor homing and penetration, we fused genetically iRGD tumor penetrating peptide to the C-terminus of TNC-C-targeting ScFV G11 (G11) (Fig. 19A–B). The G11 and

G11-iRGD were labeled with FAM fluorophore for detection in subsequent studies. To evaluate the effects of iRGD fusion and FAM labeling on the G11 binding profile, we performed binding studies using G11 and G11-iRGD on TNC-C and αvβ3 integrins (the primary receptor of iRGD peptide) under cell-free conditions. The G11-iRGD showed an increase in TNC-C binding and ~8-fold higher binding to αvβ3 integrins over control proteins (Fig. 19C). The increased binding was likely due to electrostatic interactions since TNC-C has a net negative charge, and iRGD, after processing into a CRGDK CendR peptide, has a net positive charge. These data show that iRGD fusion and FAM labeling of G11 had no adverse effects on the binding ability to target modules of iRGD-G11 to their cognate receptors.

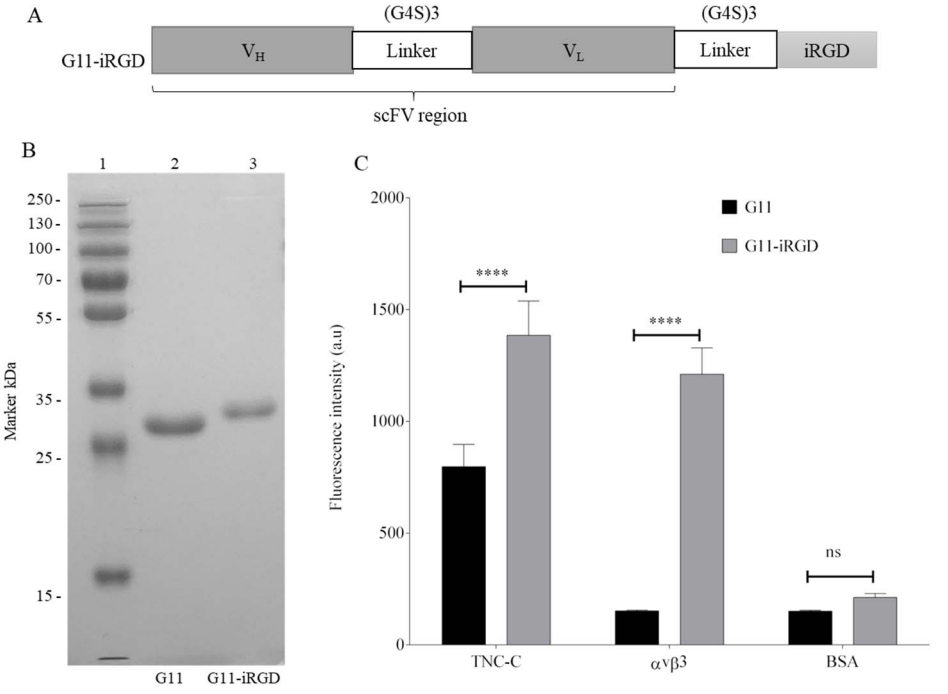

Figure 19. Cell-free binding of G11 and G11-iRGD to integrins and TNC-C. (A) Schematic representation of single-chain antibody constructs. (B) The purified recombinant scFv G11 and scFv G11-iRGD were analysed by SDS-PAGE. The size of molecular weight marker fragments (in kDa) shown on the left. (C) The binding of recombinant G11 and G11-iRGD to immobilized TNC-C and αvβ3 integrins in ELISA assay. The parental G11 binds to TNC-C but not to αvβ3 integrins or control BSA. The iRGD-G11 interacts with both TNC-C and αvβ3 integrins. The data are from 7 independent experiments. The P-value determined using the unpaired student t-test. Error bars: mean ± SEM, **** – $p < 0.0001$; ns – not significant.

5.3.1. Systemic *in vivo* biodistribution and extravasation of G11 and G11-iRGD antibodies

We performed a comparative analysis of G11 and G11-iRGD Abs in s.c. U87-MG mice. The U87-MG tumor model expresses abundant TNC-C and exhibits the upregulation of angiogenic integrins. FAM-G11 or FAM-G11-iRGD were IV injected and circulated for 1–48 h for mapping biodistribution. Confocal imaging demonstrated that the parental G11 antibody is mostly associated with tumor blood vessels and their immediate vicinity (upper rows in Fig. 20A–B). At 24 and 48 h time points, G11 also showed some extravascular FAM signal, likely due to baseline vascular leakiness. In contrast to G11, the FAM G11-iRGD showed extravasation from the tumor blood vessels already at 1 h after injection (bottom rows in Fig. 20A–B), suggesting that iRGD fusion facilitated antibody extravasation and penetration in the malignant tissue.

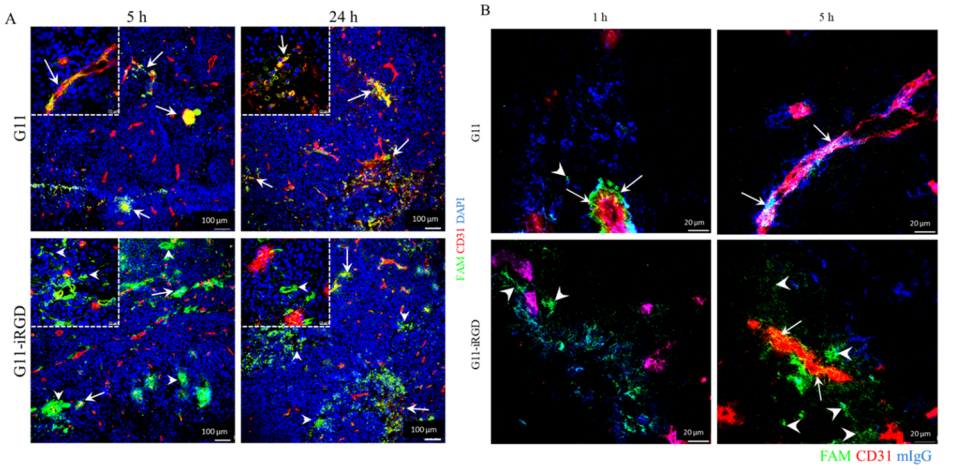

Figure 20. Biodistribution and tumor-specific extravasation of systemic G11-iRGD in U87-MG tumor lesions. (A) FAM-labeled G11 and G11-iRGD Abs were IV injected and organs collected after 1, 5, 24, and 48 h circulation. The tumor cryosections prepared from tissues collected at 5 and 24 h post-injection was stained with anti-FAM (green), vascular endothelial marker anti-CD31 (red), and nuclear counterstain DAPI (blue). Arrows point at tumor blood vessel G11 and G11-iRGD. Arrowheads point at G11-iRGD in the extravascular tumor parenchyma (20 µm in blow-up insets, scale bar: 100 µm, n=3). (B) The s.c U87-MG GBM tumor tissues from 1 and 5 h were stained with primary Abs reactive with fluorescein (green), vascular endothelial marker CD31 (red), and for endogenous mouse antibodies (mIgG) used (blue). Arrows point to scFv signals in blood vessels and arrowheads at sites of extravasation. Scale bars: 20 µm.

5.4. Targeting glioma-associated P32 with linTT1 peptide

(Publication IV)

In resting cells in the adult organism, the p32 protein is expressed intracellularly. However, inactivated cells (e.g., in tumor vascular and lymphatic endothelial cells, tumor macrophages, and malignant cells, as well as immune cells in atherosclerotic lesions) p32 also appears in the plasma membrane (Laakkonen et al.,

2002, 2004; Fogal et al., 2008). The cell surface expression of p32 in GBM lesions in the lentivirally-induced 005 mouse model has previously been documented (Agemy et al., 2013).

However, the broader relevance of the expression of p32 across GBM models and applicability of peptide-based affinity targeting of p32 protein in GBM had not been established. Therefore, we first studied the intratumoral expression of p32 in a panel of orthotopic (WTGBM, VEGF-KO, NCH421k) and subcutaneous (U87-MG) GBM models that represent different invasive/angiogenic GBM phenotypes. In orthotopic WT-GBM, VEGF-KO-GBM, and NCH421k models, we observed p32 expression at the core of the tumor and in the malignant foci (Fig. 21A). In the s.c. U87-MG model, p32 immunoreactivity was present primarily at the rim of the tumor (Fig. 21A). Importantly, p32 expression was upregulated in clinical glioma samples (glioblastoma, diffuse astrocytoma, and oligodendroglioma), with the expression was detected around the blood vessels occasionally, in the bulk of the tumor (Fig. 21B). The expression of p32 in GBM suggested potential applications for the LinTT1 peptide for targeted delivery into the GBM lesions.

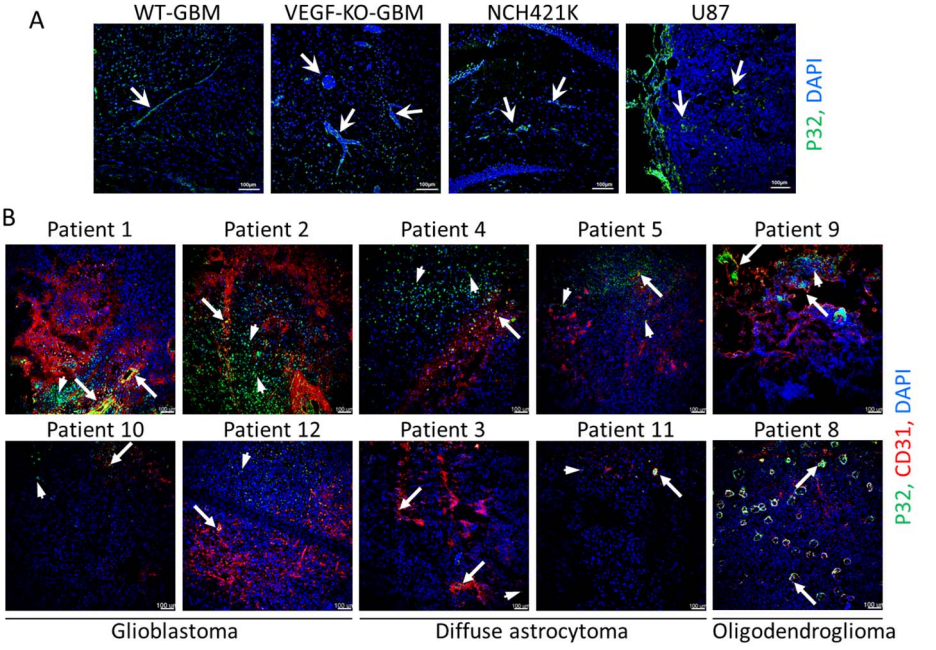

Figure 21. Expression of p32 in mouse GBM models and clinical GBM samples. (A) orthotopic (WT-GBM, VEGF-KO-GBM, NCH421k) and subcutaneous (U87-MG) tumors were cryosectioned and subjected to p32 staining with rabbit anti-p32 antibody (green) and the nuclei with DAPI (blue). (B) The snap-frozen surgical explants of human glioma were sectioned and stained with rabbit anti-p32 antibody (green), anti-CD31-positive blood vessels (red), and nucleus with DAPI (blue). The arrows indicate p32-positive areas in GBM lesions, and scale bars are 100 μm.

For targeting p32-positive GBM lesions, we used LinTT1 tumor penetrating peptide identified using *in vitro* phage display on immobilized p32 (Paasonen et al., 2016). The peptide had been used in the past for the systemic delivery of NPs to triple-negative breast cancer (Sharma et al., 2017; Simón-Gracia et al., 2018b) and for locoregional targeting of peritoneal carcinomatosis (Hunt et al., 2017). NWs functionalized with FAM-LinTT1 or FAM alone were systemically administered into GBM-bearing mice, and tissues were collected for imaging after 5 h circulation. The confocal imaging of LinTT1-NWs showed that ~3–8 fold increased tumor accumulation in the malignant tissue compared to control FAM-NW particles (Fig. 22). In control tissues, both targeted and non-targeted particles were present at similar levels. The data suggested that LinTT1 targeting peptide improves specific homing and delivery across GBM models.

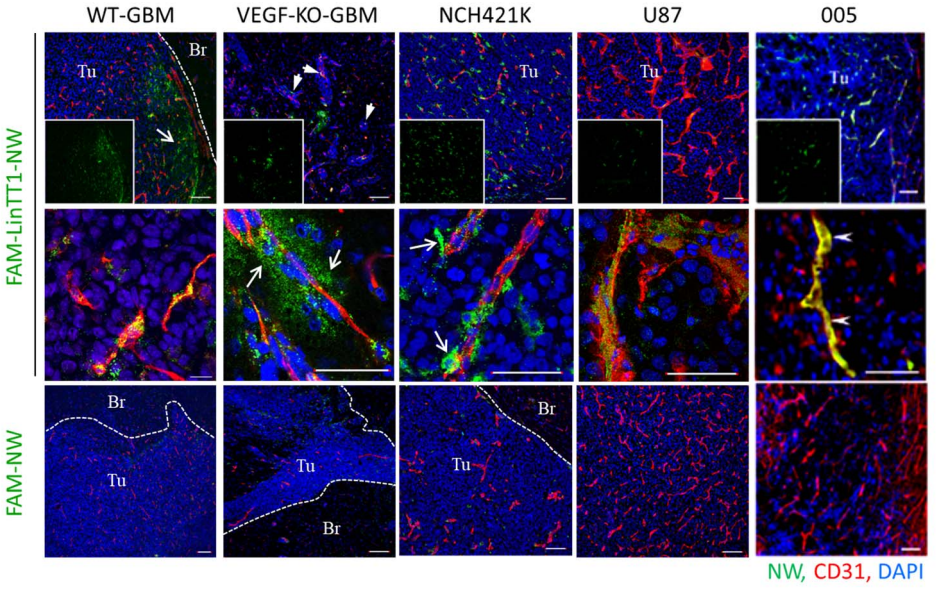

Figure 22. Systemic LinTT1-NWs home to GBM lesions. Mice bearing GBM xenografts of the mouse (005, WT-GBM, VEGF-KO-GBM – intracranial) or human origin (NCH421k – intracranial, U87-MG – subcutaneous) were IV injected with 7.5 mg/kg FAM-LinTT1-NW or FAM-NW. After 5 h of circulation, mice perfused, and organs were collected for cryosection. The sections were stained with anti-FAM (NWs), anti-CD31 (blood vessels), DAPI (cell nuclei), and subjected to confocal imaging. Tu – tumor, BP – brain parenchyma. FAM channel alone shown in insets. Arrowheads indicate the LinTT1-NW signal. Scale bars – 100µm. The middle row panel show 50 µm in high magnification of the LinTT1-NW signal.

We then evaluated the anti-glioma therapeutic potential of LinTT1-functionalized NWs loaded with proapoptotic $_{D}$[KLAKLAK]$_2$ peptide. The amphiphilic proapoptotic peptide D[KLAKLAK]$_2$, known to destabilize the mitochondrial membranes, has been used as an anti-cancer payload in numerous studies (Agemy et al., 2013, 2011; Laakkonen et al., 2004). The experimental GBM therapy with LinTT1-functionalized NWs was performed on s.c. U87-MG and orthotopic 005 GBM models. Compared to control groups, the s.c. U87-MG tumor mice treated with LinTT1-$_{D}$[KLAKLAK]$_2$-NWs showed inhibition of tumor progression and significantly reduced tumor growth (Fig. 23A). Similarly, orthotopic 005 GBM tumor mice treated with LinTT1-$_{D}$[KLAKLAK]$_2$-NWs showed much-improved survival and tumor growth inhibition compared to control-treated groups (Fig. 23B).

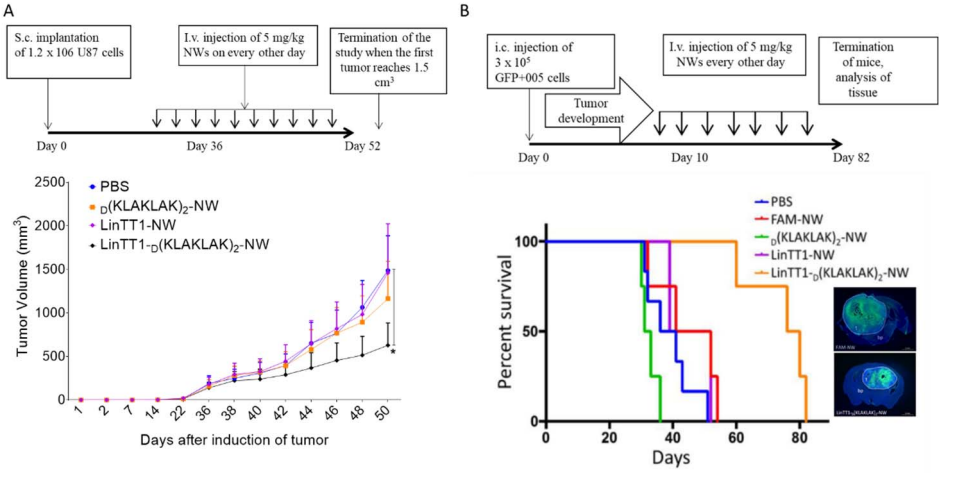

Figure 23. Experimental therapy with LinTT1-D(KLAKLAK)$_2$-NWs inhibits tumor progression in U87MG and 005 GBM models. Mice bearing (A) subcutaneous U87-MG and (B) orthotopic 005 xenografts were IV injected with PBS or of different NWs formulations (NW, $_{D}$[KLAKLAK]^2-NWs, LinTT1-NWs or LinTT1-$_{D}$[KLAKLAK]^2-NWs; all at 5 mg/kg Fe in 100 µl) as illustrated in tumor treatment study design in the top panel. Injections were performed every other day, with a total of eight injections for U87-MG (n=8 mice/group) and seven injections for 005 GBM (n=6 mice/group). Tumor size, body weight, and motor functions were recorded daily, and animals were sacrificed when tumors reached the limits allowed by the animal ethics committee. The tumor volume data were analyzed with a 2-way ANOVA; error bars: mean ± SD; * – $p < 0.01$. The survival data are expressed as Kaplan-Meyer plots. The representative brain section of orthotopic GFP-005 GBM (shown in dotted line) images shown from day 36 and 82 of mice treated with FAM-NW and FAM-LinTT1-$_{D}$[KLAKLAK]^2-NWs. T: tumor, BP: brain parenchyma.

5.5. IP3 peptide interacts with HA

(Publication V)

For identification of peptides for locoregional targeting of peritoneal carcinomatosis, we used *ex vivo* and intraperitoneal *in vivo* biopanning with a T7 peptide CX7C phage library on MKN-45P peritoneal gastric carcinoma. After biopanning, the peptide-encoding phage genome was subjected to High Throughput Sequencing (HTS) with Ion Torrent System. The analysis of next-generation sequencing data with a custom bioinformatics script resulted in the identification of IP1(CDAPRSRRC) and IP3 (CKRDLSRRC) peptides. Upon i.p. administration in MKN-45P mice, the IP3-displaying phage showed better homing than IP1 and iRGD peptide phage (Fig. 24A). Interestingly, the IP3 peptide sequence contains hyaluronic acid (HA)-binding LSRPR motif (Amemiya et al., 2005). The HA is an ECM component prominently upregulated in many solid tumors, including in peritoneal MKN-45P carcinoma. The ELISA based binding assay showed that FAM-labelled IP3 peptide was able to bind to immobilized HA ~6.4-fold higher than the control G7 peptide (Fig. 24B).

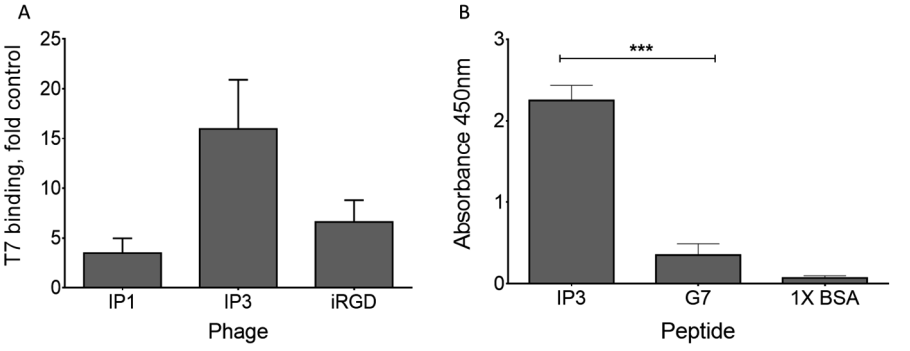

Figure 24. IP3 peptide homes to MKN-45P tumors and interacts with HA in a cell-free system. (A) The candidate peptide phages (IP1 and IP3) and control phages (iRGD and insertless) were evaluated for i.p. *in vivo* homing to MKN-45P peritoneal tumors in mice. The phage titers are expressed fold-over insert less control phage. Error bars: SEM, n = 3. (B) IP3 peptide binds to immobilized HA. HA-coated ELISA plates were incubated with FAM-IP3 peptide for interaction and bound peptide detected with anti-FAM antibody as a primary antibody, rabbit-HRP conjugate as a secondary antibody, and a chromogenic reaction. Statistical analysis was performed by Student unpaired t-test. Error bars: SEM, n = 8, ***$p < 0.001$.

This interaction was inhibited in a concentration-dependent manner by pre-treatment with 1 mg hyaluronidase (HAase) (Fig. 25A). The pretreatment with heat-inactivated HAase did not inhibit the IP3 binding to HA (Fig. 25B).

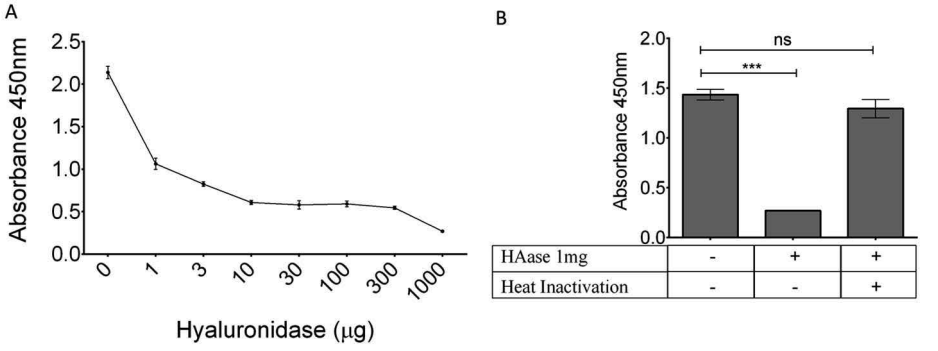

Figure 25. Hyaluronidase activity inhibits the IP3 peptide binding to HA. (A) HA was pre-incubated with different concentrations of hyaluronidase at 37 °C for 2 h, immobilized to ELISA plate, and incubated with FAM-labelled IP3 peptide. The IP3 was detected with anti-FAM antibody, rabbit-HRP conjugate, and a chromogenic reaction. (B). The HA was incubated with either untreated or heat-inactivated hyaluronidase and was used as a target for IP3 binding. One-way ANOVA performed statistical analysis with GraphPad Software, n = 4, *** $P \leq 0.001$, ns $P > 0.05$.

6. DISCUSSION

6.1. Significance

Various monospecific affinity targeting strategies for cancer delivery have been employed with limited success due to tumor heterogeneity and limited quantities of available receptors. The research work presented in this thesis describes the development of multi-targeted tumor penetrating peptides for simultaneous targeting of two or more markers in the tumor microenvironment to overcome the spatiotemporal heterogeneity in the expression of target molecules and to address the issues related to the limited number of systemically available target receptors. The peptides were identified using cell-free biopanning and validated *in vivo* using a panel of clinically relevant tumor models. Our studies established the preclinical proof of utility for the peptide-guided precision delivery for NPs loaded with anti-cancer payloads and imaging agents to solid tumors. The homing peptides identified in this work are translationally relevant as they are not species-specific and bind to both mouse and human target proteins. These results warrant future efforts on the development of these novel multitargeted homing peptides towards clinical application.

6.2. Main findings

The studies in this thesis resulted in identification of novel multi-targeted peptides and their preclinical evaluation for detection and therapy of solid tumors. We have identified three different tumor-targeting peptides PL1 (PPRRGLIKLKTS), PL3 (AGRGRLVR), and IP3 (CKRDLSRRC) and characterized their receptor interactions. We found that surface functionalization of NPs with these affinity targeting peptides increased their systemic selectivity to solid tumors and improved the therapeutic efficacy of NPs loaded with the anti-tumor payload. Further, we established the utility of previously identified tumor penetrating peptide, LinTT1 (AKRGARSTA), for targeting brain tumors. Finally, we showed that the genetic fusion of iRGD tumor penetrating peptide facilitates extra-vasation and stromal penetration of the complex.

6.2.1. Development of bispecific tenascin-C and fibronectin targeted PL1 peptide for theranostic application in solid tumors

The expression of ECM proteins isoforms TNC-C and FN-EDB are upregulated in most solid tumors but not detectable in non-malignant adult tissues (Khan et al., 2005; Trachsel et al., 2007; Silacci et al., 2006; Carnemolla et al., 1999; Park et al., 2012). Compared to receptors expressed on the surface of malignant cells, TNC-C and FN-EDB provide a more stable and high capacity target for affinity

ligands (Lingasamy et al., 2019; Järveläinen et al., 2009). Monospecific affinity ligands for FN-EDB ScFV L19 (Nilsson et al., 2001), ZD2(Han et al., 2015)) and TNC (ScFV G11 (Silacci et al., 2006), TNC aptamer (Daniels et al., 2003), and TNC-binding FHK peptide (Kim et al., 2012a) have been applied for precision delivery of solid preclinical tumors. Importantly, some of the ligands have reached clinical testing for tumor delivery of cytokines (e.g., IL2, TNF) and radionuclides (Kumra & Reinhardt, 2016; Spenlé et al., 2015).

Using the T7 phage display, we have identified 12 amino acid peptide PL1 (PPRRGLIKLKTS) that targets both FN-EDB and TNC-C. The systemic PL1 NWs and AgNPs selectively accumulated in a receptor-dependent manner in GBM and prostate carcinoma lesions. Further, based on our previous studies (Toome et al., 2017; Willmore et al., 2016), we adopted LA-ICP-MS based 2D mapping for parallel visualization of isotopically barcoded peptide AgNPs and control AgNPs. This ratiometric analysis demonstrated that PL1 targeted AgNPs show brain tumor-specific accumulation with very low baseline uptake in the healthy brain. Interestingly, we observed the internalization of PL1 peptide-guided AgNPs in cultured U87-MG cells. In follow-up studies, we aim to establish details of the PL1 peptide-mediated internalization pathway.

The FN-EDB and TNC-C are known markers for angiogenesis. Using the angiogenesis model induced by intradermal injection of VEGF-driving adeno-virus, we showed by intravital multiphoton microscopy that in live mice, PL-NWs home to angiogenic vessels suggesting applications for diseases that involve aberrant growth of neovessels, such as age-related macular degeneration (Brack et al., 2004; Santimaria et al., 2003; Folkman, 1995). We have also demonstrated potential applications for PL1-guided NPs as MR contrast agents for tumor detection and imaging. Finally, the experimental therapy of GBM tumor mice with PL1 targeted therapeutic NPs showed significantly reduced tumor volume and increased the lifespan of tumor mice compared to control groups. The FN-EDB domain is 100%, and the TNC-C domain is 96% conserved between mouse and human, and we observed in overlay studies on human glioma sample cryosections that PL1-NWs bind selectively to the FN-EDB and TNC-C positive areas. Collectively, these results warrant further preclinical development of PL1 guided drugs and imaging agents for the systemic targeting of solid tumors.

6.2.2. Development of tenascin-C and neuropilin-1 dual targeting PL3 peptide for cancer drug delivery

ECM targeting affinity ligands can reach extravascular tumor tissue passively through the EPR effect (Raavé et al., 2018), and adding tumor penetrating properties to the peptides may result in improved delivery. In our second study, we identified a novel peptide, PL3 (AGRGRLVR), that is able to bind to TNC-C and cell and tissue penetration receptor NRP-1. The NRP-1 binding is mediated by the CendR consensus motif RLVR of PL3 peptide; this interaction activates internalization and trans-tissue transport pathway (Teesalu et al., 2013, 2009). In

in vitro binding studies, we observed that PL3 peptide-binds specifically to the TNC-C and NRP1 b1b2 domain but not to Fn-EDB and NRP1 b1b2 with mutated CendR binding pocket. PL3 guided NPs showed NRP-1 dependent internalization in NRP-1-positive U87-MG and PPC1 cells but not in NRP-1-negative M21 melanoma cells. The internalization properties of PL3 peptide are similar to tLyP-1 tumor penetrating peptide that targets cell surface p32 and NRP-1 (Roth et al., 2012).

The systemic administration of two types of synthetic PL3-functionalized nanocarriers, NWs and AgNPs, resulted in their tumor homing and accumulation. This improved delivery appeared specific, as blocking TNC-C and NRP-1 binding sites with inhibitory Abs resulted in decreased tumor homing. In a proof-of-concept experimental therapy study, treatment with PL3-$_D$[KLAKLAK]$_2$-NWs significantly reduced tumor volume, and prolonged the survival rate of mice. The PL3 peptide targeted NWs, and not control nontargeted NWs, showed binding to TNC-C and NRP-1 positive regions of cryosections of human GBM, suggesting translational relevance. Overall, the studies indicate that PL3 targeting may have applications for delivering diagnostic and drug payloads in solid tumors.

6.2.3. Engineering an iRGD peptide-antibody fusion allows bifunctional targeted tumor penetration

Tumor targeting Abs are widely used and evaluated as drug carriers to improve therapeutic drug efficacy and decrease systemic toxicities. The TNC-C targeting single-chain antibody (ScFV G11) was developed for the delivery of cytotoxic or immunomodulatory payloads to solid tumors such as glioma, melanoma, pancreas, breast, and lung tumors (Silacci et al., 2006; Spenlé et al., 2015). However, bulky antibody-drug-conjugates (ADC), able to successfully target systemically accessible receptors, are less well suited for the delivery of payloads into extra-vascular tumor parenchyma. This is due to the tissue extravasation of ADCs depending entirely on the EPR effect, resulting in the uneven distribution in the tumor tissue that limits their clinical benefits (Adler & Dimitrov, 2012; Chau et al., 2019; Kalim et al., 2017). The prototypic TPP iRGD is widely used for co-administration and conjugated-based targeting of extravascular tumor parenchyma (Sugahara et al., 2009; Ruoslahti, 2017; Teesalu et al., 2013; Sugahara et al., 2010). We hypothesized that iRGD peptide conjugation to the non-internalizing G11 antibody might alleviate this problem by increasing the accessibility of tumor ECM from systemic space and activating the extravascular transport pathway for deep tumor extravasation.

We demonstrated the genetic fusion of iRGD to ECM targeting single-chain antibody G11 resulted in bispecific affinity ligand (iRGD-G11) with preserved ligand-binding specificities, able to bind both intended receptors (TNC-C and αvβ3 integrins). The modification of ScFV with iRGD and FAM labeling increased binding to TNC-C by 2-fold and vβ3 integrins 8-fold. In agreement with cell-free studies, systemic iRGD-G11 in s.c. U87-MG GBM models showed

significantly increased tumor accumulation compared to the parental G11 scFv antibody. Besides, 1 h after injection, iRGD-G11 was already detected in the extravascular tumor space, whereas the parental G11 signal in the same areas was absent. These data suggest that iRGD fusion improves tumor delivery and penetration of an ECM-targeting non-internalizing antibody – a broadly applicable strategy that could be used for other antibody-drug conjugates (ADC) to achieve improved delivery and better therapeutic efficiency.

6.2.4. LinTT1 peptide targeted nanoparticles selectively homes to brain tumors

The cryptic tumor penetrating peptide linTT1 (AKRGARSTA) was identified from the T7 phage library as a superior p32/gC1qR binding peptide (Paasonen et al., 2016; Sharma et al., 2017). In the past, homing of linTT1 guided NPs was studied extensively in mouse models of breast carcinoma and peritoneal carcinomatosis (PC) (Sharma et al., 2017; Hunt et al., 2017). The relevance of the linTT1 peptide/p32 axis for targeting gliomas had not been studied in the past. The p32 protein expression was observed in all 5 phenotypically diverse GBM mouse models and human clinical GBM specimens, in agreement with a previous study (Agemy et al., 2013; Fogal et al., 2015). The linTT1 functionalized NPs were found to accumulate in P32-positive regions in tumor lesions in all the GBM models. The homing of linTT1 was mainly observed in tumor-associated macrophages (TAM), a cell population with upregulated expression of cell surface P32 across solid tumors (Fogal et al., 2010; Chanmee et al., 2014; Mantovani et al., 2002), and intriguingly, in transdifferentiated tumor-derived vascular endothelial cells. Experimental therapy of GBM mice with LinTT1-$_D$(KLAKLAK)$_2$-NWs resulted in a significant reduction in tumor growth and improved survival compared to other control groups. This study demonstrated that LinTT1 TPP could be used to achieve tumor accumulation and delivery of different NPs to glioma lesions.

6.2.5. Identification of hyaluronan targeting IP3 peptide for peritoneal tumor delivery

HA is a large negatively charged ECM glycosaminoglycan carbohydrate polymer with biological functions ranging from the physiological role in ECM structural organization, cell adhesion, migration, angiogenesis, morphogenesis, to involvement in disease pathogenesis, e.g., cancer progression and dissemination and inflammatory responses (Simón-Gracia et al., 2018a; Zhang et al., 2018). The HA is abundantly upregulated in many cancers, including bladder, breast, prostate, lung, colon, peritoneal, and ovarian cancers (Wu et al., 2020). We used a combination of *ex vivo* and I.P. *in vivo* phage display screens in the MKN-45P gastric tumor mice model to identify a 9-residue cyclic IP3 (CKRDLSRRC) peptide that

selectively homes to peritoneal tumors upon IP administration. The IP3 peptide contains a hyaluronan-binding LSRPR motif, and indeed, *in vitro* binding studies demonstrated that IP3 binds to HA, and the treatment with hyaluronidase has abolished the binding. The IP administered IP3 peptide-coated synthetic AgNPs showed tumor-specific accumulation in the mouse peritoneal tumors of gastric and colon origin. Our results suggest that IP3 peptide may be useful for loco-regional IP delivery of drugs and imaging payloads to peritoneal tumors.

The HA regulation demonstrated to increase vascular permeability, immune modulation, regulation of angiogenesis, and apoptosis (Caon et al., 2020; Nikitovic et al., 2015; Misra et al., 2015). Therefore, HA targeted interruption of its receptor (e.g., CD44) interaction, and regulating HA synthesis and metabolism could be a promising therapeutic strategy for many types of tumors, wound healing, inflammatory disease, tissue fibrosis, and contact hypersensitivity.

6.3. Future directions

In this thesis, we have developed and preclinically validated a panel of novel peptides for precision-guided delivery to solid tumors. In the follow-up studies, these peptides can be developed further towards diagnostic and therapeutic clinical applications. Taking advantage of specific targeting properties of peptides, we consider the development of noninvasive precision-guided radioactive probes such as technetium-99m (^{99m}Tc) and gallium-68 (^{68}Ge) contrast agents for diagnostic imaging and patient stratification with PET imaging.

Further, for therapeutic applications, we will focus on three aspects. Firstly, since our peptides target the tumor microenvironment, we will evaluate peptide targeted cytokines such as (IL-2, 7, and 12, TNF-α) for developing as immunomodulatory therapeutics for cancer treatment. The second possible direction is to focus on the development of peptide-guided chemotherapeutics such as monomethyl auristatin E (MMAE) as adjuvant therapy for cancer treatment. The currently marketed cancer nanomedicines are passively targeted. Therefore, to improve efficacy and toxicity profiles, the drug-loaded NPs will be evaluated for active targeting with our peptides. Finally, we consider the development of our peptides into a next-generation modular proteolytically actuated tumor penetrating peptides.

7. CONCLUSIONS

1. Novel bispecific PL1 peptide targeting tumor extracellular matrix (ECM) proteins TNC-C and Fn-EDB allow specific targeting of Fn-EDB/TNC-C-positive solid tumors for precision delivery of anti-cancer drugs and imaging agents.

2. Tumor-penetrating peptide PL3 peptide is a bispecific peptide with an affinity towards ECM component TNC-C and cell- and tissue penetration receptor NRP-1. Systemic PL3 peptide targeted nanoparticles (NPs) show tumor-specific homing and tissue penetration that can be used for improved tumor imaging and therapy.

3. Genetic fusion of iRGD peptide to non-internalizing anti- TNC antibody G11 results in improved tumor homing and penetration.

4. LinTT1-targeted NPs accumulate in p32 positive areas in GBM lesions. The LinTT1 targeted proapoptotic NW shows therapeutic efficacy in GBM xeno-graft models.

5. Locoregional IP hyaluronan-specific IP3 peptide guided NPs home to the peritoneal carcinomatosis by targeting the HA in the tumor ECM.

8. SUMMARY IN ESTONIAN

Kasvajaid penetreerivate polüspetsiifiliste kullerpeptiidide väljatöötamine

Kasvajaliste haiguste ravivõimalused on piiratud, kuna süsteemne keemiaravi on madala efektiivsusega ning patsiendile manustatavat ravimidoosi piiravad kõrvalnähud tervetes kudedes. Üheks võimaluseks ravimite ja kontrastainete efektiivsemaks muutmiseks ja kõrvalnähtude vähendamiseks on nende laadimine nanoosakestesse. Nanoosakeste abil on võimalik parandada ravimite lahustuvust, koeselektiivsust ja vabanemist sihtmärkkoes. Vähiravimite ja nanoosakeste koeselektiivsuse ja efektiivsuse parandamiseks saab neid suunata keemiliselt konjugeeritud kullerpeptiididega. Kullerpeptiidide kasutamisel kasvajeliste haiguste täppisteraapiaks vajavad tähelepanu kaks probleemi: (1) vereringest ligipääsetavate rakupinna retseptorvalkude limiteeriv kogus, mis seab piirid kasvajakoesse sel viisil afiinsus-suunatavale ravimikogusele; ja (2) maliigsete rakkude geneetiline ebastabiilsus, mis võib põhjustada resistentsuse kujunemise afiinsus-suunatud ravimite suhtes.

Käesolevas töös kirjeldatud prekliinilistes uuringutes töötati välja kullerpeptiidid, mis seonduvad kahe või enama rakuvälise maatriksi vähispetsiifilise vormiga. PL1 (järjestus: PPRRGLIKLKTS) on kaksik-spetsiifiline peptiid, seondub selektiivselt Tenastsiin-C C-domääni ning Fibronektiini EDB domääniga. Need mõlemad molekulid on indutseeritud paljudes soliidtuumorites, ning samaaegselt kahele märklaudmolekulile suunatud kullerpeptiidi abil on võimalik saavutada nanoosakeste kõrgem ja ühtlasem akumulatsioon kasvajalistes kudedes. Teine peptiid, PL3 (järjestus: AGRGRLVR) seondub lisaks Tenastsiin-C C-domäänile neuropiliin-1ga – see interaktsioon käivitab vähispetsiifilise internalisatsiooni ja koepenetratsiooni rajad. Töös näidati, et võrreldes tavapäraste ühe molekulaarse märklauaga seonduvate peptiididega tagavad käesolevas töös identifitseeritud multispetsiilised peptiidid terapeutiliste ja diagnostiliste nanoosakeste parema akumuleerumise hiirtes modelleeritud soliidtuumorites. Töös näidati, et kullerpeptiididega suunamine parandab raudoksiidi nanoosakeste kontrasti kasvajakoe elupuhusel kuvamisel magnetresonantstomograafia abil. Eksperimentaalteraapia hiiremudelil näitas, et pro-apoptootiliste nanoosakeste suunamine meie poolt identifitseeritud vähiselektiivsete peptiididega võimendab osakeste terapeutilist efektiivsust.

Töö tulemusi on võimalik rakendada kasvajaliste protsesside senisest tundlikumaks detektsiooniks ja efektiivsemaks raviks.

9. REFERENCES

Abdollahpour-Alitappeh, M., Lotfinia, M., Gharibi, T., Mardaneh, J., Farhadihosseinabadi, B., Larki, P., Faghfourian, B., Sepehr, K.S., Abbaszadeh-Goudarzi, K., Abbaszadeh-Goudarzi, G., Johari, B., Zali, M.R., and Bagheri, N. (2019). Antibody–drug conjugates (ADCs) for cancer therapy: Strategies, challenges, and successes. *Journal of Cellular Physiology*. *234*(5), 5628–5642.

Acevedo, L.M., Barillas, S., Weis, S.M., Göthert, J.R., and Cheresh, D.A. (2008). Semaphorin 3A suppresses VEGF-mediated angiogenesis yet acts as a vascular permeability factor. *Blood*. *111*(5), 2674–2680.

Acharya, B., Meka, R.R., Venkatesha, S.H., Lees, J.R., Teesalu, T., and Moudgil, K.D. (2020). A novel CNS-homing peptide for targeting neuroinflammatory lesions in experimental autoimmune encephalomyelitis. *Molecular and Cellular Probes*. *51*.

Adler, M.J., and Dimitrov, D.S. (2012). Therapeutic Antibodies Against Cancer. *Hematology/Oncology Clinics of North America*. *26*(3), 447–481.

Agemy, L., Friedmann-Morvinski, D., Kotamraju, V.R., Roth, L., Sugahara, K.N., Girard, O.M., Mattrey, R.F., Verma, I.M., and Ruoslahti, E. (2011). Targeted nanoparticle enhanced proapoptotic peptide as potential therapy for glioblastoma. *Proceedings of the National Academy of Sciences of the United States of America*. *108*(42), 17450–17455.

Agemy, L., Kotamraju, V.R., Friedmann-Morvinski, D., Sharma, S., Sugahara, K.N., and Ruoslahti, E. (2013). Proapoptotic peptide-mediated cancer therapy targeted to cell surface p32. *Molecular Therapy*. *21*(12), 2195–2204.

Alberici, L., Roth, L., Sugahara, K.N., Agemy, L., Kotamraju, V.R., Teesalu, T., Bordignon, C., Traversari, C., Rizzardi, G.P., and Ruoslahti, E. (2013). De Novo design of a tumor-penetrating peptide. *Cancer Research*. *73*(2), 804–812.

Alibakhshi, A., Abarghooi Kahaki, F., Ahangarzadeh, S., Yaghoobi, H., Yarian, F., Arezumand, R., Ranjbari, J., Mokhtarzadeh, A., and de la Guardia, M. (2017). Targeted cancer therapy through antibody fragments-decorated nanomedicines. *Journal of Controlled Release*. *268*, 323–334.

Amamoto, R., Yagi, M., Song, Y.H., Oda, Y., Tsuneyoshi, M., Naito, S., Yokomizo, A., Kuroiwa, K., Tokunaga, S., Kato, S., Hiura, H., Samori, T., Kang, D., and Uchiumi, T. (2011). Mitochondrial p32/C1QBP is highly expressed in prostate cancer and is associated with shorter prostate-specific antigen relapse time after radical prostatectomy. *Cancer Science*. *102*(3), 639–647.

Amemiya, K., Nakatani, T., Saito, A., Suzuki, A., and Munakata, H. (2005). Hyaluronan-binding motif identified by panning a random peptide display library. *Biochimica et Biophysica Acta – General Subjects*. *1724*(1–2), 94–99.

Andrieu, J., Re, F., Russo, L., and Nicotra, F. (2019). Phage-displayed peptides targeting specific tissues and organs. *Journal of Drug Targeting*. *27*(5–6), 555–565.

Anselmo, A.C., and Mitragotri, S. (2015). A Review of Clinical Translation of Inorganic Nanoparticles. *AAPS Journal*. *17*(5), 1041–1054.

Anselmo, A.C., and Mitragotri, S. (2016). Nanoparticles in the clinic. *Bioengineering & Translational Medicine*. *1*(1), 10–29.

Anselmo, A.C., and Mitragotri, S. (2019). Nanoparticles in the clinic: An update. *Bioengineering & Translational Medicine*. *4*(3), 10–29.

Araste, F., Abnous, K., Hashemi, M., Taghdisi, S.M., Ramezani, M., and Alibolandi, M. (2018). Peptide-based targeted therapeutics: Focus on cancer treatment. *Journal of Controlled Release*. *292*, 141–162.

Bábíčková, J., Tóthová, Ľ., Boor, P., and Celec, P. (2013). In vivo phage display – A discovery tool in molecular biomedicine. *Biotechnology Advances*. *31*(8), 1247–1259.

Bailly, C., Thuru, X., and Quesnel, B. (2020). Combined cytotoxic chemotherapy and immunotherapy of cancer: modern times. *NAR Cancer*. *2*(1).

Bashir, M.R., Bhatti, L., Marin, D., and Nelson, R.C. (2015). Emerging applications for ferumoxytol as a contrast agent in MRI. *Journal of Magnetic Resonance Imaging*. *41*(4), 884–898.

Beck, A., Goetsch, L., Dumontet, C., and Corvaïa, N. (2017). Strategies and challenges for the next generation of antibody-drug conjugates. *Nature Reviews Drug Discovery*. *16*(5), 315–337.

Becker, P.M., Waltenberger, J., Yachechko, R., Mirzapoiazova, T., Sham, J.S.K., Lee, C.G., Elias, J.A., and Verin, A.D. (2005). Neuropilin-1 regulates vascular endothelial growth factor-mediated endothelial permeability. *Circulation Research*. *96*(12), 1257–1265.

Bertrand, N., Wu, J., Xu, X., Kamaly, N., and Farokhzad, O.C. (2014). Cancer nanotechnology: The impact of passive and active targeting in the era of modern cancer biology. *Advanced Drug Delivery Reviews*. *66*, 2–25.

Birchler, M.T., Milisavlijevic, D., Pfaltz, M., Neri, D., Odermatt, B., Schmid, S., and Stoeckli, S.J. (2003). Expression of the extra domain B of fibronectin, a marker of angiogenesis, in head and neck tumors. *Laryngoscope*. *113*(7), 1231–1237.

Blanco, E., Shen, H., and Ferrari, M. (2015). Principles of nanoparticle design for overcoming biological barriers to drug delivery. *Nature Biotechnology*. *33*(9), 941–951.

Bobo, D., Robinson, K.J., Islam, J., Thurecht, K.J., and Corrie, S.R. (2016). Nanoparticle-Based Medicines: A Review of FDA-Approved Materials and Clinical Trials to Date. *Pharmaceutical Research*. *33*(10), 2373–2387.

Bonvalot, S., Rutkowski, P.L., Thariat, J., Carrère, S., Ducassou, A., Sunyach, M.P., Agoston, P., Hong, A., Mervoyer, A., Rastrelli, M., Moreno, V., Li, R.K., Tiangco, B., Herraez, A.C., Gronchi, A., Mangel, L., Sy-Ortin, T., Hohenberger, P., de Baère, T., Le Cesne, A., Helfre, S., Saada-Bouzid, E., Borkowska, A., Anghel, R., Co, A., Gebhart, M., Kantor, G., Montero, A., Loong, H.H., Vergés, R., Lapeire, L., Dema, S., Kacso, G., Austen, L., Moureau-Zabotto, L., Servois, V., Wardelmann, E., Terrier, P., Lazar, A.J., Bovée, J.V.M.G., Le Péchoux, C., and Papai, Z. (2019). NBTXR3, a first-in-class radioenhancer hafnium oxide nanoparticle, plus radiotherapy versus radiotherapy alone in patients with locally advanced soft-tissue sarcoma (Act.In.Sarc): a multicentre, phase 2–3, randomised, controlled trial. *The Lancet Oncology*. *20*(8), 1148–1159.

Borsi, L., Allemanni, G., Castellani, P., Rosellini, C., Di Vinci, A., and Zardi, L. (1985). Structural differences in the cell binding region of human fibronectin molecules isolated from cultured normal and tumor-derived human cells. *FEBS Letters*. *192*(1), 71–74.

Borsi, L., Castellani, P., Risso, A.M., Leprini, A., and Zardi, L. (1990). Transforming growth factor-β regulates the splicing pattern of fibronectin messenger RNA precursor. *FEBS Letters*. *261*(1), 175–178.

Bougnaud, S., Golebiewska, A., Oudin, A., Keunen, O., Harter, P.N., Mäder, L., Azuaje, F., Fritah, S., Stieber, D., Kaoma, T., Vallar, L., Brons, N.H.C., Daubon, T., Miletic, H., Sundstrøm, T., Herold-Mende, C., Mittelbronn, M., Bjerkvig, R., and Niclou, S.P. (2016). Molecular crosstalk between tumour and brain parenchyma instructs histopathological features in glioblastoma. *Oncotarget*. *7*(22), 31955–31971.

Bourdon, M.A., Wikstrand, C.J., Bigner, D.D., Matthews, T.J., and Furthmayr, H. (1983). Human glioma-mesenchymal extracellular matrix antigen defined by monoclonal antibody. *Cancer Research*. *43*(6), 2796–2805.

Brack, S.S., Dinkelborg, L.M., and Neri, D. (2004). Molecular targeting of angiogenesis for imaging and therapy. *European Journal of Nuclear Medicine and Molecular Imaging*. *31*(9), 1327–1341.

Braun, G.B., Friman, T., Pang, H.B., Pallaoro, A., De Mendoza, T.H., Willmore, A.M.A., Kotamraju, V.R., Mann, A.P., She, Z.G., Sugahara, K.N., Reich, N.O., Teesalu, T., and Ruoslahti, E. (2014). Etchable plasmonic nanoparticle probes to image and quantify cellular internalization. *Nature Materials*. *13*(9), 904–911.

Braun, G.B., Sugahara, K.N., Yu, O.M., Kotamraju, V.R., Mölder, T., Lowy, A.M., Ruoslahti, E., and Teesalu, T. (2016). Urokinase-controlled tumor penetrating peptide. *Journal of Controlled Release*. *232*, 188–195.

Bray, F., Ferlay, J., Soerjomataram, I., Siegel, R.L., Torre, L.A., and Jemal, A. (2018). Global cancer statistics 2018: GLOBOCAN estimates of incidence and mortality worldwide for 36 cancers in 185 countries. *CA: A Cancer Journal for Clinicians*. *68*(6), 394–424.

Brösicke, N., and Faissner, A. (2015). Role of tenascins in the ECM of gliomas. *Cell Adhesion and Migration*. *9*(1–2), 131–140.

Cantelmo, A.R., Conradi, L.C., Brajic, A., Goveia, J., Kalucka, J., Pircher, A., Chaturvedi, P., Hol, J., Thienpont, B., Teuwen, L.A., Schoors, S., Boeckx, B., Vriens, J., Kuchnio, A., Veys, K., Cruys, B., Finotto, L., Treps, L., Stav-Noraas, T.E., Bifari, F., Stapor, P., Decimo, I., Kampen, K., De Bock, K., Haraldsen, G., Schoonjans, L., Rabelink, T., Eelen, G., Ghesquière, B., Rehman, J., Lambrechts, D., Malik, A.B., Dewerchin, M., and Carmeliet, P. (2016). Inhibition of the Glycolytic Activator PFKFB3 in Endothelium Induces Tumor Vessel Normalization, Impairs Metastasis, and Improves Chemotherapy. *Cancer Cell*. *30*(6), 968–985.

Caon, I., Bartolini, B., Parnigoni, A., Caravà, E., Moretto, P., Viola, M., Karousou, E., Vigetti, D., and Passi, A. (2020). Revisiting the hallmarks of cancer: The role of hyaluronan. *Seminars in Cancer Biology*. *62*, 9–19.

Carmeliet, P., and Jain, R.K. (2000). Angiogenesis in cancer and other diseases. *Nature*. *407*(6801), 249–257.

Carnemolla, B., Balza, E., Siri, A., Zardi, L., Nicotra, M.R., Bigotti, A., and Natali, P.G. (1989). A tumor-associated fibronectin isoform generated by alternative splicing of messenger RNA precursors. *Journal of Cell Biology*. *108*(3), 1139–1148.

Carnemolla, B., Castellani, P., Ponassi, M., Borsi, L., Urbini, S., Nicolo, G., Dorcaratto, A., Viale, G., Winter, G., Neri, D., and Zardi, L. (1999). Identification of a glioblastoma-associated Tenascin-C isoform by a high affinity recombinant antibody. *American Journal of Pathology*. *154*(5), 1345–1352.

Castellani, P., Viale, G., Dorcaratto, A., Nicolo, G., Kaczmarek, J., Querze, G., and Zardi, L. (1994). The fibronectin isoform containing the ed-b oncofetal domain: A marker of angiogenesis. *International Journal of Cancer*. *59*(5), 612–618.

Chabner, B.A., and Roberts, T.G. (2005). Chemotherapy and the war on cancer. *Nature Reviews Cancer*. *5*(1), 65–72.

Chanmee, T., Ontong, P., Konno, K., and Itano, N. (2014). Tumor-associated macrophages as major players in the tumor microenvironment. *Cancers*. *6*(3), 1670–1690.

Chau, C.H., Steeg, P.S., and Figg, W.D. (2019). Antibody–drug conjugates for cancer. *The Lancet*. *394*(10200), 793–804.

Chaudhary, B., Khaled, Y.S., Ammori, B.J., and Elkord, E. (2014). Neuropilin 1: Function and therapeutic potential in cancer. *Cancer Immunology, Immunotherapy*. *63*(2), 81–99.

Chen, E.C., Fathi, A.T., and Brunner, A.M. (2018). Reformulating acute myeloid leukemia: Liposomal cytarabine and daunorubicin (CPX-351) as an emerging therapy for secondary AML. *OncoTargets and Therapy*. *11*, 3425–3434.

Chen, Y.B., Jiang, C.T., Zhang, G.Q., Wang, J.S., and Pang, D. (2009). Increased expression of hyaluronic acid binding protein 1 is correlated with poor prognosis in patients with breast cancer. *Journal of Surgical Oncology*. *100*(5), 382–386.

Chiquet-Ehrismann, R., Mackie, E.J., Pearson, C.A., and Sakakura, T. (1986). Tenascin: an extracellular matrix protein involved in tissue interactions during fetal development and oncogenesis. *Cell*. *47*(1), 131–139.

Christian, S., Pilch, J., Akerman, M.E., Porkka, K., Laakkonen, P., and Ruoslahti, E. (2003). Nucleolin expressed at the cell surface is a marker of endothelial cells in angiogenic blood vessels. *Journal of Cell Biology*. *163*(4), 871–878.

Chung, A.S., Lee, J., and Ferrara, N. (2010). Targeting the tumour vasculature: Insights from physiological angiogenesis. *Nature Reviews Cancer*. *10*(7), 505–514.

Clackson, T., Hoogenboom, H.R., Griffiths, A.D., and Winter, G. (1991). Making antibody fragments using phage display libraries. *Nature*. *352*(6336), 624–628.

Colombi, M., Barlati, S., Kornblihtt, A., Baralle, F.E., and Vaheri, A. (1986). A family of fibronectin mRNAs in human normal and transformed cells. *BBA – Gene Structure and Expression*. *868*(4), 207–214.

Crisci, S., Amitrano, F., Saggese, M., Muto, T., Sarno, S., Mele, S., Vitale, P., Ronga, G., Berretta, M., and Di Francia, R. (2019). Overview of current targeted anti-cancer drugs for therapy in onco-hematology. *Medicina (Lithuania)*. *55*(8), 414.

Cureton, N., Korotkova, I., Baker, B., Greenwood, S., Wareing, M., Kotamraju, V.R., Teesalu, T., Cellesi, F., Tirelli, N., Ruoslahti, E., Aplin, J.D., and Harris, L.K. (2017). Selective targeting of a novel vasodilator to the uterine vasculature to treat impaired uteroplacental perfusion in pregnancy. *Theranostics*. *7*(15), 3715–3731.

D'Ovidio, M.C., Mastracchio, A., Marzullo, A., Ciabatta, M., Pini, B., Uccini, S., Zardi, L., and Ruco, L.P. (1998). Intratumoral microvessel density and expression of ED-A/ED-B sequences of fibronectin in breast carcinoma. *European Journal of Cancer*. *34*(7), 1081–1085.

Daniels, D.A., Chen, H., Hicke, B.J., Swiderek, K.M., and Gold, L. (2003). A tenascin-C aptamer identified by tumor cell SELEX: Systematic evolution of ligands by exponential enrichment. *Proceedings of the National Academy of Sciences of the United States of America*. *100*(26), 15416–15421.

Deng, X., Wang, L., You, X., Dai, P., and Zeng, Y. (2018). Advances in the T7 phage display system (Review). *Molecular Medicine Reports*. *17*(1), 714–720.

Desgrosellier, J.S., and Cheresh, D.A. (2010). Integrins in cancer: Biological implications and therapeutic opportunities. *Nature Reviews Cancer*. *10*(1), 9–22.

DeVita, V.T., and Chu, E. (2008). A history of cancer chemotherapy. *Cancer Research*. *68*(21), 8643–8653.

Ding, Y., Zhou, J., Wang, S., Li, Y., Mi, Y., Gao, S., Xu, Y., Chen, Y., and Yan, J. (2018). Anti-neuropilin-1 monoclonal antibody suppresses the migration and invasion of human gastric cancer cells via Akt dephosphorylation. *Experimental and Therapeutic Medicine*. *16*(2), 537–546.

Dörries, U., and Schachner, M. (1994). Tenascin mRNA isoforms in the developing mouse brain. *Journal of Neuroscience Research*. *37*(3), 336–347.

Dudley, A.C. (2012). Tumor endothelial cells. *Cold Spring Harbor Perspectives in Medicine*. *2*(3).

Dumontet, C., and Jordan, M.A. (2010). Microtubule-binding agents: A dynamic field of cancer therapeutics. *Nature Reviews Drug Discovery*. *9*(10), 790–803.

Ellerby, H.M., Arap, W., Ellerby, L.M., Kain, R., Andrusiak, R., Del Rio, G., Krajewski, S., Lombardo, C.R., Rao, R., Ruoslahti, E., Bredesen, D.E., and Pasqualini, R. (1999). Anti-cancer activity of targeted pro-apoptotic peptides. *Nature Medicine*. *5*(9), 1032–1038.

Ellis, L.M. (2006). The role of neuropilins in cancer. *Molecular Cancer Therapeutics*. *5*(5), 1099–1107.

Fogal, V., Babic, I., Chao, Y., Pastorino, S., Mukthavaram, R., Jiang, P., Cho, Y.J., Pingle, S.C., Crawford, J.R., Piccioni, D.E., and Kesari, S. (2015). Mitochondrial p32 is upregulated in Myc expressing brain cancers and mediates glutamine addiction. *Oncotarget*. *6*(2), 1157–1170.

Fogal, V., Richardson, A.D., Karmali, P.P., Scheffler, I.E., Smith, J.W., and Ruoslahti, E. (2010). Mitochondrial p32 Protein Is a Critical Regulator of Tumor Metabolism via Maintenance of Oxidative Phosphorylation. *Molecular and Cellular Biology*. *30*(6), 1303–1318.

Fogal, V., Zhang, L., Krajewski, S., and Ruoslahti, E. (2008). Mitochondrial/cell-surface protein p32/gC1qR as a molecular target in tumor cells and tumor stroma. *Cancer Research*. *68*(17), 7210–7218.

Folkman, J. (1995). Angiogenesis in cancer, vascular, rheumatoid and other disease. *Nature Medicine*. *1*(1), 27–30.

Frey, K., Fiechter, M., Schwager, K., Belloni, B., Barysch, M.J., Neri, D., and Dummer, R. (2011). Different patterns of fibronectin and tenascin-C splice variants expression in primary and metastatic melanoma lesions. *Experimental Dermatology*. *20*(8), 685–688.

Fu, D., Calvo, J.A., and Samson, L.D. (2012). Balancing repair and tolerance of DNA damage caused by alkylating agents. *Nature Reviews Cancer*. *12*(2), 104–120.

Fukamauchi, F., Mataga, N., Wang, Y.J., Sato, S., Yoshiki, A., and Kusakabe, M. (1996). Abnormal behavior and neurotransmissions of tenascin gene knockout mouse. *Biochemical and Biophysical Research Communications*. *221*(1), 151–156.

Fukuda, T., Yoshida, N., Kataoka, Y., Manabe, R. ichiroh, Mizuno-Horikawa, Y., Sato, M., Kuriyama, K., Yasui, N., and Sekiguchi, K. (2002). Mice lacking the EDB segment of fibronectin develop normally but exhibit reduced cell growth and fibronectin matrix assembly in vitro. *Cancer Research*. *62*(19), 5603–5610.

Gerber, D.E. (2008). Targeted therapies: a new generation of cancer treatments. *American family physician*. *77*(3), 311–9.

Ghebrehiwet, B., and Peerschke, E.I.B. (1998). Structure and function of gC1q-R: A multiligand binding cellular protein. *Immunobiology*. *199*(2), 225–238.

Giblin, S.P., and Midwood, K.S. (2015). Tenascin-C: Form versus function. *Cell Adhesion and Migration*. *9*(1–2), 48–82.

Gilkes, D.M., Semenza, G.L., and Wirtz, D. (2014). Hypoxia and the extracellular matrix: Drivers of tumour metastasis. *Nature Reviews Cancer*. *14*(6), 430–439.

Goel, H.L., Pursell, B., Chang, C., Shaw, L.M., Mao, J., Simin, K., Kumar, P., Vander Kooi, C.W., Shultz, L.D., Greiner, D.L., Norum, J.H., Toftgard, R., Kuperwasser, C., and Mercurio, A.M. (2013). GLI1 regulates a novel neuropilin-2/α6β1 integrin based autocrine pathway that contributes to breast cancer initiation. *EMBO Molecular Medicine*. *5*(4), 488–508.

Goel, S., Duda, D.G., Xu, L., Munn, L.L., Boucher, Y., Fukumura, D., and Jain, R.K. (2011). Normalization of the vasculature for treatment of cancer and other diseases. *Physiological Reviews*. *91*(3), 1071–1121.

Hamidi, H., and Ivaska, J. (2018). Every step of the way: integrins in cancer progression and metastasis. *Nature Reviews Cancer*. *18*(9), 1–16.

Han, Z., Zhou, Z., Shi, X., Wang, J., Wu, X., Sun, D., Chen, Y., Zhu, H., Magi-Galluzzi, C., and Lu, Z.R. (2015). EDB fibronectin specific peptide for prostate cancer targeting. *Bioconjugate Chemistry*. *26*(5), 830–838.

Hanahan, D., and Folkman, J. (1996). Patterns and emerging mechanisms of the angiogenic switch during tumorigenesis. *Cell*. *86*(3), 353–364.

Hanahan, D., and Weinberg, R.A. (2011). Hallmarks of cancer: The next generation. *Cell*. *144*(5), 646–674.

Heldin, C.H., Rubin, K., Pietras, K., and Östman, A. (2004). High interstitial fluid pressure – An obstacle in cancer therapy. *Nature Reviews Cancer*. *4*(10), 806–813.

Hida, K., Hida, Y., Amin, D.N., Flint, A.F., Panigrahy, D., Morton, C.C., and Klagsbrun, M. (2004). Tumor-associated endothelial cells with cytogenetic abnormalities. *Cancer Research*. *64*(22), 8249–8255.

Hoffman, J.A., Giraudo, E., Singh, M., Zhang, L., Inoue, M., Porkka, K., Hanahan, D., and Ruoslahti, E. (2003). Progressive vascular changes in a transgenic mouse model of squamous cell carcinoma. *Cancer Cell*. *4*(5), 383–391.

Hollingsworth, R.E., and Jansen, K. (2019). Turning the corner on therapeutic cancer vaccines. *npj Vaccines*. *4*(1), 1–10.

Hoshyar, N., Gray, S., Han, H., and Bao, G. (2016). The effect of nanoparticle size on in vivo pharmacokinetics and cellular interaction. *Nanomedicine*. *11*(6), 673–692.

Hua, S., de Matos, M.B.C., Metselaar, J.M., and Storm, G. (2018). Current trends and challenges in the clinical translation of nanoparticulate nanomedicines: Pathways for translational development and commercialization. *Frontiers in Pharmacology*. *9*(JUL), 790.

Huang, C.-Y.Y., Ju, D.-T.T., Chang, C.-F.F., Muralidhar Reddy, P., and Velmurugan, B.K. (2017a). A review on the effects of current chemotherapy drugs and natural agents in treating non-small cell lung cancer. *BioMedicine*. *7*(4), 23.

Huang, R., Andersen, L.M.K., and Rofstad, E.K. (2017b). Metastatic pathway and the microvascular and physicochemical microenvironments of human melanoma xenografts. *Journal of Translational Medicine*. *15*(1).

Hunt, H., Simón-Gracia, L., Tobi, A., Teesalu, T., Kotamraju, V.R., Sharma, S., Sugahara, K.N., Ruoslahti, E., Teesalu, T., Nigul, M., and Sugahara, K.N. (2017). Targeting of p32 in peritoneal carcinomatosis with intraperitoneal linTT1 peptide-guided pro-apoptotic nanoparticles. *Journal of Controlled Release*. *260*, 142–153.

Hussain, S., Rodriguez-Fernandez, M., Braun, G.B., Doyle, F.J., and Ruoslahti, E. (2014). Quantity and accessibility for specific targeting of receptors in tumours. *Scientific Reports*. *4*(1), 5232.

Hynes, R.O. (2002). Integrins: Bidirectional, allosteric signaling machines. *Cell*. *110*(6), 673–687.

Ikemoto, H., Lingasamy, P., Willmore, A.M.A., Hunt, H., Kurm, K., Tammik, O., Scodeller, P., Simón-Gracia, L., Kotamraju, V.R., Lowy, A.M., Sugahara, K.N., and Teesalu, T. (2017). Hyaluronan-binding peptide for targeting peritoneal carcinomatosis. *Tumor Biology*. *39*(5), 1010428317701628.

Ishiwata, T., Takahashi, K., Shimanuki, Y., Ohashi, R., Cui, R., Takahashi, F., Shimizu, K., Miura, K., and Fukuchi, Y. (2005). Serum tenascin-C as a potential predictive marker

of angiogenesis in non-small cell lung cancer. *Anticancer Research*. *25*(1 B), 489–495.

Jain, R.K. (2005). Normalization of tumor vasculature: An emerging concept in anti-angiogenic therapy. *Science*. *307*(5706), 58–62.

Jain, R.K., Duda, D.G., Clark, J.W., and Loeffler, J.S. (2006). Lessons from phase III clinical trials on anti-VEGF therapy for cancer. *Nature Clinical Practice Oncology*. *3*(1), 24–40.

Järveläinen, H., Sainio, A., Koulu, M., Wight, T.N., and Penttinen, R. (2009). Extracellular matrix molecules: Potential targets in pharmacotherapy. *Pharmacological Reviews*. *61*(2), 198–223.

Jeong, W. jin, Bu, J., Kubiatowicz, L.J., Chen, S.S., Kim, Y.S., and Hong, S. (2018). Peptide–nanoparticle conjugates: a next generation of diagnostic and therapeutic platforms? *Nano Convergence*. *5*(1), 38.

Joester, A., and Faissner, A. (1999). Evidence for combinatorial variability of tenascin-C isoforms and developmental regulation in the mouse central nervous system. *Journal of Biological Chemistry*. *274*(24), 17144–17151.

Johannsen, M., Spitaleri, G., Curigliano, G., Roigas, J., Weikert, S., Kempkensteffen, C., Roemer, A., Kloeters, C., Rogalla, P., Pecher, G., Miller, K., Berndt, A., Kosmehl, H., Trachsel, E., Kaspar, M., Lovato, V., González-Iglesias, R., Giovannoni, L., Menssen, H.D., Neri, D., and De Braud, F. (2010). The tumour-targeting human L19-IL2 immunocytokine: Preclinical safety studies, phase i clinical trial in patients with solid tumours and expansion into patients with advanced renal cell carcinoma. *European Journal of Cancer*. *46*(16), 2926–2935.

Le Joncour, V., and Laakkonen, P. (2018). Seek & Destroy, use of targeting peptides for cancer detection and drug delivery. *Bioorganic and Medicinal Chemistry*. *26*(10), 2797–2806.

Jones, F.S., and Jones, P.L. (2000). The tenascin family of ECM glycoproteins: Structure, function, and regulation during embryonic development and tissue remodeling. *Developmental Dynamics*. *218*(2), 235–259.

Joyce, J.A., Laakkonen, P., Bernasconi, M., Bergers, G., Ruoslahti, E., and Hanahan, D. (2003). Stage-specific vascular markers revealed by phage display in a mouse model of pancreatic islet tumorigenesis. *Cancer Cell*. *4*(5), 393–403.

Kalim, M., Chen, J., Wang, S., Lin, C., Ullah, S., Liang, K., Ding, Q., Chen, S., and Zhan, J.B. (2017). Intracellular trafficking of new anticancer therapeutics: Antibody–drug conjugates. *Drug Design, Development and Therapy*. *11*, 2265–2276.

Karjalainen, K., Jaalouk, D.E., Bueso-Ramos, C.E., Zurita, A.J., Kuniyasu, A., Eckhardt, B.L., Marini, F.C., Lichtiger, B., O'Brien, S., Kantarjian, H.M., Cortes, J.E., Koivunen, E., Arap, W., and Pasqualini, R. (2011). Targeting neuropilin-1 in human leukemia and lymphoma. *Blood*. *117*(3), 920–927.

Kaspar, M., Zardi, L., and Neri, D. (2006). Fibronectin as target for tumor therapy. *International Journal of Cancer*. *118*(6), 1331–1339.

Kaur, H., Bruno, J.G., Kumar, A., and Sharma, T.K. (2018). Aptamers in the therapeutics and diagnostics pipelines. *Theranostics*. *8*(15), 4016–4032.

Kawasaki, T., Kitsukawa, T., Bekku, Y., Matsuda, Y., Sanbo, M., Yagi, T., and Fujisawa, H. (1999). A requirement for neuropilin-1 in embryonic vessel formation. *Development*. *126*(21), 4895–4902.

Kelly, K.A., Bardeesy, N., Anbazhagan, R., Gurumurthy, S., Berger, J., Alencar, H., DePinho, R.A., Mahmood, U., and Weissleder, R. (2008). Targeted nanoparticles for

imaging incipient pancreatic ductal adenocarcinoma. *PLoS Medicine*. *5*(4), 0657–0668.

Kennedy, P.J., Oliveira, C., Granja, P.L., and Sarmento, B. (2017). Antibodies and associates: Partners in targeted drug delivery. *Pharmacology and Therapeutics*. *177*, 129–145.

Keunen, O., Johansson, M., Oudin, A., Sanzey, M., Rahim, S.A.A., Fack, F., Thorsen, F., Taxt, T., Bartos, M., Jirik, R., Miletic, H., Wang, J., Stieber, D., Stuhr, L., Moen, I., Rygh, C.B., Bjerkvig, R., and Niclou, S.P. (2011). Anti-VEGF treatment reduces blood supply and increases tumor cell invasion in glioblastoma. *Proceedings of the National Academy of Sciences of the United States of America*. *108*(9), 3749–3754.

Khan, Z.A., Chan, B.M., Uniyal, S., Barbin, Y.P., Farhangkhoee, H., Chen, S., and Chakrabarti, S. (2005). EDB fibronectin and angiogenesis – A novel mechanistic pathway. *Angiogenesis*. *8*(3), 183–196.

Kim, K.J., Li, B., Winer, J., Armanini, M., Gillett, N., Phillips, H.S., and Ferrara, N. (1993). Inhibition of vascular endothelial growth factor-induced angiogenesis suppresses tumour growth in vivo. *Nature*. *362*(6423), 841–844.

Kim, M.Y., Kim, O.R., Choi, Y.S., Lee, H., Park, K., Lee, C.T., Kang, K.W., and Jeong, S. (2012a). Selection and characterization of tenascin C targeting peptide. *Molecules and Cells*. *33*(1), 71–77.

Kim, S., Kim, D., Jung, H.H., Lee, I.H., Kim, J. Il, Suh, J.Y., and Jon, S. (2012b). Bio-inspired design and potential biomedical applications of a novel class of high-affinity peptides. *Angewandte Chemie – International Edition*. *51*(8), 1890–1894.

King, A., Ndifon, C., Lui, S., Widdows, K., Kotamraju, V.R., Agemy, L., Teesalu, T., Glazier, J.D., Cellesi, F., Tirelli, N., Aplin, J.D., Ruoslahti, E., and Harris, L.K. (2016). Tumor-homing peptides as tools for targeted delivery of payloads to the placenta. *Science Advances*. *2*(5), e1600349.

Kirpotin, D.B., Drummond, D.C., Shao, Y., Shalaby, M.R., Hong, K., Nielsen, U.B., Marks, J.D., Benz, C.C., and Park, J.W. (2006). Antibody targeting of long-circulating lipidic nanoparticles does not increase tumor localization but does increase internalization in animal models. *Cancer Research*. *66*(13), 6732–6740.

Koga, A., Aoyagi, K., Imaizumi, T., Miyagi, M., and Shirouzu, K. (2011). Comparison between the gastric cancer cell line MKN-45 and the high-Potential peritoneal dissemination gastric cancer cell line MKN-45P. *Kurume Medical Journal*. *58*(3), 73–79.

Kremer, J.C., Prudner, B.C., Lange, S.E.S., Bean, G.R., Schultze, M.B., Brashears, C.B., Radyk, M.D.A., Redlich, N., Tzeng, S.C., Kami, K., Shelton, L., Li, A., Morgan, Z., Bomalaski, J.S., Tsukamoto, T., McConathy, J., Michel, L.S., Held, J.M., and Van Tine, B.A. (2017). Arginine Deprivation Inhibits the Warburg Effect and Upregulates Glutamine Anaplerosis and Serine Biosynthesis in ASS1-Deficient Cancers. *Cell Reports*. *18*(4), 991–1004.

Kumra, H., and Reinhardt, D.P. (2016). Fibronectin-targeted drug delivery in cancer. *Advanced Drug Delivery Reviews*. *97*, 101–110.

Kuncic, Z. (2015). Cancer nanomedicine: Challenges and opportunities. *Medical Journal of Australia*. *203*(5), 204-205.e1.

Laakkonen, P., Åkerman, M.E., Biliran, H., Yang, M., Ferrer, F., Karpanen, T., Hoffman, R.M., and Ruoslahti, E. (2004). Antitumor activity of a homing peptide that targets tumor lymphatics and tumor cells. *Proceedings of the National Academy of Sciences of the United States of America*. *101*(25), 9381–9386.

Laakkonen, P., Porkka, K., Hoffman, J.A., and Ruoslahti, E. (2002). A tumor-homing peptide with a targeting specificity related to lymphatic vessels. *Nature Medicine*. *8*(7), 751–755.

Lambert, S., Bouttier, M., Vassy, R., Seigneuret, M., Petrow-Sadowski, C., Janvier, S., Heveker, N., Ruscetti, F.W., Perret, G., Jones, K.S., and Pique, C. (2009). HTLV-1 uses HSPG and neuropilin-1 for entry by molecular mimicry of VEGF165. *Blood*. *113*(21), 5176–5185.

Lee, S.Y., Kang, M.S., Jeong, W.Y., Han, D.W., and Kim, K.S. (2020). Hyaluronic acid-based theranostic nanomedicines for targeted cancer therapy. *Cancers*. *12*(4), 940.

Van Leeuwen, H.C., and O'Hare, P. (2001). Retargeting of the mitochondrial protein p32/gC1Qr to a cytoplasmic compartment and the cell surface. *Journal of Cell Science*. *114*(11), 2115–2123.

Lingasamy, P., Laarmann, A.-H., and Teesalu, T. (2020a). Tumor penetrating peptide-functionalized Tenascin-C antibody for glioblastoma targeting. *Current cancer drug targets*. *20*, 1–11.

Lingasamy, P., and Teesalu, T. (2020). Homing peptides for cancer therapy. *In* Bio-Nanomedicine for Cancer Therapy, H. Santos & F. Fontana (Eds.),. Springer Nature Switzerland AG. X, 420.

Lingasamy, P., Tobi, A., Haugas, M., Hunt, H., Paiste, P., Asser, T., Rätsep, T., Kotamraju, V.R., Bjerkvig, R., and Teesalu, T. (2019). Bi-specific tenascin-C and fibronectin targeted peptide for solid tumor delivery. *Biomaterials*. *219*, 119373.

Lingasamy, P., Tobi, A., Kurm, K., Kopanchuk, S., Sudakov, A., Salumäe, M., Rätsep, T., Asser, T., Bjerkvig, R., and Teesalu, T. (2020b). Tumor-penetrating peptide for systemic targeting of Tenascin-C. *Scientific Reports*. *10*(1), 5809.

Link, W. (2015). Anti-cancer Drugs: Discovery, Development and Therapy. *In* International Manual of Oncology Practice. Springer International Publishing, Cham. 81–94.

List, T., and Neri, D. (2013). Immunocytokines: A review of molecules in clinical development for cancer therapy. *Clinical Pharmacology: Advances and Applications*. *5*(SUPPL. 1), 29–45.

Liu, R., Li, X., Xiao, W., and Lam, K.S. (2017). Tumor-targeting peptides from combinatorial libraries. *Advanced Drug Delivery Reviews*. *110–111*, 13–37.

Lopes, A., Vandermeulen, G., and Préat, V. (2019). Cancer DNA vaccines: current preclinical and clinical developments and future perspectives. *Journal of Experimental and Clinical Cancer Research*. *38*(1), 1–24.

Lu, L., Qi, H., Zhu, J., Sun, W.X., Zhang, B., Tang, C.Y., and Cheng, Q. (2017). Vascular-homing peptides for cancer therapy. *Biomedicine and Pharmacotherapy*. *92*, 187–195.

Mackie, E.J., and Tucker, R.P. (1999). The tenascin-C knockout revisited. *Journal of Cell Science*. *112*(22), 3847–3853.

Maggiorella, L., Barouch, G., Devaux, C., Pottier, A., Deutsch, E., Bourhis, J., Borghi, E., and Levy, L. (2012). Nanoscale radiotherapy with hafnium oxide nanoparticles. *Future Oncology*. *8*(9), 1167–1181.

Maj, E., Papiernik, D., and Wietrzyk, J. (2016). Antiangiogenic cancer treatment: The great discovery and greater complexity (Review). *International Journal of Oncology*. *49*(5), 1773–1784.

Mamluk, R., Gechtman, Z., Kutcher, M.E., Gasiunas, N., Gallagher, J., and Klagsbrun, M. (2002). Neuropilin-1 binds vascular endothelial growth factor 165, placenta

growth factor-2, and heparin via its b1b2 domain. *Journal of Biological Chemistry*. *277*(27), 24818–24825.

Mann, A.P., Scodeller, P., Hussain, S., Braun, G.B., Mölder, T., Toome, K., Ambasudhan, R., Teesalu, T., Lipton, S.A., and Ruoslahti, E. (2017). Identification of a peptide recognizing cerebrovascular changes in mouse models of Alzheimer's disease. *Nature Communications*. *8*(1), 1403.

Mann, A.P., Scodeller, P., Hussain, S., Joo, J., Kwon, E., Braun, G.B., Mölder, T., She, Z.G., Kotamraju, V.R., Ranscht, B., Krajewski, S., Teesalu, T., Bhatia, S., Sailor, M.J., and Ruoslahti, E. (2016). A peptide for targeted, systemic delivery of imaging and therapeutic compounds into acute brain injuries. *Nature Communications*. *7*(1), 11980.

Mantovani, A., Sozzani, S., Locati, M., Allavena, P., and Sica, A. (2002). Macrophage polarization: Tumor-associated macrophages as a paradigm for polarized M2 mononuclear phagocytes. *Trends in Immunology*. *23*(11), 549–555.

Marumoto, T., Tashiro, A., Friedmann-Morvinski, D., Scadeng, M., Soda, Y., Gage, F.H., and Verma, I.M. (2009). Development of a novel mouse glioma model using lentiviral vectors. *Nature Medicine*. *15*(1), 110–116.

Matochko, W.L., and Derda, R. (2015). Next-generation sequencing of phage-displayed peptide libraries. *Methods in Molecular Biology*. *1248*, 249–266.

Matsumura, Y., and Maeda, H. (1986). A New Concept for Macromolecular Therapeutics in Cancer Chemotherapy: Mechanism of Tumoritropic Accumulation of Proteins and the Antitumor Agent Smancs. *Cancer Research*. *46*(8), 6387–6392.

Mazzone, M., Dettori, D., Leite de Oliveira, R., Loges, S., Schmidt, T., Jonckx, B., Tian, Y.M., Lanahan, A.A., Pollard, P., Ruiz de Almodovar, C., De Smet, F., Vinckier, S., Aragonés, J., Debackere, K., Luttun, A., Wyns, S., Jordan, B., Pisacane, A., Gallez, B., Lampugnani, M.G., Dejana, E., Simons, M., Ratcliffe, P., Maxwell, P., and Carmeliet, P. (2009). Heterozygous Deficiency of PHD2 Restores Tumor Oxygenation and Inhibits Metastasis via Endothelial Normalization. *Cell*. *136*(5), 839–851.

McDonald, J.A. (1988). Extracellular matrix assembly. *Annual Review of Cell Biology*. *4*, 183–207.

Meyer, K., and Palmer, J.W. (1934). The Polysaccharide of the Vitreous Humor. *Journal of Biological Chemistry*. *107*(3), 629–634.

Midwood, K.S., and Orend, G. (2009). The role of tenascin-C in tissue injury and tumorigenesis. *Journal of Cell Communication and Signaling*. *3*(3–4), 287–310.

Mishra, J., and Panda, J.J. (2019). Short peptide-based smart targeted cancer nanotherapeutics: A glimmer of hope. *Therapeutic Delivery*. *10*(3), 135–138.

Misra, S., Hascall, V.C., Markwald, R.R., and Ghatak, S. (2015). Interactions between hyaluronan and its receptors (CD44, RHAMM) regulate the activities of inflammation and cancer. *Frontiers in Immunology*. *6*(MAY), 201.

Nakamura, F., and Goshima, Y. (2002). Structural and functional relation of neuropilins. *Advances in Experimental Medicine and Biology*. *515*, 55–69.

Nasarre, C., Roth, M., Jacob, L., Roth, L., Koncina, E., Thien, A., Labourdette, G., Poulet, P., Hubert, P., Crémel, G., Roussel, G., Aunis, D., and Bagnard, D. (2010). Peptide-based interference of the transmembrane domain of neuropilin-1 inhibits glioma growth in vivo. *Oncogene*. *29*(16), 2381–2392.

Navya, P.N., Kaphle, A., Srinivas, S.P., Bhargava, S.K., Rotello, V.M., and Daima, H.K. (2019). Current trends and challenges in cancer management and therapy using designer nanomaterials. *Nano Convergence*. *6*(1), 1–30.

Necas, J., Bartosikova, L., Brauner, P., and Kolar, J. (2008). Hyaluronic acid (hyaluronan): A review. *Veterinarni Medicina*. *53*(8), 397–411.

Neri, D., and Bicknell, R. (2005). Tumour vascular targeting. *Nature Reviews Cancer*. *5*(6), 436–446.

Ng, T.S.C., Garlin, M.A., Weissleder, R., and Miller, M.A. (2020). Improving nanotherapy delivery and action through image-guided systems pharmacology. *Theranostics*. *10*(3), 968–997.

Nikitovic, D., Tzardi, M., Berdiaki, A., Tsatsakis, A., and Tzanakakis, G.N. (2015). Cancer microenviroment and inflammation: Role of hyaluronan. *Frontiers in Immunology*. *6*(MAR).

Niland, S., and Eble, J.A. (2019). Neuropilins in the context of tumor vasculature. *International Journal of Molecular Sciences*. *20*(3), 639.

Nilsson, F., Kosmehl, H., Zardi, L., and Neri, D. (2001). Targeted delivery of tissue factor to the ED-B domain of fibronectin, a marker of angiogenesis, mediates the infarction of solid tumors in mice. *Cancer research*. *61*(2), 711–6.

van Obberghen-Schilling, E., Tucker, R.P., Saupe, F., Gasser, I., Cseh, B., and Orend, G. (2011). Fibronectin and tenascin-C: Accomplices in vascular morphogenesis during development and tumor growth. *International Journal of Developmental Biology*. *55*(4–5), 511–525.

Oh, P., Li, Y., Yu, J., Durr, E., Krasinska, K.M., Carver, L.A., Testa, J.E., and Schnitzer, J.E. (2004). Subtractive proteomic mapping of the endothelial surface in lung and solid tumours for tissue-specific therapy. *Nature*. *429*(6992), 629–635.

Ohnishi, T., Hiraga, S., Izumoto, S., Matsumura, H., Kanemura, Y., Arita, N., and Hayakawa, T. (1998). Role of fibronectin-stimulated tumor cell migration in glioma invasion in vivo: Clinical significance of fibronectin and fibronectin receptor expressed in human glioma tissues. *Clinical and Experimental Metastasis*. *16*(8), 729–741.

Orend, G., and Chiquet-Ehrismann, R. (2006). Tenascin-C induced signaling in cancer. *Cancer Letters*. *244*(2), 143–163.

Oyama, F., Hirohashi, S., Shimosato, Y., Titani, K., and Sekiguchi, K. (1990). Oncodevelopmental Regulation of the Alternative Splicing of Fibronectin PreMessenger RNA in Human Lung Tissues. *Cancer Research*. *50*(4), 1075–1078.

Paasonen, L., Sharma, S., Braun, G.B., Kotamraju, V.R., Chung, T.D.Y., She, Z.G., Sugahara, K.N., Yliperttula, M., Wu, B., Pellecchia, M., Ruoslahti, E., and Teesalu, T. (2016). New p32/gC1qR Ligands for Targeted Tumor Drug Delivery. *ChemBioChem*. *17*(7), 570–575.

Paganelli, G., Grana, C., Chinol, M., Cremonesi, M., De Cicco, C., De Braud, F., Robertson, C., Zurrida, S., Casadio, C., Zoboli, S., Siccardi, A.G., and Veronesi, U. (1999). Antibody-guided three-step therapy for high grade glioma with yttrium-90 biotin. *European Journal of Nuclear Medicine*. *26*(4), 348–357.

Pagani, F., Zagato, L., Vergani, C., Casari, G., Sidoli, A., and Baralle, F.E. (1991). Tissue-specific splicing pattern of fibronectin messenger RNA precursor during development and aging in rat. *Journal of Cell Biology*. *113*(5), 1223–1229.

Park, J., Kim, S., Saw, P.E., Lee, I.H., Yu, M.K., Kim, M., Lee, K., Kim, Y.C., Jeong, Y.Y., and Jon, S. (2012). Fibronectin extra domain B-specific aptide conjugated nanoparticles for targeted cancer imaging. *Journal of Controlled Release*. *163*(2), 111–118.

Park, J.H., Von Maltzahn, G., Zhang, L., Schwartz, M.P., Ruoslahti, E., Bhatia, S.N., and Sailor, M.J. (2008). Magnetic iron oxide nanoworms for tumor targeting and imaging. *Advanced Materials*. *20*(9), 1630–1635.

Park, J.W., Hong, K., Kirpotin, D.B., Colbern, G., Shalaby, R., Baselga, J., Shao, Y., Nielsen, U.B., Marks, J.D., Moore, D., Papahadjopoulos, D., and Benz, C.C. (2002). Anti-HER2 immunoliposomes: Enhanced efficacy attributable to targeted delivery. *Clinical Cancer Research*. *8*(4), 1172–1181.

Pasqualini, R., and Ruoslahti, E. (1996). Organ targeting in vivo using phage display peptide libraries. *Nature*. *380*(6572), 364–366.

Patra, J.K., Das, G., Fraceto, L.F., Campos, E.V.R., Rodriguez-Torres, M.D.P., Acosta-Torres, L.S., Diaz-Torres, L.A., Grillo, R., Swamy, M.K., Sharma, S., Habtemariam, S., and Shin, H.S. (2018). Nano based drug delivery systems: Recent developments and future prospects 10 Technology 1007 Nanotechnology 03 Chemical Sciences 0306 Physical Chemistry (incl. Structural) 03 Chemical Sciences 0303 Macromolecular and Materials Chemistry 11 Medical and He. *Journal of Nanobiotechnology*. *16*(1), 71.

Pemmari, T., Ivanova, L., May, U., Lingasamy, P., Tobi, A., Pasternack, A., Prince, S., Ritvos, O., Makkapati, S., Teesalu, T., Cairo, M.S., Järvinen, T.A.H., and Liao, Y. (2020a). Exposed CendR Domain in Homing Peptide Yields Skin-Targeted Therapeutic in Epidermolysis Bullosa. *Molecular Therapy*. *28*(8), 1833–1845.

Pemmari, T., Koho, T., and Järvinen, T.A.H. (2020b). Probing Vasculature by In Vivo Phage Display for Target Organ-Specific Delivery in Regenerative Medicine. *In* Vascularization for Tissue Engineering and Regenerative Medicine. Springer International Publishing, Cham. 1–26.

Pierschbacher, M.D., and Ruoslahti, E. (1984). Cell attachment activity of fibronectin can be duplicated by small synthetic fragments of the molecule. *Nature*. *309*(5963), 30–33.

Pini, A., Viti, F., Santucci, A., Carnemolla, B., Zardi, L., Neri, P., and Neri, D. (1998). Design and use of a phage display library: Antibodies with subnanomolar affinity against a marker of angiogenesis eluted from a two-dimensional gel. *Journal of Biological Chemistry*. *273*(34), 21769–21776.

Prud'homme, G.J., and Glinka, Y. (2012). Neuropilins are multifunctional coreceptors involved in tumor initiation, growth, metastasis and immunity. *Oncotarget*. *3*(9), 921–939.

Pufall, M.A. (2015). Glucocorticoids and cancer. *Advances in Experimental Medicine and Biology*. *872*, 315–333.

Pujuguet, P., Hammann, A., Moutet, M., Samuel, J.L., Martin, F., and Martin, M. (1996). Expression of fibronectin ED-A+ and ED-B+ isoforms by human and experimental colorectal cancer: Contribution of cancer cells and tumor-associated myofibroblasts. *American Journal of Pathology*. *148*(2), 579–592.

Pytela, R., Pierschbacher, M.D., and Ruoslahti, E. (1985). Identification and isolation of a 140 kd cell surface glycoprotein with properties expected of a fibronectin receptor. *Cell*. *40*(1), 191–198.

Quail, D.F., and Joyce, J.A. (2013). Microenvironmental regulation of tumor progression and metastasis. *Nature Medicine*. *19*(11), 1423–1437.

Raavé, R., van Kuppevelt, T.H., and Daamen, W.F. (2018). Chemotherapeutic drug delivery by tumoral extracellular matrix targeting. *Journal of Controlled Release*. *274*, 1–8.

Rafii, S., Lyden, D., Benezra, R., Hattori, K., and Heissig, B. (2002). Vascular and haematopoietic stem cells: Novel targets for anti-angiogenesis therapy? *Nature Reviews Cancer*. *2*(11), 826–835.

Rajabi, M., and Mousa, S.A. (2017). The role of angiogenesis in cancer treatment. *Biomedicines*. *5*(2), 34.

Rak, J., Yu, J.L., Kerbel, R.S., and Coomber, B.L. (2002). What do oncogenic mutations have to do with angiogenesis/vascular dependence of tumors? *Cancer Research*. *62*(7), 1931–1934.

Riva, P., Franceschi, G., Frattarelli, M., Lazzari, S., Riva, N., Giuliani, G., Casi, M., Sarti, G., Guiducci, G., Giorgetti, G., Gentile, R., Santimaria, M., Jermann, E., and Maeke, H.R. (1999). Loco-regional radioimmunotherapy of high-grade malignant gliomas using specific monoclonal antibodies labeled with 90Y: A phase I study. *Clinical Cancer Research*. *5*(10 SUPPL.), 3275s-3280s.

Rosenblum, D., Joshi, N., Tao, W., Karp, J.M., and Peer, D. (2018). Progress and challenges towards targeted delivery of cancer therapeutics. *Nature Communications*. *9*(1), 1–12.

Roth-Kleiner, M., Hirsch, E., and Schittny, J.C. (2004). Fetal Lungs of Tenascin-C-Deficient Mice Grow Well, but Branch Poorly in Organ Culture. *American Journal of Respiratory Cell and Molecular Biology*. *30*(3), 360–366.

Roth, L., Agemy, L., Kotamraju, V.R., Braun, G., Teesalu, T., Sugahara, K.N., Hamzah, J., and Ruoslahti, E. (2012). Transtumoral targeting enabled by a novel neuropilin-binding peptide. *Oncogene*. *31*(33), 3754–3763.

Rothenberg, M.L. (1997). Topoisomerase I inhibitors: Review and update. *Annals of Oncology*. *8*(9), 837–855.

Ruoslahti, E. (1988). Fibronectin and its receptors. *Annual Review of Biochemistry*. *57*(1), 375–413.

Ruoslahti, E. (2002). Specialization of tumour vasculature. *Nature Reviews Cancer*. *2*(2), 83–90.

Ruoslahti, E. (2012). Peptides as targeting elements and tissue penetration devices for nanoparticles. *Advanced Materials*. *24*(28), 3747–3756.

Ruoslahti, E. (2017). Tumor penetrating peptides for improved drug delivery. *Advanced drug delivery reviews*. *110–111*, 3–12.

Ruoslahti, E., Bhatia, S.N., and Sailor, M.J. (2010). Targeting of drugs and nanoparticles to tumors. *Journal of Cell Biology*. *188*(6), 759–768.

Rybak, J.N., Roesli, C., Kaspar, M., Villa, A., and Neri, D. (2007). The extra-domain A of fibronectin is a vascular marker of solid tumors and metastases. *Cancer Research*. *67*(22), 10948–10957.

Säälik, P., Lingasamy, P., Toome, K., Mastandrea, I., Rousso-Noori, L., Tobi, A., Simón-Gracia, L., Hunt, H., Paiste, P., Kotamraju, V.R., Bergers, G., Asser, T., Rätsep, T., Ruoslahti, E., Bjerkvig, R., Friedmann-Morvinski, D., and Teesalu, T. (2019). Peptide-guided nanoparticles for glioblastoma targeting. *Journal of Controlled Release*. *308*, 109–118.

Saha, P., and Datta, K. (2018). Multifuctional, multicompartmental hyaluronan-binding protein 1 (HABP1/p32/gC1qR): Implication in cancer progression and metastasis. *Oncotarget*. *9*(12), 10784–10807.

Santimaria, M., Moscatelli, G., Viale, G.L., Giovannoni, L., Neri, G., Viti, F., Leprini, A., Borsi, L., Castellani, P., Zardi, L., Neri, D., and Riva, P. (2003). Immunoscintigraphic detection of the ED-B domain of fibronectin, a marker of angiogenesis, in patients with cancer. *Clinical Cancer Research*. *9*(2), 571–579.

Saw, P.E., and Song, E.W. (2019). Phage display screening of therapeutic peptide for cancer targeting and therapy. *Protein and Cell*. *10*(11), 787–807.

Schanté, C.E., Zuber, G., Herlin, C., and Vandamme, T.F. (2011). Chemical modifications of hyaluronic acid for the synthesis of derivatives for a broad range of biomedical applications. *Carbohydrate Polymers*. *85*(3), 469–489.

Schliemann, C., and Neri, D. (2007). Antibody-based targeting of the tumor vasculature. *Biochimica et Biophysica Acta – Reviews on Cancer*. *1776*(2), 175–192.

Schliemann, C., Palumbo, A., Zuberbühler, K., Villa, A., Kaspar, M., Trachsel, E., Klapper, W., Menssen, H.D., and Neri, D. (2009a). Complete eradication of human B-cell lymphoma xenografts using rituximab in combination with the immunocytokine L19-IL2. *Blood*. *113*(10), 2275–2283.

Schliemann, C., Wiedmer, A., Pedretti, M., Szczepanowski, M., Klapper, W., and Neri, D. (2009b). Three clinical-stage tumor targeting antibodies reveal differential expression of oncofetal fibronectin and tenascin-C isoforms in human lymphoma. *Leukemia Research*. *33*(12), 1718–1722.

Schwarzbauer, J.E., Tamkun, J.W., Lemischka, I.R., and Hynes, R.O. (1983). Three different fibronectin mRNAs arise by alternative splicing within the coding region. *Cell*. *35*(2 PART 1), 421–431.

Scodeller, P., and Asciutto, E.K. (2020). Targeting tumors using peptides. *Molecules*. *25*(4), 808.

Sharma, S., Kotamraju, V.R., Mölder, T., Tobi, A., Teesalu, T., and Ruoslahti, E. (2017). Tumor-Penetrating Nanosystem Strongly Suppresses Breast Tumor Growth. *Nano Letters*. *17*(3), 1356–1364.

Sherwood, L.M., Parris, E.E., and Folkman, J. (1971). Tumor Angiogenesis: Therapeutic Implications. *New England Journal of Medicine*. *285*(21), 1182–1186.

Shi, J., Kantoff, P.W., Wooster, R., and Farokhzad, O.C. (2017). Cancer nanomedicine: Progress, challenges and opportunities. *Nature Reviews Cancer*. *17*(1), 20–37.

Shimaoka, M., and Springer, T.A. (2003). Therapeutic antagonists and conformational regulation of integrin function. *Nature Reviews Drug Discovery*. *2*(9), 703–716.

Silacci, M., Brack, S.S., Späth, N., Buck, A., Hillinger, S., Arni, S., Weder, W., Zardi, L., and Neri, D. (2006). Human monoclonal antibodies to domain C of tenascin-C selectively target solid tumors in vivo. *Protein Engineering, Design and Selection*. *19*(10), 471–478.

Simón-Gracia, L., Hunt, H., and Teesalu, T. (2018a). Peritoneal carcinomatosis targeting with tumor homing peptides. *Molecules*. *23*(5).

Simón-Gracia, L., Scodeller, P., Fuentes, S.S., Vallejo, V.G., Ríos, X., Sebastián, E.S., Sidorenko, V., Di Silvio, D., Suck, M., De Lorenzi, F., Rizzo, L.Y., Stillfried, S. von, Kilk, K., Lammers, T., Moya, S.E., and Teesalu, T. (2018b). Application of polymersomes engineered to target p32 protein for detection of small breast tumors in mice. *Oncotarget*. *9*(27), 18682–18697.

Smith, G.P. (1985). Filamentous fusion phage: Novel expression vectors that display cloned antigens on the virion surface. *Science*. *228*(4705), 1315–1317.

Smith, G.P., and Petrenko, V.A. (1997). Phage display. *Chemical Reviews*. *97*(2), 391–410.

Song, S., Ewald, A.J., Stallcup, W., Werb, Z., and Bergers, G. (2005). PDGFRβ+ perivascular progenitor cells in tumours regulate pericyte differentiation and vascular survival. *Nature Cell Biology*. *7*(9), 870–879.

Spenlé, C., Saupe, F., Midwood, K., Burckel, H., Noel, G., and Orend, G. (2015). Tenascin-C: Exploitation and collateral damage in cancer management. *Cell Adhesion and Migration*. *9*(1–2), 141–153.

Stallcup, W.B., and Huang, F.J. (2008). A role for the NG2 proteoglycan in glioma progression. *Cell adhesion & migration*. *2*(3), 192–201.

Stasikowska-Kanicka, O., Wągrowska-Danilewicz, M., and Danilewicz, M. (2018). Immunohistochemical study on neuropilin 1 (NRP1) immunoexpression in oral squamous cell carcinoma. *Folia Histochemica et Cytobiologica*. *56*(2), 98–105.

Staton, C.A., Kumar, I., Reed, M.W.R., and Brown, N.J. (2007). Neuropilins in physiological and pathological angiogenesis. *Journal of Pathology*. *212*(3), 237–248.

Stephenson, J.M., Banerjee, S., Saxena, N.K., Cherian, R., and Banerjee, S.K. (2002). Neuropilin-1 is differentially expressed in myoepithelial cells and vascular smooth muscle cells in preneoplastic and neoplastic human breast: A possible marker for the progression of breast cancer. *International Journal of Cancer*. *101*(5), 409–414.

Storz, P., Hausser, A., Link, G., Dedio, J., Ghebrehiwet, B., Pfizenmaier, K., and Johannes, F.J. (2000). Protein kinase C μ is regulated by the multifunctional chaperon protein p32. *Journal of Biological Chemistry*. *275*(32), 24601–24607.

Sugahara, K.N., Teesalu, T., Karmali, P.P., Kotamraju, V.R., Agemy, L., Girard, O.M., Hanahan, D., Mattrey, R.F., and Ruoslahti, E. (2009). Tissue-Penetrating Delivery of Compounds and Nanoparticles into Tumors. *Cancer Cell*. *16*(6), 510–520.

Sugahara, K.N., Teesalu, T., Prakash Karmali, P., Ramana Kotamraju, V., Agemy, L., Greenwald, D.R., and Ruoslahti, E. (2010). Coadministration of a tumor-penetrating peptide enhances the efficacy of cancer drugs. *Science*. *328*(5981), 1031–1035.

Takada, Y., Ye, X., and Simon, S. (2007). The integrins. *Genome Biology*. *8*(5), 215.

Takagi, S., Tsuji, T., Amagai, T., Takamatsu, T., and Fujisawa, H. (1987). Specific cell surface labels in the visual centers of Xenopus laevis tadpole identified using monoclonal antibodies. *Developmental Biology*. *122*(1), 90–100.

Takashima, S., Kitakaze, M., Asakura, M., Asanuma, H., Sanada, S., Tashiro, F., Niwa, H., Miyazaki, J.I., Hirota, S., Kitamura, Y., Kitsukawa, T., Fujisawa, H., Klagsbrun, M., and Hori, M. (2002). Targeting of both mouse neuropilin-1 and neuropilin-2 genes severely impairs developmental yolk sac and embryonic angiogenesis. *Proceedings of the National Academy of Sciences of the United States of America*. *99*(6), 3657–3662.

Talasila, K.M., Soentgerath, A., Euskirchen, P., Rosland, G. V., Wang, J., Huszthy, P.C., Prestegarden, L., Skaftnesmo, K.O., Sakariassen, P.Ø., Eskilsson, E., Stieber, D., Keunen, O., Brekka, N., Moen, I., Nigro, J.M., Vintermyr, O.K., Lund-Johansen, M., Niclou, S., Mørk, S.J., Enger, P.Ø., Bjerkvig, R., and Miletic, H. (2013). EGFR wild-type amplification and activation promote invasion and development of glioblastoma independent of angiogenesis. *Acta Neuropathologica*. *125*(5), 683–698.

Talmadge, J.E. (2011). Immune cell infiltration of primary and metastatic lesions: Mechanisms and clinical impact. *Seminars in Cancer Biology*. *21*(2), 131–138.

Tamkun, J.W., Schwarzbauer, J.E., and Hynes, R.O. (1984). A single rat fibronectin gene generates three different mRNAs by alternative splicing of a complex exon. *Proceedings of the National Academy of Sciences of the United States of America*. *81*(16 I), 5140–5144.

Tammela, T., and Alitalo, K. (2010). Lymphangiogenesis: Molecular Mechanisms and Future Promise. *Cell*. *140*(4), 460–476.

Tanaka, H., El-Karef, A., Kaito, M., Kinoshita, N., Fujita, N., Horiike, S., Watanabe, S., Yoshida, T., and Adachi, Y. (2006). Circulating level of large splice variants of

tenascin-C is a marker of piecemeal necrosis activity in patients with chronic hepatitis C. *Liver International*. *26*(3), 311–318.

Teesalu, T., and Lingasamy, P. (2020). Bi-Specific Extracellular Matrix Binding Peptides and Methods of Use Thereof (PCT Patent No. WO2020161602).

Teesalu, T., Sugahara, K.N., Kotamraju, V.R., and Ruoslahti, E. (2009). C-end rule peptides mediate neuropilin-1-dependent cell, vascular, and tissue penetration. *Proceedings of the National Academy of Sciences of the United States of America*. *106*(38), 16157–16162.

Teesalu, T., Sugahara, K.N., and Ruoslahti, E. (2012). Mapping of vascular ZIP codes by phage display. *Methods in Enzymology*. *503*, 35–56.

Teesalu, T., Sugahara, K.N., and Ruoslahti, E. (2013). Tumor-penetrating peptides. *Frontiers in Oncology*. *3 AUG*, 216.

Tonini, T., Rossi, F., and Claudio, P.P. (2003). Molecular basis of angiogenesis and cancer. *Oncogene*. *22*(43), 6549–6556.

Toome, K., Willmore, A.M.A., Paiste, P., Tobi, A., Sugahara, K.N., Kirsimäe, K., Ruoslahti, E., Braun, G.B., and Teesalu, T. (2017). Ratiometric: In vivo auditioning of targeted silver nanoparticles. *Nanoscale*. *9*(28), 10094–10100.

Torrieri, G., Fontana, F., Figueiredo, P., Liu, Z., Ferreira, M.P.A., Talman, V., Martins, J.P., Fusciello, M., Moslova, K., Teesalu, T., Cerullo, V., Hirvonen, J., Ruskoaho, H., Balasubramanian, V., and Santos, H.A. (2020). Dual-peptide functionalized acetalated dextran-based nanoparticles for sequential targeting of macrophages during myocardial infarction. *Nanoscale*. *12*(4), 2350–2358.

Trachsel, E., Kaspar, M., Bootz, F., Detmar, M., and Neri, D. (2007). A human mAb specific to oncofetal fibronectin selectively targets chronic skin inflammation in vivo. *Journal of Investigative Dermatology*. *127*(4), 881–886.

Tse, B.W.C., Volpert, M., Ratther, E., Stylianou, N., Nouri, M., McGowan, K., Lehman, M.L., McPherson, S.J., Roshan-Moniri, M., Butler, M.S., Caradec, J., Gregory-Evans, C.Y., McGovern, J., Das, R., Takhar, M., Erho, N., Alshalafa, M., Davicioni, E., Schaeffer, E.M., Jenkins, R.B., Ross, A.E., Karnes, R.J., Den, R.B., Fazli, L., Gregory, P.A., Gleave, M.E., Williams, E.D., Rennie, P.S., Buttyan, R., Gunter, J.H., Selth, L.A., Russell, P.J., Nelson, C.C., and Hollier, B.G. (2017). Neuropilin-1 is upregulated in the adaptive response of prostate tumors to androgen-targeted therapies and is prognostic of metastatic progression and patient mortality. *Oncogene*. *36*(24), 3417–3427.

Tsesmetzis, N., Paulin, C.B.J., Rudd, S.G., and Herold, N. (2018). Nucleobase and nucleoside analogues: Resistance and re-sensitisation at the level of pharmacokinetics, pharmacodynamics and metabolism. *Cancers*. *10*(7), 240.

Tucker, R.P., and Chiquet-Ehrismann, R. (2015). Tenascin-C: Its functions as an integrin ligand. *International Journal of Biochemistry and Cell Biology*. *65*, 165–168.

Tucker, R.P., Spring, J., Baumgartner, S., Martin, D., Hagios, C., Poss, P.M., and Chiquet-Ehrismann, R. (1994). Novel tenascin variants with a distinctive pattern of expression in the avian embryo. *Development*. *120*(3), 637–647.

Valkenburg, K.C., De Groot, A.E., and Pienta, K.J. (2018). Targeting the tumour stroma to improve cancer therapy. *Nature Reviews Clinical Oncology*. *15*(6), 366–381.

Veiksina, S., Kopanchuk, S., Mazina, O., Link, R., Lille, A., and Rinken, A. (2015). Homogeneous fluorescence anisotropy-based assay for characterization of ligand binding dynamics to GPCRs in budded baculoviruses: The case of Cy3B-NDP-α-MSH binding to MC4 receptors. *In* Methods in Molecular Biology. Springer New York. 37–50.

Veiksina, S., Kopanchuk, S., and Rinken, A. (2014). Budded baculoviruses as a tool for a homogeneous fluorescence anisotropy-based assay of ligand binding to G protein-coupled receptors: The case of melanocortin 4 receptors. *Biochimica et Biophysica Acta – Biomembranes*. *1838*(1 PARTB), 372–381.

Venning, F.A., Wullkopf, L., and Erler, J.T. (2015). Targeting ECM disrupts cancer progression. *Frontiers in Oncology*. *5*(OCT), 224.

Ventola, C.L. (2017). Progress in nanomedicine: Approved and investigational nano-drugs. *P and T*. *42*(12), 742–755.

Viale, G.L., Castellani, P., Dorcaratto, A., Pau, A., Sehrbundt, E., Siri, A., Birò, A., Zardi, L., Lesniak, M.S., Rigamonti, D., and Piepmeier, J.M. (2002). Occurrence of a glioblastoma-associated Tenascin-C isoform in cerebral cavernomas and neighboring vessels. *Neurosurgery*. *50*(4), 838–842.

Villa, A., Trachsel, E., Kaspar, M., Schliemann, C., Sommavilla, R., Rybak, J.N., Rösli, C., Borsi, L., and Neri, D. (2008). A high-affinity human monoclonal antibody specific to the alternatively spliced EDA domain of fibronectin efficiently targets tumor neo-vasculature in vivo. *International Journal of Cancer*. *122*(11), 2405–2413.

Vivekanandhan, S., and Mukhopadhyay, D. (2019). Genetic status of KRAS influences Transforming Growth Factor-beta (TGF-β) signaling: An insight into Neuropilin-1 (NRP1) mediated tumorigenesis. *Seminars in Cancer Biology*. *54*, 72–79.

Vrettos, E.I., Mező, G., and Tzakos, A.G. (2018). On the design principles of peptide–drug conjugates for targeted drug delivery to the malignant tumor site. *Beilstein Journal of Organic Chemistry*. *14*, 930–954.

Wang, J., Liu, Y., Teesalu, T., Sugahara, K.N., Kotamrajua, V.R., Adams, J.D., Ferguson, B.S., Gong, Q., Oh, S.S., Csordas, A.T., Cho, M., Ruoslahti, E., Xiao, Y., and Soh, H.T. (2011). Selection of phage-displayed peptides on live adherent cells in microfluidic channels. *Proceedings of the National Academy of Sciences of the United States of America*. *108*(17), 6909–6914.

Wang, T., Chen, C., Larcher, L.M., Barrero, R.A., and Veedu, R.N. (2019). Three decades of nucleic acid aptamer technologies: Lessons learned, progress and opportunities on aptamer development. *Biotechnology Advances*. *37*(1), 28–50.

Ween, M.P., Oehler, M.K., and Ricciardelli, C. (2011). Role of versican, hyaluronan and CD44 in ovarian cancer metastasis. *International Journal of Molecular Sciences*. *12*(2), 1009–1029.

Weide, B., Eigentler, T., Catania, C., Ascierto, P.A., Cascinu, S., Becker, J.C., Hauschild, A., Romanini, A., Danielli, R., Dummer, R., Trefzer, U., Elia, G., Neri, D., and Garbe, C. (2019). A phase II study of the L19IL2 immunocytokine in combination with dacarbazine in advanced metastatic melanoma patients. *Cancer Immunology, Immunotherapy*. *68*(9), 1547–1559.

Wierzbicka-Patynowski, I., and Schwarzbauer, J.E. (2003). The ins and outs of fibronectin matrix assembly. *Journal of Cell Science*. *116*(16), 3269–3276.

Wilhelm, S., Tavares, A.J., Dai, Q., Ohta, S., Audet, J., Dvorak, H.F., and Chan, W.C.W. (2016). Analysis of nanoparticle delivery to tumours. *Nature Reviews Materials*. *1*(ue 5), 16014.

Willmore, A.M.A., Simón-Gracia, L., Toome, K., Paiste, P., Kotamraju, V.R., Mölder, T., Sugahara, K.N., Ruoslahti, E., Braun, G.B., and Teesalu, T. (2016). Targeted silver nanoparticles for ratiometric cell phenotyping. *Nanoscale*. *8*(17), 9096–9101.

Wu, W., Chen, L., Wang, Y., Jin, J., Xie, X., and Zhang, J. (2020). Hyaluronic acid predicts poor prognosis in breast cancer patients: A protocol for systematic review and meta analysis. *Medicine*. *99*(22), e20438.

Yang, Y.H., Rajaiah, R., Ruoslahti, E., and Moudgil, K.D. (2011). Peptides targeting inflamed synovial vasculature attenuate autoimmune arthritis. *Proceedings of the National Academy of Sciences of the United States of America*. *108*(31), 12857–12862.

Yoo, J., Park, C., Yi, G., Lee, D., and Koo, H. (2019). Active targeting strategies using biological ligands for nanoparticle drug delivery systems. *Cancers*. *11*(5).

Yu, H., Teng, C., Liu, Q., Xin, T., Xing, L., Dong, G., Jiang, Q., Lv, Y., Song, X., Huang, D., Li, Y., Shen, W., Jin, Y., and Zhang, F. (2013). Elevated expression of hyaluronic acid binding protein 1 (HABP1)/P32/C1QBP is a novel indicator for lymph node and peritoneal metastasis of epithelial ovarian cancer patients. *Tumor Biology*. *34*(6), 3981–3987.

Zanotelli, M.R., and Reinhart-King, C.A. (2018). Mechanical forces in tumor angiogenesis. *In* Advances in Experimental Medicine and Biology. Springer New York LLC. 91–112.

Zhang, Y., Sun, T., and Jiang, C. (2018). Biomacromolecules as carriers in drug delivery and tissue engineering. *Acta Pharmaceutica Sinica B*. *8*(1), 34–50.

Zhao, J., Liu, T., Yu, G., and Wang, J. (2015). Overexpression of HABP1 correlated with clinicopathological characteristics and unfavorable prognosis in endometrial cancer. *Tumor Biology*. *36*(2), 1299–1306.

Zhao, Z., Ukidve, A., Kim, J., and Mitragotri, S. (2020). Targeting Strategies for Tissue-Specific Drug Delivery. *Cell*. *181*(1), 151–167.

Zhong, W., Pang, L., Feng, H., Dong, H., Wang, S., Cong, H., Shen, Y., and Bing, Y. (2020). Recent advantage of hyaluronic acid for anti-cancer application: a review of "3S" transition approach. *Carbohydrate Polymers*. *238*, 116204.

ACKNOWLEDGMENTS

This research work was performed at the Lab of Cancer Biology group at the University of Tartu. Firstly my sincere thanks go to my supervisor, professor Tambet Teesalu, for providing me the opportunity to research in the exciting cross-disciplinary field of a peptide targeted delivery on cancer. Throughout my Ph.D. studies, he was available for discussion anytime, provided constant support and guidance. Thanks for his support, great discussions, and his ideas during the years.

Thanks to all current and former cancer biology lab members for being fantastic colleagues and having a great working environment. It was a great pleasure to work with all of you. I would also like to thank all my great collaborators and co-authors for their contribution and support, particularly Dr. Päärn Paiste for the ICP-MS and Dr. Sergei Kopanchuk for the FA assay. Thanks to rector professor Toomas Asser and associate professor Tõnu Rätsep for the patient samples and their support. Many thanks to professor Erkki Ruoslahti and professor Rolf Bjerkvig for the valuable technical suggestions and proofreading of articles.

I am very thankful to peer-reviewers associate professor Karin Kogerman and Dr. Olesja Bodarenko for their time, helpful comments, suggestions, and constructive criticism for improving the Ph.D. thesis.

I want to dedicate this work to my late parents, Lingasamy and Selvi, who have supported me throughout their lifetime. Thanks to my grandparents and cousins for their support and help during my childhood education. Finally, I would like to thank my wonderful wife Vijayachitra Modhukur, and my lovely son Vikas Prakash for giving me all the emotional support during all these years.

PUBLICATIONS

CURRICULUM VITAE

Name: Prakash Lingasamy
Date of Birth: March 02, 1984, Dharapuram, TN, India
Citizenship: Indian
Address: Lab of Cancer Biology,
Institute of Biomedicine and Translational Medicine,
University of Tartu, Ravila 14b 50411, Tartu
Phone: +372 5889 1103
E-mail: prakash@ut.ee, prakashbio@gmail.com

Education:

2012 – …	Ph.D. student, Faculty of Medicine, University of Tartu
2006–2009	M.Sc. Biotechnology- specialized in Molecular Biotechnology, Royal Institute of Technology (KTH), Stockholm, Sweden
2002–2005	B.Tech. Industrial Biotechnology, Anna University, India
1999–2002	Diploma in Computer Technology, T.R.N. Polytechnic College, India

Professional employments:

2015–2020	University of Tartu, Cancer Biology Group, Institute of Biomedicine and Translational Medicine, Specialist
2009–2012	University Hospital Inselspital, University of Berne, Switzerland, Research Scientist
2008–2009	Lonza AG, Switzerland, Downstream process development, Intern
2008	Denmark Technical University (DTU), Denmark, Researcher
2005–2006	PPTS Pvt. Ltd, India, Clinical Trial Research Trainee
2004–2005	Virchow Biotech Pvt. Ltd, India, Research assistant

Dissertations supervised:

2019	Anett-Hildegard Laarmann, Master's Degree, 2019, Development of tumor penetrating antibodies, University of Tartu
2015	Markko Salumäe, Master's Degree, 2015, Identification of peptide motifs that bind to Nucleolin and FnIII-C domain of Tenascin-C, University of Tartu

Publications, Patents, and Book chapters:
Publications:

1. **Lingasamy, P.**, Laarmann, A., Teesalu, T., Tumor penetrating peptide-functionalized Tenascin C targeting antibody for glioblastoma targeting, *Current Cancer Drug Targets*, 2020 Oct 1;20:11–1.
2. Pemmari, T., Ivanova, L., May, M., **Lingasamy, P.**, Pasternack,A., Tobi, A., Pasternack, A., Prince, S., Ritvos, O., Makkapati, S., Teesalu, T., Cairo, MS.,

Järvinen, TAH., Liao, Y., Exposed CendR Domain in Homing Peptide Yields Skin-Targeted Therapeutic in Epidermolysis Bullosa, *Molecular therapy : the journal of the American Society of Gene Therapy*, 2020 May 20;S1525-0016(20)30251-3.

3. **Lingasamy, P**., Tobi, A, Kurm, k., Sudakov, A., Salumäe, M., Rätsep, T., Asser, T., Bjerkvig, R., Teesalu, T., Tumor-penetrating peptide for systemic targeting of Tenascin-C, *Scientific Reports*, 2020 Apr 2;10(1):5809
4. **Lingasamy, P**., Tobi, A., Haugas, M., Hunt, H., Paiste, P., Asser, T., Rätsep, T., Kotamraju, V. R., Bjerkvig, R., Teesalu, T., Bi-specific tenascin-C and fibronectin targeted peptide for solid tumor delivery, *Biomaterials*, 2019 Oct;219:119373.
5. Säälik, P.*, **Lingasamy, P**.*, Toome, K., Mastandrea, I., Rousso-Noori, L., Tobi, A., Simón-Gracia, L., Hunt, H., Paiste, P., Kotamraju, V. R., Bergers, G., Asser, T., Rätsep, T., Ruoslahti, E., Bjerkvig, R., Friedmann-Morvinski, D., Teesalu, T., Peptide-guided nanoparticles for glioblastoma targeting, *Journal of Controlled Release*, 2019 Aug 28;308:109–118.
6. Ikemoto, H., **Lingasamy, P**., Willmore, A. M. A., Hunt, H., Kurm, K., Tammik, O., Scodeller, P., Simón-Gracia, L., Kotamraju, V. R., Lowy, A. M., Sugahara, K. N., Teesalu, T., Hyaluronan-binding peptide for targeting peritoneal carcinomatosis, *Tumor Biology*, 2017 May; 39(5):1010428317701628.
7. Favre, B., Begré, N., Bouameur, J. E., **Lingasamy, P.**, Conover, G. M., Fontao, L., Borradori, L., Desmoplakin interacts with the coil 1 of different types of intermediate filament proteins and displays high affinity for assembled intermediate filaments, *PLoS ONE*, 2018 Oct 4;13(10):e0205038.
8. Bouameur, J. E., Favre, B., Fontao, L., **Lingasamy, P.**, Begré, N., Borradori, L., 2014: Interaction of plectin with keratins 5 and 14: Dependence on several plectin domains and keratin quaternary structure. *Journal of Investigative Dermatology*., 134, 2776–2783.
9. Bouameur, J. E., Schneider, Y., Begre, N., Hobbs, R. P., **Lingasamy, P.**, Fontao, L., Green, K. J., Favre, B., Borradori, L., Phosphorylation of serine 4642 in the C-terminus of plectin by MNK2 and PKA modulates its interaction with intermediate filaments. *Journal of Cell Science*, 2014 Nov,134(11):2776–2783.
10. Favre, B.*, Schneider, Y.*, **Lingasamy, P.***, Bouameur, J. E., Begré, N., Gontier, Y., Steiner-Champliaud, M. F., Frias, M. A., Borradori, L., Fontao, L., Plectin interacts with the rod domain of type III intermediate filament proteins desmin and vimentin. *European Journal of Cell Biology,* 2011 May;90(5):390–400.

Patents:

1. Title of Invention: "BI-SPECIFIC EXTRACELLULAR MATRIX BINDING PEPTIDES AND METHODS OF USE THEREOF", Tambet Teesalu and **Prakash Lingasamy,** Our Ref.: TARTU 100 (095468/00002) and Registered US Provisional Patent Application Number: 62800879, International PCT No: IB2020/050847

Book chapters:

1. **Lingasamy, P.,** & Teesalu, T. (2020). Chapter XX: Homing peptides for cancer therapy. In Bio-Nanomedicine for Cancer Therapy, H. Santos & F. Fontana (Eds.) (1st ed., pp. X, 420). *Springer Nature Switzerland AG* (In press).

ELULOOKIRJELDUS

Nimi:	Prakash Lingasamy
Sünniaeg:	2. märts, 1984, Dharapuram, TN, India
Kodakondsus:	India
Kontaktandmed:	Tartu Ülikool, arstiteaduskond, bio- ja siirdemeditsiini instituut, Vähibioloogia laboratoorium
Telefon:	+372 588 91103
E-mail:	prakash@ut.ee, prakashbio@gmail.com

Hariduskäik:

2012 – …	Doktorant, Tartu Ülikool, arstiteaduskond, bio- ja siirdemeditsiini instituut
2006–2009	M.Sc. Biotehnoloogia – Kuninglik Tehnhnoloogiainstituut (KTH), Stockholm, Rootsi.
2002–2005	B.Tech., Anna University, India.
1999–2002	Diplom informaatikas, T.R.N. Polytechnic College, India.

Teenistuskäik:

2015–2020	Spetsialist, Tartu Ülikool, arstiteaduskond, bio- ja siirdemeditsiini instituut
2009–2012	Teadur, Berni Ülikool, Sveits.
2008–2009	Intern, Lonza AG, Sveits.
2008	Teadur, Denmark Technical University (DTU), Denmark, Taani.
2005–2006	Kliiniliste ravimiuuringute praktikant, PPTS Pvt. Ltd, India.
2004–2005	Assistent, Virchow Biotech Pvt. Ltd, India.

Juhendatud väitekirjad:

2019	Anett-Hildegard Laarmann, M.Sc. 2019, “Development of tumor penetrating antibodies”, Tartu Ülikool.
2015	Markko Salumäe, M.Sc. kraad 2015, “Identification of peptide motifs that bind to Nucleolin and FnIII-C domain of Tenascin-C”, Tartu Ülikool.

Publikatsioonid, Patendid ja Raamatute peatükid:

Publikatsioonid:

1. **Lingasamy, P.**, Laarmann, A., Teesalu, T., Tumor penetrating peptide-functionalized Tenascin C targeting antibody for glioblastoma targeting, *Current Cancer Drug Targets*, 2020 Oct 1;20:11–1.

2. Pemmari, T., Ivanova, L., May, M., **Lingasamy, P.**, Pasternack,A., Tobi, A., Pasternack, A., Prince, S., Ritvos, O., Makkapati, S., Teesalu, T., Cairo, MS., Järvinen, TAH., Liao, Y., Exposed CendR Domain in Homing Peptide Yields Skin-Targeted Therapeutic in Epidermolysis Bullosa, *Molecular therapy : the journal of the American Society of Gene Therapy*, 2020 May 20;S1525-0016(20)30251-3.
3. **Lingasamy, P**., Tobi, A, Kurm, k., Sudakov, A., Salumäe, M., Rätsep, T., Asser, T., Bjerkvig, R., Teesalu, T., Tumor-penetrating peptide for systemic targeting of Tenascin-C, *Scientific Reports*, 2020 Apr 2;10(1):5809
4. **Lingasamy, P**., Tobi, A., Haugas, M., Hunt, H., Paiste, P., Asser, T., Rätsep, T., Kotamraju, V. R., Bjerkvig, R., Teesalu, T., Bi-specific tenascin-C and fibronectin targeted peptide for solid tumor delivery, *Biomaterials*, 2019 Oct;219:119373.
5. Säälik, P.*, **Lingasamy, P**.*, Toome, K., Mastandrea, I., Rousso-Noori, L., Tobi, A., Simón-Gracia, L., Hunt, H., Paiste, P., Kotamraju, V. R., Bergers, G., Asser, T., Rätsep, T., Ruoslahti, E., Bjerkvig, R., Friedmann-Morvinski, D., Teesalu, T., Peptide-guided nanoparticles for glioblastoma targeting, *Journal of Controlled Release*, 2019 Aug 28;308:109–118.
6. Ikemoto, H., **Lingasamy, P**., Willmore, A. M. A., Hunt, H., Kurm, K., Tammik, O., Scodeller, P., Simón-Gracia, L., Kotamraju, V. R., Lowy, A. M., Sugahara, K. N., Teesalu, T., Hyaluronan-binding peptide for targeting peritoneal carcinomatosis, *Tumor Biology*, 2017 May; 39(5):1010428317701628.
7. Favre, B., Begré, N., Bouameur, J. E., **Lingasamy, P.**, Conover, G. M., Fontao, L., Borradori, L., Desmoplakin interacts with the coil 1 of different types of intermediate filament proteins and displays high affinity for assembled intermediate filaments, *PLoS ONE*, 2018 Oct 4;13(10):e0205038.
8. Bouameur, J. E., Favre, B., Fontao, L., **Lingasamy, P.**, Begré, N., Borradori, L., 2014: Interaction of plectin with keratins 5 and 14: Dependence on several plectin domains and keratin quaternary structure. *Journal of Investigative Dermatology*., 134, 2776–2783.
9. Bouameur, J. E., Schneider, Y., Begre, N., Hobbs, R. P., **Lingasamy, P.**, Fontao, L., Green, K. J., Favre, B., Borradori, L., Phosphorylation of serine 4642 in the C-terminus of plectin by MNK2 and PKA modulates its interaction with intermediate filaments. *Journal of Cell Science*, 2014 Nov,134(11):2776–2783.
10. Favre, B.*, Schneider, Y.*, **Lingasamy, P.***, Bouameur, J. E., Begré, N., Gontier, Y., Steiner-Champliaud, M. F., Frias, M. A., Borradori, L., Fontao, L., Plectin interacts with the rod domain of type III intermediate filament proteins desmin and vimentin. *European Journal of Cell Biology,* 2011 May;90(5):390–400.

Patendid:

1. Title of Invention: "BI-SPECIFIC EXTRACELLULAR MATRIX BINDING PEPTIDES AND METHODS OF USE THEREOF", Tambet Teesalu and **Prakash Lingasamy,** Our Ref.: TARTU 100 (095468/00002) and Registered US Provisional Patent Application Number: 62800879, International PCT No: IB2020/050847

Raamatute peatükid:

1. Lingasamy, P., & Teesalu, T. (2020). Chapter XX: Homing peptides for cancer therapy. In Bio-Nanomedicine for Cancer Therapy, H. Santos & F. Fontana (Eds.) (1st ed., pp. X, 420). *Springer Nature Switzerland AG* (In press).

DISSERTATIONES MEDICINAE UNIVERSITATIS TARTUENSIS

1. **Heidi-Ingrid Maaroos**. The natural course of gastric ulcer in connection with chronic gastritis and *Helicobacter pylori*. Tartu, 1991.
2. **Mihkel Zilmer**. Na-pump in normal and tumorous brain tissues: Structural, functional and tumorigenesis aspects. Tartu, 1991.
3. **Eero Vasar**. Role of cholecystokinin receptors in the regulation of behaviour and in the action of haloperidol and diazepam. Tartu, 1992.
4. **Tiina Talvik**. Hypoxic-ischaemic brain damage in neonates (clinical, biochemical and brain computed tomographical investigation). Tartu, 1992.
5. **Ants Peetsalu**. Vagotomy in duodenal ulcer disease: A study of gastric acidity, serum pepsinogen I, gastric mucosal histology and *Helicobacter pylori*. Tartu, 1992.
6. **Marika Mikelsaar**. Evaluation of the gastrointestinal microbial ecosystem in health and disease. Tartu, 1992.
7. **Hele Everaus**. Immuno-hormonal interactions in chronic lymphocytic leukaemia and multiple myeloma. Tartu, 1993.
8. **Ruth Mikelsaar**. Etiological factors of diseases in genetically consulted children and newborn screening: dissertation for the commencement of the degree of doctor of medical sciences. Tartu, 1993.
9. **Agu Tamm**. On metabolic action of intestinal microflora: clinical aspects. Tartu, 1993.
10. **Katrin Gross**. Multiple sclerosis in South-Estonia (epidemiological and computed tomographical investigations). Tartu, 1993.
11. **Oivi Uibo**. Childhood coeliac disease in Estonia: occurrence, screening, diagnosis and clinical characterization. Tartu, 1994.
12. **Viiu Tuulik**. The functional disorders of central nervous system of chemistry workers. Tartu, 1994.
13. **Margus Viigimaa**. Primary haemostasis, antiaggregative and anticoagulant treatment of acute myocardial infarction. Tartu, 1994.
14. **Rein Kolk**. Atrial versus ventricular pacing in patients with sick sinus syndrome. Tartu, 1994.
15. **Toomas Podar**. Incidence of childhood onset type 1 diabetes mellitus in Estonia. Tartu, 1994.
16. **Kiira Subi**. The laboratory surveillance of the acute respiratory viral infections in Estonia. Tartu, 1995.
17. **Irja Lutsar**. Infections of the central nervous system in children (epidemiologic, diagnostic and therapeutic aspects, long term outcome). Tartu, 1995.
18. **Aavo Lang**. The role of dopamine, 5-hydroxytryptamine, sigma and NMDA receptors in the action of antipsychotic drugs. Tartu, 1995.
19. **Andrus Arak**. Factors influencing the survival of patients after radical surgery for gastric cancer. Tartu, 1996.

20. **Tõnis Karki**. Quantitative composition of the human lactoflora and method for its examination. Tartu, 1996.
21. **Reet Mändar**. Vaginal microflora during pregnancy and its transmission to newborn. Tartu, 1996.
22. **Triin Remmel**. Primary biliary cirrhosis in Estonia: epidemiology, clinical characterization and prognostication of the course of the disease. Tartu, 1996.
23. **Toomas Kivastik**. Mechanisms of drug addiction: focus on positive reinforcing properties of morphine. Tartu, 1996.
24. **Paavo Pokk**. Stress due to sleep deprivation: focus on $GABA_A$ receptor-chloride ionophore complex. Tartu, 1996.
25. **Kristina Allikmets**. Renin system activity in essential hypertension. Associations with atherothrombogenic cardiovascular risk factors and with the efficacy of calcium antagonist treatment. Tartu, 1996.
26. **Triin Parik**. Oxidative stress in essential hypertension: Associations with metabolic disturbances and the effects of calcium antagonist treatment. Tartu, 1996.
27. **Svetlana Päi**. Factors promoting heterogeneity of the course of rheumatoid arthritis. Tartu, 1997.
28. **Maarike Sallo**. Studies on habitual physical activity and aerobic fitness in 4 to 10 years old children. Tartu, 1997.
29. **Paul Naaber**. *Clostridium difficile* infection and intestinal microbial ecology. Tartu, 1997.
30. **Rein Pähkla**. Studies in pinoline pharmacology. Tartu, 1997.
31. **Andrus Juhan Voitk**. Outpatient laparoscopic cholecystectomy. Tartu, 1997.
32. **Joel Starkopf**. Oxidative stress and ischaemia-reperfusion of the heart. Tartu, 1997.
33. **Janika Kõrv**. Incidence, case-fatality and outcome of stroke. Tartu, 1998.
34. **Ülla Linnamägi**. Changes in local cerebral blood flow and lipid peroxidation following lead exposure in experiment. Tartu, 1998.
35. **Ave Minajeva**. Sarcoplasmic reticulum function: comparison of atrial and ventricular myocardium. Tartu, 1998.
36. **Oleg Milenin**. Reconstruction of cervical part of esophagus by revascularised ileal autografts in dogs. A new complex multistage method. Tartu, 1998.
37. **Sergei Pakriev**. Prevalence of depression, harmful use of alcohol and alcohol dependence among rural population in Udmurtia. Tartu, 1998.
38. **Allen Kaasik**. Thyroid hormone control over β-adrenergic signalling system in rat atria. Tartu, 1998.
39. **Vallo Matto**. Pharmacological studies on anxiogenic and antiaggressive properties of antidepressants. Tartu, 1998.
40. **Maire Vasar**. Allergic diseases and bronchial hyperreactivity in Estonian children in relation to environmental influences. Tartu, 1998.
41. **Kaja Julge**. Humoral immune responses to allergens in early childhood. Tartu, 1998.

42. **Heli Grünberg**. The cardiovascular risk of Estonian schoolchildren. A cross-sectional study of 9-, 12- and 15-year-old children. Tartu, 1998.
43. **Epp Sepp**. Formation of intestinal microbial ecosystem in children. Tartu, 1998.
44. **Mai Ots**. Characteristics of the progression of human and experimental glomerulopathies. Tartu, 1998.
45. **Tiina Ristimäe**. Heart rate variability in patients with coronary artery disease. Tartu, 1998.
46. **Leho Kõiv**. Reaction of the sympatho-adrenal and hypothalamo-pituitary-adrenocortical system in the acute stage of head injury. Tartu, 1998.
47. **Bela Adojaan**. Immune and genetic factors of childhood onset IDDM in Estonia. An epidemiological study. Tartu, 1999.
48. **Jakov Shlik**. Psychophysiological effects of cholecystokinin in humans. Tartu, 1999.
49. **Kai Kisand**. Autoantibodies against dehydrogenases of α-ketoacids. Tartu, 1999.
50. **Toomas Marandi**. Drug treatment of depression in Estonia. Tartu, 1999.
51. **Ants Kask**. Behavioural studies on neuropeptide Y. Tartu, 1999.
52. **Ello-Rahel Karelson**. Modulation of adenylate cyclase activity in the rat hippocampus by neuropeptide galanin and its chimeric analogs. Tartu, 1999.
53. **Tanel Laisaar**. Treatment of pleural empyema — special reference to intrapleural therapy with streptokinase and surgical treatment modalities. Tartu, 1999.
54. **Eve Pihl**. Cardiovascular risk factors in middle-aged former athletes. Tartu, 1999.
55. **Katrin Õunap**. Phenylketonuria in Estonia: incidence, newborn screening, diagnosis, clinical characterization and genotype/phenotype correlation. Tartu, 1999.
56. **Siiri Kõljalg**. *Acinetobacter* – an important nosocomial pathogen. Tartu, 1999.
57. **Helle Karro**. Reproductive health and pregnancy outcome in Estonia: association with different factors. Tartu, 1999.
58. **Heili Varendi**. Behavioral effects observed in human newborns during exposure to naturally occurring odors. Tartu, 1999.
59. **Anneli Beilmann**. Epidemiology of epilepsy in children and adolescents in Estonia. Prevalence, incidence, and clinical characteristics. Tartu, 1999.
60. **Vallo Volke**. Pharmacological and biochemical studies on nitric oxide in the regulation of behaviour. Tartu, 1999.
61. **Pilvi Ilves**. Hypoxic-ischaemic encephalopathy in asphyxiated term infants. A prospective clinical, biochemical, ultrasonographical study. Tartu, 1999.
62. **Anti Kalda**. Oxygen-glucose deprivation-induced neuronal death and its pharmacological prevention in cerebellar granule cells. Tartu, 1999.
63. **Eve-Irene Lepist**. Oral peptide prodrugs – studies on stability and absorption. Tartu, 2000.

64. **Jana Kivastik**. Lung function in Estonian schoolchildren: relationship with anthropometric indices and respiratory symptomas, reference values for dynamic spirometry. Tartu, 2000.
65. **Karin Kull**. Inflammatory bowel disease: an immunogenetic study. Tartu, 2000.
66. **Kaire Innos**. Epidemiological resources in Estonia: data sources, their quality and feasibility of cohort studies. Tartu, 2000.
67. **Tamara Vorobjova**. Immune response to *Helicobacter pylori* and its association with dynamics of chronic gastritis and epithelial cell turnover in antrum and corpus. Tartu, 2001.
68. **Ruth Kalda**. Structure and outcome of family practice quality in the changing health care system of Estonia. Tartu, 2001.
69. **Annika Krüüner**. *Mycobacterium tuberculosis* – spread and drug resistance in Estonia. Tartu, 2001.
70. **Marlit Veldi**. Obstructive Sleep Apnoea: Computerized Endopharyngeal Myotonometry of the Soft Palate and Lingual Musculature. Tartu, 2001.
71. **Anneli Uusküla**. Epidemiology of sexually transmitted diseases in Estonia in 1990–2000. Tartu, 2001.
72. **Ade Kallas**. Characterization of antibodies to coagulation factor VIII. Tartu, 2002.
73. **Heidi Annuk**. Selection of medicinal plants and intestinal lactobacilli as antimicrobil components for functional foods. Tartu, 2002.
74. **Aet Lukmann**. Early rehabilitation of patients with ischaemic heart disease after surgical revascularization of the myocardium: assessment of health-related quality of life, cardiopulmonary reserve and oxidative stress. A clinical study. Tartu, 2002.
75. **Maigi Eisen**. Pathogenesis of Contact Dermatitis: participation of Oxidative Stress. A clinical – biochemical study. Tartu, 2002.
76. **Piret Hussar**. Histology of the post-traumatic bone repair in rats. Elaboration and use of a new standardized experimental model – bicortical perforation of tibia compared to internal fracture and resection osteotomy. Tartu, 2002.
77. **Tõnu Rätsep**. Aneurysmal subarachnoid haemorrhage: Noninvasive monitoring of cerebral haemodynamics. Tartu, 2002.
78. **Marju Herodes**. Quality of life of people with epilepsy in Estonia. Tartu, 2003.
79. **Katre Maasalu**. Changes in bone quality due to age and genetic disorders and their clinical expressions in Estonia. Tartu, 2003.
80. **Toomas Sillakivi**. Perforated peptic ulcer in Estonia: epidemiology, risk factors and relations with *Helicobacter pylori*. Tartu, 2003.
81. **Leena Puksa**. Late responses in motor nerve conduction studies. F and A waves in normal subjects and patients with neuropathies. Tartu, 2003.
82. **Krista Lõivukene**. *Helicobacter pylori* in gastric microbial ecology and its antimicrobial susceptibility pattern. Tartu, 2003.

83. **Helgi Kolk**. Dyspepsia and *Helicobacter pylori* infection: the diagnostic value of symptoms, treatment and follow-up of patients referred for upper gastrointestinal endoscopy by family physicians. Tartu, 2003.
84. **Helena Soomer**. Validation of identification and age estimation methods in forensic odontology. Tartu, 2003.
85. **Kersti Oselin**. Studies on the human MDR1, MRP1, and MRP2 ABC transporters: functional relevance of the genetic polymorphisms in the *MDR1* and *MRP1* gene. Tartu, 2003.
86. **Jaan Soplepmann**. Peptic ulcer haemorrhage in Estonia: epidemiology, prognostic factors, treatment and outcome. Tartu, 2003.
87. **Margot Peetsalu**. Long-term follow-up after vagotomy in duodenal ulcer disease: recurrent ulcer, changes in the function, morphology and *Helicobacter pylori* colonisation of the gastric mucosa. Tartu, 2003.
88. **Kersti Klaamas**. Humoral immune response to *Helicobacter pylori* a study of host-dependent and microbial factors. Tartu, 2003.
89. **Pille Taba**. Epidemiology of Parkinson's disease in Tartu, Estonia. Prevalence, incidence, clinical characteristics, and pharmacoepidemiology. Tartu, 2003.
90. **Alar Veraksitš**. Characterization of behavioural and biochemical phenotype of cholecystokinin-2 receptor deficient mice: changes in the function of the dopamine and endopioidergic system. Tartu, 2003.
91. **Ingrid Kalev**. CC-chemokine receptor 5 (CCR5) gene polymorphism in Estonians and in patients with Type I and Type II diabetes mellitus. Tartu, 2003.
92. **Lumme Kadaja**. Molecular approach to the regulation of mitochondrial function in oxidative muscle cells. Tartu, 2003.
93. **Aive Liigant**. Epidemiology of primary central nervous system tumours in Estonia from 1986 to 1996. Clinical characteristics, incidence, survival and prognostic factors. Tartu, 2004.
94. **Andres, Kulla**. Molecular characteristics of mesenchymal stroma in human astrocytic gliomas. Tartu, 2004.
95. **Mari Järvelaid**. Health damaging risk behaviours in adolescence. Tartu, 2004.
96. **Ülle Pechter**. Progression prevention strategies in chronic renal failure and hypertension. An experimental and clinical study. Tartu, 2004.
97. **Gunnar Tasa**. Polymorphic glutathione S-transferases – biology and role in modifying genetic susceptibility to senile cataract and primary open angle glaucoma. Tartu, 2004.
98. **Tuuli Käämbre**. Intracellular energetic unit: structural and functional aspects. Tartu, 2004.
99. **Vitali Vassiljev**. Influence of nitric oxide syntase inhibitors on the effects of ethanol after acute and chronic ethanol administration and withdrawal. Tartu, 2004.

100. **Aune Rehema**. Assessment of nonhaem ferrous iron and glutathione redox ratio as markers of pathogeneticity of oxidative stress in different clinical groups. Tartu, 2004.
101. **Evelin Seppet**. Interaction of mitochondria and ATPases in oxidative muscle cells in normal and pathological conditions. Tartu, 2004.
102. **Eduard Maron**. Serotonin function in panic disorder: from clinical experiments to brain imaging and genetics. Tartu, 2004.
103. **Marje Oona**. *Helicobacter pylori* infection in children: epidemiological and therapeutic aspects. Tartu, 2004.
104. **Kersti Kokk**. Regulation of active and passive molecular transport in the testis. Tartu, 2005.
105. **Vladimir Järv**. Cross-sectional imaging for pretreatment evaluation and follow-up of pelvic malignant tumours. Tartu, 2005.
106. **Andre Õun**. Epidemiology of adult epilepsy in Tartu, Estonia. Incidence, prevalence and medical treatment. Tartu, 2005.
107. **Piibe Muda**. Homocysteine and hypertension: associations between homocysteine and essential hypertension in treated and untreated hypertensive patients with and without coronary artery disease. Tartu, 2005.
108. **Külli Kingo**. The interleukin-10 family cytokines gene polymorphisms in plaque psoriasis. Tartu, 2005.
109. **Mati Merila**. Anatomy and clinical relevance of the glenohumeral joint capsule and ligaments. Tartu, 2005.
110. **Epp Songisepp**. Evaluation of technological and functional properties of the new probiotic *Lactobacillus fermentum* ME-3. Tartu, 2005.
111. **Tiia Ainla**. Acute myocardial infarction in Estonia: clinical characteristics, management and outcome. Tartu, 2005.
112. **Andres Sell**. Determining the minimum local anaesthetic requirements for hip replacement surgery under spinal anaesthesia – a study employing a spinal catheter. Tartu, 2005.
113. **Tiia Tamme**. Epidemiology of odontogenic tumours in Estonia. Pathogenesis and clinical behaviour of ameloblastoma. Tartu, 2005.
114. **Triine Annus**. Allergy in Estonian schoolchildren: time trends and characteristics. Tartu, 2005.
115. **Tiia Voor**. Microorganisms in infancy and development of allergy: comparison of Estonian and Swedish children. Tartu, 2005.
116. **Priit Kasenõmm**. Indicators for tonsillectomy in adults with recurrent tonsillitis – clinical, microbiological and pathomorphological investigations. Tartu, 2005.
117. **Eva Zusinaite**. Hepatitis C virus: genotype identification and interactions between viral proteases. Tartu, 2005.
118. **Piret Kõll**. Oral lactoflora in chronic periodontitis and periodontal health. Tartu, 2006.
119. **Tiina Stelmach**. Epidemiology of cerebral palsy and unfavourable neurodevelopmental outcome in child population of Tartu city and county, Estonia Prevalence, clinical features and risk factors. Tartu, 2006.

120. **Katrin Pudersell**. Tropane alkaloid production and riboflavine excretion in the field and tissue cultures of henbane (*Hyoscyamus niger* L.). Tartu, 2006.
121. **Külli Jaako**. Studies on the role of neurogenesis in brain plasticity. Tartu, 2006.
122. **Aare Märtson**. Lower limb lengthening: experimental studies of bone regeneration and long-term clinical results. Tartu, 2006.
123. **Heli Tähepõld**. Patient consultation in family medicine. Tartu, 2006.
124. **Stanislav Liskmann**. Peri-implant disease: pathogenesis, diagnosis and treatment in view of both inflammation and oxidative stress profiling. Tartu, 2006.
125. **Ruth Rudissaar**. Neuropharmacology of atypical antipsychotics and an animal model of psychosis. Tartu, 2006.
126. **Helena Andreson**. Diversity of *Helicobacter pylori* genotypes in Estonian patients with chronic inflammatory gastric diseases. Tartu, 2006.
127. **Katrin Pruus**. Mechanism of action of antidepressants: aspects of serotoninergic system and its interaction with glutamate. Tartu, 2006.
128. **Priit Põder**. Clinical and experimental investigation: relationship of ischaemia/reperfusion injury with oxidative stress in abdominal aortic aneurysm repair and in extracranial brain artery endarterectomy and possibilities of protection against ischaemia using a glutathione analogue in a rat model of global brain ischaemia. Tartu, 2006.
129. **Marika Tammaru**. Patient-reported outcome measurement in rheumatoid arthritis. Tartu, 2006.
130. **Tiia Reimand**. Down syndrome in Estonia. Tartu, 2006.
131. **Diva Eensoo**. Risk-taking in traffic and Markers of Risk-Taking Behaviour in Schoolchildren and Car Drivers. Tartu, 2007.
132. **Riina Vibo**. The third stroke registry in Tartu, Estonia from 2001 to 2003: incidence, case-fatality, risk factors and long-term outcome. Tartu, 2007.
133. **Chris Pruunsild**. Juvenile idiopathic arthritis in children in Estonia. Tartu, 2007.
134. **Eve Õiglane-Šlik**. Angelman and Prader-Willi syndromes in Estonia. Tartu, 2007.
135. **Kadri Haller**. Antibodies to follicle stimulating hormone. Significance in female infertility. Tartu, 2007.
136. **Pille Ööpik**. Management of depression in family medicine. Tartu, 2007.
137. **Jaak Kals**. Endothelial function and arterial stiffness in patients with atherosclerosis and in healthy subjects. Tartu, 2007.
138. **Priit Kampus**. Impact of inflammation, oxidative stress and age on arterial stiffness and carotid artery intima-media thickness. Tartu, 2007.
139. **Margus Punab**. Male fertility and its risk factors in Estonia. Tartu, 2007.
140. **Alar Toom**. Heterotopic ossification after total hip arthroplasty: clinical and pathogenetic investigation. Tartu, 2007.

141. **Lea Pehme**. Epidemiology of tuberculosis in Estonia 1991–2003 with special regard to extrapulmonary tuberculosis and delay in diagnosis of pulmonary tuberculosis. Tartu, 2007.
142. **Juri Karjagin**. The pharmacokinetics of metronidazole and meropenem in septic shock. Tartu, 2007.
143. **Inga Talvik**. Inflicted traumatic brain injury shaken baby syndrome in Estonia – epidemiology and outcome. Tartu, 2007.
144. **Tarvo Rajasalu**. Autoimmune diabetes: an immunological study of type 1 diabetes in humans and in a model of experimental diabetes (in RIP-B7.1 mice). Tartu, 2007.
145. **Inga Karu**. Ischaemia-reperfusion injury of the heart during coronary surgery: a clinical study investigating the effect of hyperoxia. Tartu, 2007.
146. **Peeter Padrik**. Renal cell carcinoma: Changes in natural history and treatment of metastatic disease. Tartu, 2007.
147. **Neve Vendt**. Iron deficiency and iron deficiency anaemia in infants aged 9 to 12 months in Estonia. Tartu, 2008.
148. **Lenne-Triin Heidmets**. The effects of neurotoxins on brain plasticity: focus on neural Cell Adhesion Molecule. Tartu, 2008.
149. **Paul Korrovits**. Asymptomatic inflammatory prostatitis: prevalence, etiological factors, diagnostic tools. Tartu, 2008.
150. **Annika Reintam**. Gastrointestinal failure in intensive care patients. Tartu, 2008.
151. **Kristiina Roots**. Cationic regulation of Na-pump in the normal, Alzheimer's and CCK_2 receptor-deficient brain. Tartu, 2008.
152. **Helen Puusepp**. The genetic causes of mental retardation in Estonia: fragile X syndrome and creatine transporter defect. Tartu, 2009.
153. **Kristiina Rull**. Human chorionic gonadotropin beta genes and recurrent miscarriage: expression and variation study. Tartu, 2009.
154. **Margus Eimre**. Organization of energy transfer and feedback regulation in oxidative muscle cells. Tartu, 2009.
155. **Maire Link**. Transcription factors FoxP3 and AIRE: autoantibody associations. Tartu, 2009.
156. **Kai Haldre**. Sexual health and behaviour of young women in Estonia. Tartu, 2009.
157. **Kaur Liivak**. Classical form of congenital adrenal hyperplasia due to 21-hydroxylase deficiency in Estonia: incidence, genotype and phenotype with special attention to short-term growth and 24-hour blood pressure. Tartu, 2009.
158. **Kersti Ehrlich**. Antioxidative glutathione analogues (UPF peptides) – molecular design, structure-activity relationships and testing the protective properties. Tartu, 2009.
159. **Anneli Rätsep**. Type 2 diabetes care in family medicine. Tartu, 2009.
160. **Silver Türk**. Etiopathogenetic aspects of chronic prostatitis: role of mycoplasmas, coryneform bacteria and oxidative stress. Tartu, 2009.

161. **Kaire Heilman**. Risk markers for cardiovascular disease and low bone mineral density in children with type 1 diabetes. Tartu, 2009.
162. **Kristi Rüütel**. HIV-epidemic in Estonia: injecting drug use and quality of life of people living with HIV. Tartu, 2009.
163. **Triin Eller**. Immune markers in major depression and in antidepressive treatment. Tartu, 2009.
164. **Siim Suutre**. The role of TGF-β isoforms and osteoprogenitor cells in the pathogenesis of heterotopic ossification. An experimental and clinical study of hip arthroplasty. Tartu, 2010.
165. **Kai Kliiman**. Highly drug-resistant tuberculosis in Estonia: Risk factors and predictors of poor treatment outcome. Tartu, 2010.
166. **Inga Villa**. Cardiovascular health-related nutrition, physical activity and fitness in Estonia. Tartu, 2010.
167. **Tõnis Org**. Molecular function of the first PHD finger domain of Autoimmune Regulator protein. Tartu, 2010.
168. **Tuuli Metsvaht**. Optimal antibacterial therapy of neonates at risk of early onset sepsis. Tartu, 2010.
169. **Jaanus Kahu**. Kidney transplantation: Studies on donor risk factors and mycophenolate mofetil. Tartu, 2010.
170. **Koit Reimand**. Autoimmunity in reproductive failure: A study on associated autoantibodies and autoantigens. Tartu, 2010.
171. **Mart Kull**. Impact of vitamin D and hypolactasia on bone mineral density: a population based study in Estonia. Tartu, 2010.
172. **Rael Laugesaar**. Stroke in children – epidemiology and risk factors. Tartu, 2010.
173. **Mark Braschinsky**. Epidemiology and quality of life issues of hereditary spastic paraplegia in Estonia and implemention of genetic analysis in everyday neurologic practice. Tartu, 2010.
174. **Kadri Suija**. Major depression in family medicine: associated factors, recurrence and possible intervention. Tartu, 2010.
175. **Jarno Habicht**. Health care utilisation in Estonia: socioeconomic determinants and financial burden of out-of-pocket payments. Tartu, 2010.
176. **Kristi Abram**. The prevalence and risk factors of rosacea. Subjective disease perception of rosacea patients. Tartu, 2010.
177. **Malle Kuum**. Mitochondrial and endoplasmic reticulum cation fluxes: Novel roles in cellular physiology. Tartu, 2010.
178. **Rita Teek**. The genetic causes of early onset hearing loss in Estonian children. Tartu, 2010.
179. **Daisy Volmer**. The development of community pharmacy services in Estonia – public and professional perceptions 1993–2006. Tartu, 2010.
180. **Jelena Lissitsina**. Cytogenetic causes in male infertility. Tartu, 2011.
181. **Delia Lepik**. Comparison of gunshot injuries caused from Tokarev, Makarov and Glock 19 pistols at different firing distances. Tartu, 2011.
182. **Ene-Renate Pähkla**. Factors related to the efficiency of treatment of advanced periodontitis. Tartu, 2011.

183. **Maarja Krass**. L-Arginine pathways and antidepressant action. Tartu, 2011.
184. **Taavi Lai**. Population health measures to support evidence-based health policy in Estonia. Tartu, 2011.
185. **Tiit Salum**. Similarity and difference of temperature-dependence of the brain sodium pump in normal, different neuropathological, and aberrant conditions and its possible reasons. Tartu, 2011.
186. **Tõnu Vooder**. Molecular differences and similarities between histological subtypes of non-small cell lung cancer. Tartu, 2011.
187. **Jelena Štšepetova**. The characterisation of intestinal lactic acid bacteria using bacteriological, biochemical and molecular approaches. Tartu, 2011.
188. **Radko Avi**. Natural polymorphisms and transmitted drug resistance in Estonian HIV-1 CRF06_cpx and its recombinant viruses. Tartu, 2011, 116 p.
189. **Edward Laane**. Multiparameter flow cytometry in haematological malignancies. Tartu, 2011, 152 p.
190. **Triin Jagomägi**. A study of the genetic etiology of nonsyndromic cleft lip and palate. Tartu, 2011, 158 p.
191. **Ivo Laidmäe**. Fibrin glue of fish (*Salmo salar*) origin: immunological study and development of new pharmaceutical preparation. Tartu, 2012, 150 p.
192. **Ülle Parm**. Early mucosal colonisation and its role in prediction of invasive infection in neonates at risk of early onset sepsis. Tartu, 2012, 168 p.
193. **Kaupo Teesalu**. Autoantibodies against desmin and transglutaminase 2 in celiac disease: diagnostic and functional significance. Tartu, 2012, 142 p.
194. **Maksim Zagura**. Biochemical, functional and structural profiling of arterial damage in atherosclerosis. Tartu, 2012, 162 p.
195. **Vivian Kont**. Autoimmune regulator: characterization of thymic gene regulation and promoter methylation. Tartu, 2012, 134 p.
196. **Pirje Hütt**. Functional properties, persistence, safety and efficacy of potential probiotic lactobacilli. Tartu, 2012, 246 p.
197. **Innar Tõru**. Serotonergic modulation of CCK-4- induced panic. Tartu, 2012, 132 p.
198. **Sigrid Vorobjov**. Drug use, related risk behaviour and harm reduction interventions utilization among injecting drug users in Estonia: implications for drug policy. Tartu, 2012, 120 p.
199. **Martin Serg**. Therapeutic aspects of central haemodynamics, arterial stiffness and oxidative stress in hypertension. Tartu, 2012, 156 p.
200. **Jaanika Kumm**. Molecular markers of articular tissues in early knee osteoarthritis: a population-based longitudinal study in middle-aged subjects. Tartu, 2012, 159 p.
201. **Kertu Rünkorg**. Functional changes of dopamine, endopioid and endocannabinoid systems in CCK2 receptor deficient mice. Tartu, 2012, 125 p.
202. **Mai Blöndal**. Changes in the baseline characteristics, management and outcomes of acute myocardial infarction in Estonia. Tartu, 2012, 127 p.

203. **Jana Lass**. Epidemiological and clinical aspects of medicines use in children in Estonia. Tartu, 2012, 170 p.
204. **Kai Truusalu**. Probiotic lactobacilli in experimental persistent *Salmonella* infection. Tartu, 2013, 139 p.
205. **Oksana Jagur**. Temporomandibular joint diagnostic imaging in relation to pain and bone characteristics. Long-term results of arthroscopic treatment. Tartu, 2013, 126 p.
206. **Katrin Sikk**. Manganese-ephedrone intoxication – pathogenesis of neurological damage and clinical symptomatology. Tartu, 2013, 125 p.
207. **Kai Blöndal**. Tuberculosis in Estonia with special emphasis on drug-resistant tuberculosis: Notification rate, disease recurrence and mortality. Tartu, 2013, 151 p.
208. **Marju Puurand**. Oxidative phosphorylation in different diseases of gastric mucosa. Tartu, 2013, 123 p.
209. **Aili Tagoma**. Immune activation in female infertility: Significance of autoantibodies and inflammatory mediators. Tartu, 2013, 135 p.
210. **Liis Sabre**. Epidemiology of traumatic spinal cord injury in Estonia. Brain activation in the acute phase of traumatic spinal cord injury. Tartu, 2013, 135 p.
211. **Merit Lamp**. Genetic susceptibility factors in endometriosis. Tartu, 2013, 125 p.
212. **Erik Salum**. Beneficial effects of vitamin D and angiotensin II receptor blocker on arterial damage. Tartu, 2013, 167 p.
213. **Maire Karelson**. Vitiligo: clinical aspects, quality of life and the role of melanocortin system in pathogenesis. Tartu, 2013, 153 p.
214. **Kuldar Kaljurand**. Prevalence of exfoliation syndrome in Estonia and its clinical significance. Tartu, 2013, 113 p.
215. **Raido Paasma**. Clinical study of methanol poisoning: handling large outbreaks, treatment with antidotes, and long-term outcomes. Tartu, 2013, 96 p.
216. **Anne Kleinberg**. Major depression in Estonia: prevalence, associated factors, and use of health services. Tartu, 2013, 129 p.
217. **Triin Eglit**. Obesity, impaired glucose regulation, metabolic syndrome and their associations with high-molecular-weight adiponectin levels. Tartu, 2014, 115 p.
218. **Kristo Ausmees**. Reproductive function in middle-aged males: Associations with prostate, lifestyle and couple infertility status. Tartu, 2014, 125 p.
219. **Kristi Huik**. The influence of host genetic factors on the susceptibility to HIV and HCV infections among intravenous drug users. Tartu, 2014, 144 p.
220. **Liina Tserel**. Epigenetic profiles of monocytes, monocyte-derived macrophages and dendritic cells. Tartu, 2014, 143 p.
221. **Irina Kerna**. The contribution of *ADAM12* and *CILP* genes to the development of knee osteoarthritis. Tartu, 2014, 152 p.

222. **Ingrid Liiv**. Autoimmune regulator protein interaction with DNA-dependent protein kinase and its role in apoptosis. Tartu, 2014, 143 p.
223. **Liivi Maddison**. Tissue perfusion and metabolism during intra-abdominal hypertension. Tartu, 2014, 103 p.
224. **Krista Ress**. Childhood coeliac disease in Estonia, prevalence in atopic dermatitis and immunological characterisation of coexistence. Tartu, 2014, 124 p.
225. **Kai Muru**. Prenatal screening strategies, long-term outcome of children with marked changes in maternal screening tests and the most common syndromic heart anomalies in Estonia. Tartu, 2014, 189 p.
226. **Kaja Rahu**. Morbidity and mortality among Baltic Chernobyl cleanup workers: a register-based cohort study. Tartu, 2014, 155 p.
227. **Klari Noormets**. The development of diabetes mellitus, fertility and energy metabolism disturbances in a Wfs1-deficient mouse model of Wolfram syndrome. Tartu, 2014, 132 p.
228. **Liis Toome**. Very low gestational age infants in Estonia. Tartu, 2014, 183 p.
229. **Ceith Nikkolo**. Impact of different mesh parameters on chronic pain and foreign body feeling after open inguinal hernia repair. Tartu, 2014, 132 p.
230. **Vadim Brjalin**. Chronic hepatitis C: predictors of treatment response in Estonian patients. Tartu, 2014, 122 p.
231. **Vahur Metsna**. Anterior knee pain in patients following total knee arthroplasty: the prevalence, correlation with patellar cartilage impairment and aspects of patellofemoral congruence. Tartu, 2014, 130 p.
232. **Marju Kase**. Glioblastoma multiforme: possibilities to improve treatment efficacy. Tartu, 2015, 137 p.
233. **Riina Runnel**. Oral health among elementary school children and the effects of polyol candies on the prevention of dental caries. Tartu, 2015, 112 p.
234. **Made Laanpere**. Factors influencing women's sexual health and reproductive choices in Estonia. Tartu, 2015, 176 p.
235. **Andres Lust**. Water mediated solid state transformations of a polymorphic drug – effect on pharmaceutical product performance. Tartu, 2015, 134 p.
236. **Anna Klugman**. Functionality related characterization of pretreated wood lignin, cellulose and polyvinylpyrrolidone for pharmaceutical applications. Tartu, 2015, 156 p.
237. **Triin Laisk-Podar**. Genetic variation as a modulator of susceptibility to female infertility and a source for potential biomarkers. Tartu, 2015, 155 p.
238. **Mailis Tõnisson**. Clinical picture and biochemical changes in blood in children with acute alcohol intoxication. Tartu, 2015, 100 p.
239. **Kadri Tamme**. High volume haemodiafiltration in treatment of severe sepsis – impact on pharmacokinetics of antibiotics and inflammatory response. Tartu, 2015, 133 p.

240. **Kai Part**. Sexual health of young people in Estonia in a social context: the role of school-based sexuality education and youth-friendly counseling services. Tartu, 2015, 203 p.
241. **Urve Paaver**. New perspectives for the amorphization and physical stabilization of poorly water-soluble drugs and understanding their dissolution behavior. Tartu, 2015, 139 p.
242. **Aleksandr Peet**. Intrauterine and postnatal growth in children with HLA-conferred susceptibility to type 1 diabetes. Tartu. 2015, 146 p.
243. **Piret Mitt**. Healthcare-associated infections in Estonia – epidemiology and surveillance of bloodstream and surgical site infections. Tartu, 2015, 145 p.
244. **Merli Saare**. Molecular Profiling of Endometriotic Lesions and Endometria of Endometriosis Patients. Tartu, 2016, 129 p.
245. **Kaja-Triin Laisaar**. People living with HIV in Estonia: Engagement in medical care and methods of increasing adherence to antiretroviral therapy and safe sexual behavior. Tartu, 2016, 132 p.
246. **Eero Merilind**. Primary health care performance: impact of payment and practice-based characteristics. Tartu, 2016, 120 p.
247. **Jaanika Kärner**. Cytokine-specific autoantibodies in AIRE deficiency. Tartu, 2016, 182 p.
248. **Kaido Paapstel**. Metabolomic profile of arterial stiffness and early biomarkers of renal damage in atherosclerosis. Tartu, 2016, 173 p.
249. **Liidia Kiisk**. Long-term nutritional study: anthropometrical and clinico-laboratory assessments in renal replacement therapy patients after intensive nutritional counselling. Tartu, 2016, 207 p.
250. **Georgi Nellis**. The use of excipients in medicines administered to neonates in Europe. Tartu, 2017, 159 p.
251. **Aleksei Rakitin**. Metabolic effects of acute and chronic treatment with valproic acid in people with epilepsy. Tartu, 2017, 125 p.
252. **Eveli Kallas**. The influence of immunological markers to susceptibility to HIV, HBV, and HCV infections among persons who inject drugs. Tartu, 2017, 138 p.
253. **Tiina Freimann**. Musculoskeletal pain among nurses: prevalence, risk factors, and intervention. Tartu, 2017, 125 p.
254. **Evelyn Aaviksoo**. Sickness absence in Estonia: determinants and influence of the sick-pay cut reform. Tartu, 2017, 121 p.
255. **Kalev Nõupuu**. Autosomal-recessive Stargardt disease: phenotypic heterogeneity and genotype-phenotype associations. Tartu, 2017, 131 p.
256. **Ho Duy Binh**. Osteogenesis imperfecta in Vietnam. Tartu, 2017, 125 p.
257. **Uku Haljasorg**. Transcriptional mechanisms in thymic central tolerance. Tartu, 2017, 147 p.
258. **Živile Riispere**. IgA Nephropathy study according to the Oxford Classification: IgA Nephropathy clinical-morphological correlations, disease progression and the effect of renoprotective therapy. Tartu, 2017, 129 p.
259. **Hiie Soeorg**. Coagulase-negative staphylococci in gut of preterm neonates and in breast milk of their mothers. Tartu, 2017, 216 p.

260. **Anne-Mari Anton Willmore**. Silver nanoparticles for cancer research. Tartu, 2017, 132 p.
261. **Ott Laius**. Utilization of osteoporosis medicines, medication adherence and the trend in osteoporosis related hip fractures in Estonia. Tartu, 2017, 134 p.
262. **Alar Aab**. Insights into molecular mechanisms of asthma and atopic dermatitis. Tartu, 2017, 164 p.
263. **Sander Pajusalu**. Genome-wide diagnostics of Mendelian disorders: from chromosomal microarrays to next-generation sequencing. Tartu, 2017, 146 p.
264. **Mikk Jürisson**. Health and economic impact of hip fracture in Estonia. Tartu, 2017, 164 p.
265. **Kaspar Tootsi**. Cardiovascular and metabolomic profiling of osteoarthritis. Tartu, 2017, 150 p.
266. **Mario Saare**. The influence of AIRE on gene expression – studies of transcriptional regulatory mechanisms in cell culture systems. Tartu, 2017, 172 p.
267. **Piia Jõgi**. Epidemiological and clinical characteristics of pertussis in Estonia. Tartu, 2018, 168 p.
268. **Elle Põldoja**. Structure and blood supply of the superior part of the shoulder joint capsule. Tartu, 2018, 116 p.
269. **Minh Son Nguyen**. Oral health status and prevalence of temporo-mandibular disorders in 65–74-year-olds in Vietnam. Tartu, 2018, 182 p.
270. **Kristian Semjonov**. Development of pharmaceutical quench-cooled molten and melt-electrospun solid dispersions for poorly water-soluble indomethacin. Tartu, 2018, 125 p.
271. **Janne Tiigimäe-Saar**. Botulinum neurotoxin type A treatment for sialorrhea in central nervous system diseases. Tartu, 2018, 109 p.
272. **Veiko Vengerfeldt**. Apical periodontitis: prevalence and etiopathogenetic aspects. Tartu, 2018, 150 p.
273. **Rudolf Bichele**. TNF superfamily and AIRE at the crossroads of thymic differentiation and host protection against *Candida albicans* infection. Tartu, 2018, 153 p.
274. **Olga Tšuiko**. Unravelling Chromosomal Instability in Mammalian Pre-implantation Embryos Using Single-Cell Genomics. Tartu, 2018, 169 p.
275. **Kärt Kriisa**. Profile of acylcarnitines, inflammation and oxidative stress in first-episode psychosis before and after antipsychotic treatment. Tartu, 2018, 145 p.
276. **Xuan Dung Ho**. Characterization of the genomic profile of osteosarcoma. Tartu, 2018, 144 p.
277. **Karit Reinson**. New Diagnostic Methods for Early Detection of Inborn Errors of Metabolism in Estonia. Tartu, 2018, 201 p.
278. **Mari-Anne Vals**. Congenital N-glycosylation Disorders in Estonia. Tartu, 2019, 148 p.

279. **Liis Kadastik-Eerme**. Parkinson's disease in Estonia: epidemiology, quality of life, clinical characteristics and pharmacotherapy. Tartu, 2019, 202 p.
280. **Hedi Hunt**. Precision targeting of intraperitoneal tumors with peptide-guided nanocarriers. Tartu, 2019, 179 p.
281. **Rando Porosk**. The role of oxidative stress in Wolfram syndrome 1 and hypothermia. Tartu, 2019, 123 p.
282. **Ene-Ly Jõgeda**. The influence of coinfections and host genetic factor on the susceptibility to HIV infection among people who inject drugs. Tartu, 2019, 126 p.
283. **Kristel Ehala-Aleksejev**. The associations between body composition, obesity and obesity-related health and lifestyle conditions with male reproductive function. Tartu, 2019, 138 p.
284. **Aigar Ottas**. The metabolomic profiling of psoriasis, atopic dermatitis and atherosclerosis. Tartu, 2019, 136 p.
285. **Elmira Gurbanova**. Specific characteristics of tuberculosis in low default, but high multidrug–resistance prison setting. Tartu, 2019, 129 p.
286. **Van Thai Nguyeni**. The first study of the treatment outcomes of patients with cleft lip and palate in Central Vietnam. Tartu, 2019, 144 p.
287. **Maria Yakoreva**. Imprinting Disorders in Estonia. Tartu, 2019, 187 p.
288. **Kadri Rekker**. The putative role of microRNAs in endometriosis pathogenesis and potential in diagnostics. Tartu, 2019, 140 p.
289. **Ülle Võhma**. Association between personality traits, clinical characteristics and pharmacological treatment response in panic disorder. Tartu, 2019, 121 p.
290. **Aet Saar**. Acute myocardial infarction in Estonia 2001–2014: towards risk-based prevention and management. Tartu, 2019, 124 p.
291. **Toomas Toomsoo**. Transcranial brain sonography in the Estonian cohort of Parkinson's disease. Tartu, 2019, 114 p.
292. **Lidiia Zhytnik**. Inter- and intrafamilial diversity based on genotype and phenotype correlations of Osteogenesis Imperfecta. Tartu, 2019, 224 p.
293. **Pilleriin Soodla**. Newly HIV-infected people in Estonia: estimation of incidence and transmitted drug resistance. Tartu, 2019, 194 p.
294. **Kristiina Ojamaa**. Epidemiology of gynecological cancer in Estonia. Tartu, 2020, 133 p.
295. **Marianne Saard**. Modern Cognitive and Social Intervention Techniques in Paediatric Neurorehabilitation for Children with Acquired Brain Injury. Tartu, 2020, 168 p.
296. **Julia Maslovskaja**. The importance of DNA binding and DNA breaks for AIRE-mediated transcriptional activation. Tartu, 2020, 162 p.
297. **Natalia Lobanovskaya**. The role of PSA-NCAM in the survival of retinal ganglion cells. Tartu, 2020, 105 p.
298. **Madis Rahu**. Structure and blood supply of the postero-superior part of the shoulder joint capsule with implementation of surgical treatment after anterior traumatic dislocation. Tartu, 2020, 104 p.

299. **Helen Zirnask**. Luteinizing hormone (LH) receptor expression in the penis and its possible role in pathogenesis of erectile disturbances. Tartu, 2020, 87 p.
300. **Kadri Toome**. Homing peptides for targeting of brain diseases. Tartu, 2020, 152 p.
301. **Maarja Hallik**. Pharmacokinetics and pharmacodynamics of inotropic drugs in neonates. Tartu, 2020, 172 p.
302. **Raili Müller**. Cardiometabolic risk profile and body composition in early rheumatoid arthritis. Tartu, 2020, 133 p.
303. **Sergo Kasvandik**. The role of proteomic changes in endometrial cells – from the perspective of fertility and endometriosis. Tartu, 2020, 191 p.
304. **Epp Kaleviste**. Genetic variants revealing the role of STAT1/STAT3 signaling cytokines in immune protection and pathology. Tartu, 2020, 189 p.
305. **Sten Saar**. Epidemiology of severe injuries in Estonia. Tartu, 2020, 104 p.
306. **Kati Braschinsky**. Epidemiology of primary headaches in Estonia and applicability of web-based solutions in headache epidemiology research. Tartu, 2020, 129 p.
307. **Helen Vaher**. MicroRNAs in the regulation of keratinocyte responses in *psoriasis vulgaris* and atopic dermatitis. Tartu, 2020, 242 p.
308. **Liisi Raam**. Molecular Alterations in the Pathogenesis of Two Chronic Dermatoses – Vitiligo and Psoriasis. Tartu, 2020, 164 p.
309. **Artur Vetkas**. Long-term quality of life, emotional health, and associated factors in patients after aneurysmal subarachnoid haemorrhage. Tartu, 2020, 127 p.
310. **Teele Kasepalu**. Effects of remote ischaemic preconditioning on organ damage and acylcarnitines' metabolism in vascular surgery. Tartu, 2020, 130 p.